GENOMIC APPROACHES TO CONGENITAL GENITOURINARY DISORDERS

APPROVED BY SUPERVISORY COMMITTEE

Linda Baker, M.D.

Andrew Zinn, M.D., Ph.D.

Jonathan Cohen, Ph.D.

Thomas Carroll, Ph.D.

DEDICATION

To my high school biology teacher, Mrs. Hughes

Thank you for making genetics so interesting

GENOMIC APPROACHES TO CONGENITAL GENITOURINARY DISORDERS

by

STEVEN MICHAEL HARRISON

DISSERTATION

Presented to the Faculty of the Graduate School of Biomedical Sciences

The University of Texas Southwestern Medical Center at Dallas

In Partial Fulfillment of the Requirements

For the Degree of

DOCTOR OF PHILOSOPHY

The University of Texas Southwestern Medical Center

Dallas, TX

May, 2014

ACKNOWLEDGEMENTS

I would like to thank my mentor Linda Baker for her support, guidance, and friendship during my time in the lab. Her enthusiasm for research was a strong motivator throughout this process. I would also like to thank my committee members Andrew Zinn, Jonathon Cohen, and Thomas Carroll for their support in my pursuit of a human genetics project and for providing invaluable perspectives and advice.

I am very grateful to everyone in Linda Baker's lab, as each member has made the lab a great place to work. Thank you to Shaohua Zhang for her incredible help on a daily basis. Thank you to both Emma Sanchez and Martinez Hill for their invaluable assistance with the clinical aspects of this research. Thank you to Daniel DaJusta, Carlos Villanueva, Melise Keays, Candace Granberg and especially Gwen Grimsby for their significant contributions to this work.

Thank you to Chao Xing, Jonathan Rios, Jason Park, Sandy Cope-Yokoyama, Sachin Hajarnis, Peter Igarashi, JT Hsieh, and many other researchers at UT Southwestern for providing support. Thank you to David Calderwood and Massimiliano Baldassarre (Yale University) for their generous sharing of plasmids and recombinant proteins. Additionally, thank you to the Prune Belly Syndrome Network for their enthusiastic willingness to participate in this research

Lastly, thank you to the many friends I've made in Dallas and to my incredible family for always being proud of me and encouraging higher education.

GENOMIC APPROACHES TO CONGENITAL GENITOURINARY DISORDERS

STEVEN MICHAEL HARRISON

The University of Texas Southwestern Medical Center at Dallas, 2014

Linda A. Baker, M.D.

Congenital genitourinary disorders are the third most common congenital anomaly worldwide (1 in 135 births) and include anomalies of both the urinary and genital systems, such as prune belly syndrome (PBS), persistent cloaca, and disorders of sex development (DSD). Understanding the genetic cause of a disease plays a major role in clinical diagnosis, management, and treatment; however the underlying causative genes for PBS and persistent cloaca are unknown while mutations in known DSD genes account for only 50% of 46,XY DSD patients. The goal of this research was to use both array-comparative genomic hybridization and whole exome sequencing to identify causative variants and candidate genes for PBS, persistent cloaca, and DSD. Sequencing the exomes of two PBS brothers identified a missense mutation in Filamin A and functional testing suggests this mutation impairs muscle cell contraction and mechanosensing. Candidate genes identified from sequencing the exomes of unrelated patients are hypothesized to have similar effects on cellular function, suggesting a common causative pathway may contribute to PBS

pathogenesis. Additionally, structural variants identified by array-comparative genomic hybridization propose both candidate regions for persistent cloaca and novel variants in DSD pathogenesis. Both genome-wide tests identified novel or rare candidate genes for further study indicating that continued genetic testing of patients with congenital genitourinary disorders will lead to a better understanding of molecular pathways of disease pathogenesis and clinical care.

TABLE OF CONTENTS

PRIOR PUBLICATIONS

Harrison S, Seideman C, Baker L. 2014. DNA copy-number variations in persistent cloaca patients. *Journal of Urology*. Epub ahead of print.

Harrison S*, Campbell I*, Keays M, Granberg C, Villanueva C, Tannin G, Zinn A, Castrillon D, Shaw C, Stankiewicz P, Baker L. 2013. Screening and familial characterization of copy-number variations in *NR5A1* in 46,XY disorders of sexual development and premature ovarian failure. *American Journal of Medical Genetics Part A*. 161A: 2487-2494.

Sheng-Wei C, Mislankar M, Misra C, Huang N, DaJusta D, **Harrison S**, McBride K, Baker L, Garg V. 2013. Genetic abnormalities in FOXP1 are associated with congenital heart defects. *Human Mutation*. 34(9): 1226-1230.

Granberg C*, **Harrison S***, Dajusta D, Zhang S, Hajarnis S, Igarashi P, Baker L. 2012. Genetic basis of prune belly syndrome: screening for HNF1β gene. *Journal of Urology*. 187(1): 272-278.

*These first authors contributed equally to the manuscript

LIST OF FIGURES

LIST OF TABLES

LIST OF ABBREVIATIONS

ABD - actin-binding domain

aCGH - array-comparative genomic hybridization

ACTA2 - alpha-smooth muscle actin

AMH - anti-Müllerian hormone

AR - androgen receptor

CHD - congential heart disease

CHD1 - calponin homology domain 1

CHD2 - calponin homology domain 2

CHO - chinese hampster ovary

CHRM3 - Muscarinic acetylcholine receptor M3

chrX - chromosome X

CIIP - congenital idiopathic intestinal pseudoobstruction

CNV - copy number variation

CSBS - congenital short bowel syndrome

dbSNP - Single Nucleotide Polymorphism Database

DGV - Database of Genomic Variants

DSD - disorders of sex development

DSTYK - dual serine-threonine and tyrosine protein kinase

E - embryonic day

ECM - extracellular matrix

f-actin - filamentous actin

FFPE - formalin-fixed paraffin-embeeded

FISH - fluorescence in situ hybridization

FLNA - filamin-A

FMD - frontometaphyseal dysplasia

GATK - genome analysis toolkit

Gb - gigabases

GD - gonadal dysgenesis

GERP - Genomic Evolutionary Rate Profiling

HHAT - hedgehog acyltransferase

HIF-1α - hypoxia-inducible factor 1α

HNF1B - hepatocyte nuclear factor 1β

HYDIN - axonemal central pair apparatus protein

Ig - immunoglobin

IGFN1 - immunoglobulin-like and fibronectin type III domain containing 1

ITGB1 - integrin, beta 1

ITGB7 - integrin, beta 7

LUTO - lower urinary tract obstruction

MAF - minor allele frequency

Mb - megabases

MLPA - multiplex ligation-dependent probe amplification

MNS - Melnick-Needles syndrome

MODY - maturity onset diabetes of the young

MUC4 - mucin 4

NGS - next-generation sequecing

NHLBI EVS - National Heart, Lung, and Blood Institute Exome Sequencing Project

NR5A1 - nuclear receptor subfamily 5, group A, member 1 gene

OMIM - Online Mendelian Inheritance in Man

OPD - otopalatodigital

OPD1 - otopalatodigital syndrome, type I

OPD2 - otopalatodigital syndrome, type II

PBS - prune belly syndrome

PCR - polymerase chain reaction

Pkdh1 - polycystic kidney and hepatic disease 1

POF - premature ovarian failure

PUV - posterior urethral valves

PVNH - periventricular heterotopia

SF1 - steroidogenic factor 1

SHH - Sonic hedgehog

SNV - single nucleotide variant

SRY - sex-determining region Y

TIF2 - transcriptional intermediary factor-2

TTN - titin

UPIIIA - Uroplakin IIIA

WES - whole exome sequencing

WGS - whole genome sequencing

WT - wild-type

CHAPTER 1: INTRODUCTION

I. Genetic basis of human phenotypes

Determining the genetic basis of human diseases is a major focus of current research as gene identification can provide important knowledge about disease mechanisms, biological pathways, and potential treatment options. Online Mendelian Inheritance in Man (OMIM), a public database of human genes and genetic phenotypes, lists nearly 7,700 Mendelian diseases but only 53% of these human diseases have a known genetic or molecular basis. Understanding the genetic cause of a disease plays a major role in clinical diagnosis, management, and treatment for mutation-carrying patients and genetic counseling for family members and future pregnancies. In the case of congenital anomalies that can be diagnosed *in utero*, having a confirmed genetic diagnosis impacts management of the pregnancy, such as pregnancy continuation or *in utero* surgical interventions. Beyond clinical management, understanding the genetic cause of a disorder provides insight into the etiology of common and complex diseases with similar phenotypes. With regards to genitourinary disorders, the incidence of prune belly syndrome (PBS) is 1:50,000 however the obstructive bladder phenotype observed in PBS patients is a common feature of patients with lower urinary tract obstruction (LUTO), incidence 1:3,000 (Bogart et al. 2006; Malin et al. 2012). Thus identification of novel mediators of bladder muscle development and function from studying a rare disorder, such as PBS, may impact treatment and therapies for the more common LUTO.

Disease-causing variations in the human genome can be classified into two categories: structural and sequence-level variations. New technological advances allow for detection of these types of variants across the whole genome; namely array-based assays to detect structural variations and large-scale sequencing approaches to detect sequence-level variations.

II. Copy-number variations and array comparative genomic hybridization

Structural variations are deletions, duplications, insertions, inversions or translocations that affect the structure of a patient's chromosomes. Structural variations that results in an abnormal number of copies of a segment of DNA are classified as Copy Number Variations (CNVs). CNVs are defined as deletions or duplications of genomic segments, ranging in size from 1 kilobase up to multiple megabases (Iafrate et al. 2004). Studies in normal populations have shown that more than 20% of the human genome is subject to CNVs (Iafrate et al. 2004; Sebat et al. 2004). However, the majority of CNVs are less than 100 kb in size, common, and not associated with disease (benign) (Itsara et al. 2009). In contrast, large CNVs (>400 kb in size) are rare and *de novo* large CNVs are often pathogenic and have been identified as major causes of intellectual disability, autism, and multiple congenital anomalies (Sebat et al. 2007; Baldwin et al. 2008; Cook & Scherer 2008). CNVs can contribute to disease by causing imbalances in gene dosage, creating fusion proteins, or disrupting a gene's sequence or regulatory elements. Discovery of CNVs in patients has identified candidate loci or genes for previously unexplained genetic anomalies (Zhang et al. 2009). The association of CNV data with clinical phenotypes can

contribute to a better understanding of disease pathogenesis by revealing genes that are dosage sensitive.

Array-comparative genomic hybridization (aCGH), also known as chromosome microarray analysis or cytogenomic microarray analysis, is a microarray-based genomic test capable of detecting CNVs throughout the genome in a single test. Array-based CNV tests have 100-fold higher resolution compared to conventional karyotyping and an average diagnostic yield of 15-20% compared to 3% diagnostic yield with karyotyping (Miller et al. 2010). Due to higher sensitivity in detection of chromosomal aberrations, aCGH is recommended in place of karyotyping and as a first-tier test in the clinical evaluation of patients with multiple congenital anomalies and/or intellectual disability (Miller et al. 2010).

As CNVs are common, assessment of identified CNVs as pathogenic, benign, or unknown clinical significance is necessary (Table 1.1). A CNV is classified as pathogenic if the imbalance contains or overlaps a known dosage-sensitive gene, if the CNV overlaps in a genomic region with defined clinical significance, or if the CNV occurs in a gene-rich region that includes morbid OMIM genes. A CNV is classified as benign if the imbalance contains no annotated genes or if the CNV fully overlaps known benign CNVs in a large control database, such as Database of Genomic Variants (DGV). A CNV is determined to be of unknown significance if the CNV is not defined by the aforementioned criteria as pathogenic or benign (Lee et al. 2007; Yu et al. 2009). In studying a patient cohort, the significance of identified likely-pathogenic CNVs can be determined based upon the inheritance pattern of the CNV, presence of overlapping/recurrent CNVs in patients with similar phenotypes, and the size and dosage effect (Vulto-van Silfhout et al. 2013).

Primary Criteria	Indicates CNV is Probably	
	Pathogenic	Benign
1. a. CNV inherited from healthy parent or similar to a CNV in healthy relative		X
b. CNV inherited from affected parent or similar to a CNV in affected relative	X	
2. CNV is completely contained within genomic imbalance in a CNV database of healthy individuals (DGV)		X
3. CNV overlaps a genomic imbalance in a CNV database for patients with ID/DD, ASD, or MCA	X	
4. CNV overlaps genomic coordinates for a known genomic-imbalance syndrome	X	
5. CNV contains morbid OMIM genes	X	
6. a. CNV is gene rich	X	
b. CNV is gene poor		X
General Findings		
1. CNV is a deletion (heterozygous or homozygous)	X	
2. a. CNV is a duplication		X
b. CNV is an amplification (greater than 1 copy gain)	X	
3. CNV is devoid of known regulatory elements		X

Table 1.1. Assessment of CNV pathogenicity. The described criteria are general assumptions. Exceptions to each case have been observed. ID/DD, intellectual disability or developmental delay; ASD, autism spectrum disorders; MCA, multiple congenital anomalies; DGV, database genomic variants. Adapted (Miller et al. 2010)

A recent study to identify CNVs via aCGH testing in 5,531 patients with intellectual disability or multiple congenital anomalies identified rare CNVs in 25% of the patients (Vulto-van Silfhout et al. 2013). This finding is consistent with previous reports that congenital anomalies are significantly more frequent in patients with clinically-significant CNVs as compared to patients with normal results (Shoukier et al. 2013). Segregation analysis detected that 41% of the identified CNVs are *de novo* and indicates that the most severe phenotypes are enriched in patients with *de novo* CNVs. The study also contends that copy-number losses are more likely to result in severe phenotypes than copy-number gains and that phenotype severity also correlates with CNV size (Zhang et al. 2009; Vulto-van Silfhout et al. 2013).

The implementation of aCGH testing has also discovered new genes implicated in disorders of sex development, congenital heart malformation, and mental retardation (Froyen et al. 2008; Zhang et al. 2009; White et al. 2012). Prior to 2004, CHARGE syndrome was described as a nonrandom pattern of congenital anomalies without genetic cause. In 2004, aCGH testing identified overlapping deletion CNVs of the gene *CHD7* in two patients (Vissers et al. 2004). After discovery by aCGH, targeted sequencing of *CHD7* identified causal mutations in ten additional CHARGE syndrome patients. A review of 379 CHARGE syndrome patients found that *CHD7* mutations now account for 67% of all cases (Zentner et al. 2010). This example proves the power of CNV testing in identifying the genetic basis of unexplained MCA disorders.

III. Sequence-level variations and whole exome sequencing

The second class of disease-causing variations is sequence-level variants. Sequence-level variants are changes affecting one or more nucleotides, such as single nucleotide variants (SNVs) or small insertions and deletions (indels). To understand the impact of sequence variants on human diseases, these variants are categorized based on the predicted impact of the variation of the translated protein. SNVs can result in synonymous mutations (amino acid sequence is not modified) or non-synonymous mutations (amino acid sequence is modified). Non-synonymous mutations can be further classified as missense mutations, in which the mutation results in a codon that codes for a different amino acid, or nonsense mutations, in which the mutation results in a premature stop codon. Nonsense mutations may result in a truncated protein, or more often, mRNAs containing the nonsense mutation are degraded by nonsense-mediated mRNA decay.

For genetic phenotypes in which a molecular cause is known, sequencing can readily identify potentially-causal mutations in candidate genes. For genetic phenotypes with no known molecular cause, discovery of possibly-pathogenic variants by individually sequencing likely-candidate genes is slow to return useful genetic information (Ono & Harley 2013). A more economical and time-effective approach to gene discovery is through next-generation sequencing (NGS). Both whole genome sequencing (WGS) and whole exome sequencing (WES) are powerful tools for disease gene identification as rapid NGS of the entire genome or exome of a patient removes the necessity of prioritizing candidate genes for sequencing.

WES focuses on the ~1% of the genome that is protein coding (exome) as 85% of disease-causing mutations are estimated to occur in the exome (Rabbani et al. 2014). The initial proof-of-concept for WES in gene discovery research was documented in 2009 by identification of the gene responsible for Freeman-Sheldon syndrome by sequencing the exomes of only four unrelated patients (Ng et al. 2009). Since 2009, the roles of over 150 genes have been discovered or distinguished by WES (Boycott et al. 2013; Rabbani et al. 2014).

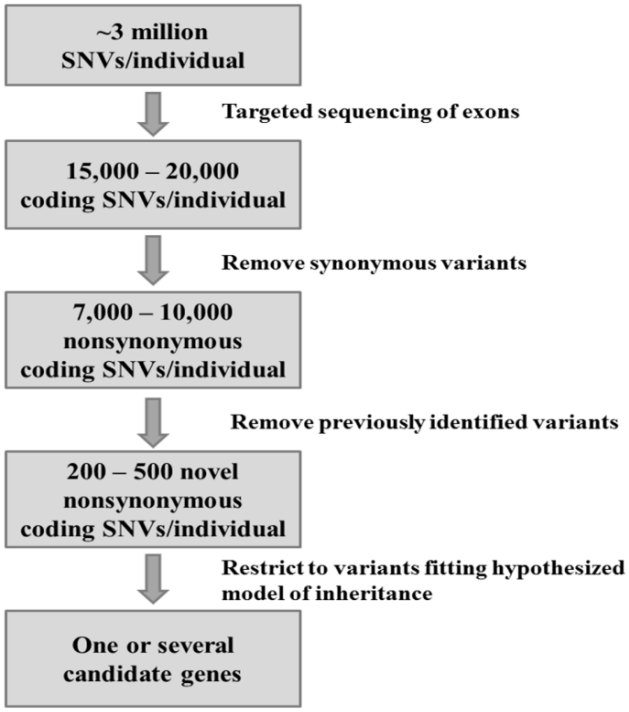

Figure 1.1. Filtering approach for exome sequencing projects aimed at novel gene discovery for Mendelian disorders. SNVs, single nucleotide variants.
Adapted from Stitziel et al. (2011)

As the goal of WES is to identify a disease-causing variant, numerous filters are applied to reduce the estimated 25,000 variants in an individual's exome to a few potential disease-causing variants (Gilissen et al. 2012). A generalized approach for filtering exome sequencing results aimed at novel gene discovery is seen in Figure 1.1. WES results are first compared to a reference genome which on average identifies ~20,000 exonic SNVs. Next, synonymous variants are excluded. As rare variants are more likely disease causing, variants are then compared to control data sets to facilitate exclusion of variants that are present at frequencies higher than the expected carrier frequency. With over 6500 exomes, the National Heart, Lung, and Blood Institute Exome Sequencing Project (NHLBI ESP) database is the largest curated and publicly available data set. On average, filtering for novel variants or rare variants with <1% population frequency will narrow the results to 500 or 200 variants per exome, respectively (Boycott et al. 2013). This filtering model assumes that the disease-causing variant is coding, alters protein sequence, and is completely penetrant; criteria that are not consistent across all disease-causing variants.

Next, additional strategies are needed to identify the causative mutation among the 200–500 novel or rare variants. Each strategy depends on the hypothesized model of inheritance (outlined in Figure 1.2). WES is often utilized in familial cases as familial recurrence of a defined phenotype strongly suggests that a disease is monogenic (Boycott et al. 2013). A linkage based strategy for familial cases (Figure 1.2.A) involves sequencing multiple affected family members to identify shared variants. In addition, by sequencing non-affected family members, familial benign variants can be excluded (assuming variant is fully penetrant). An identical variant identified in affected family members is highly suggestive that the implicated gene is causal in disorder pathogenesis.

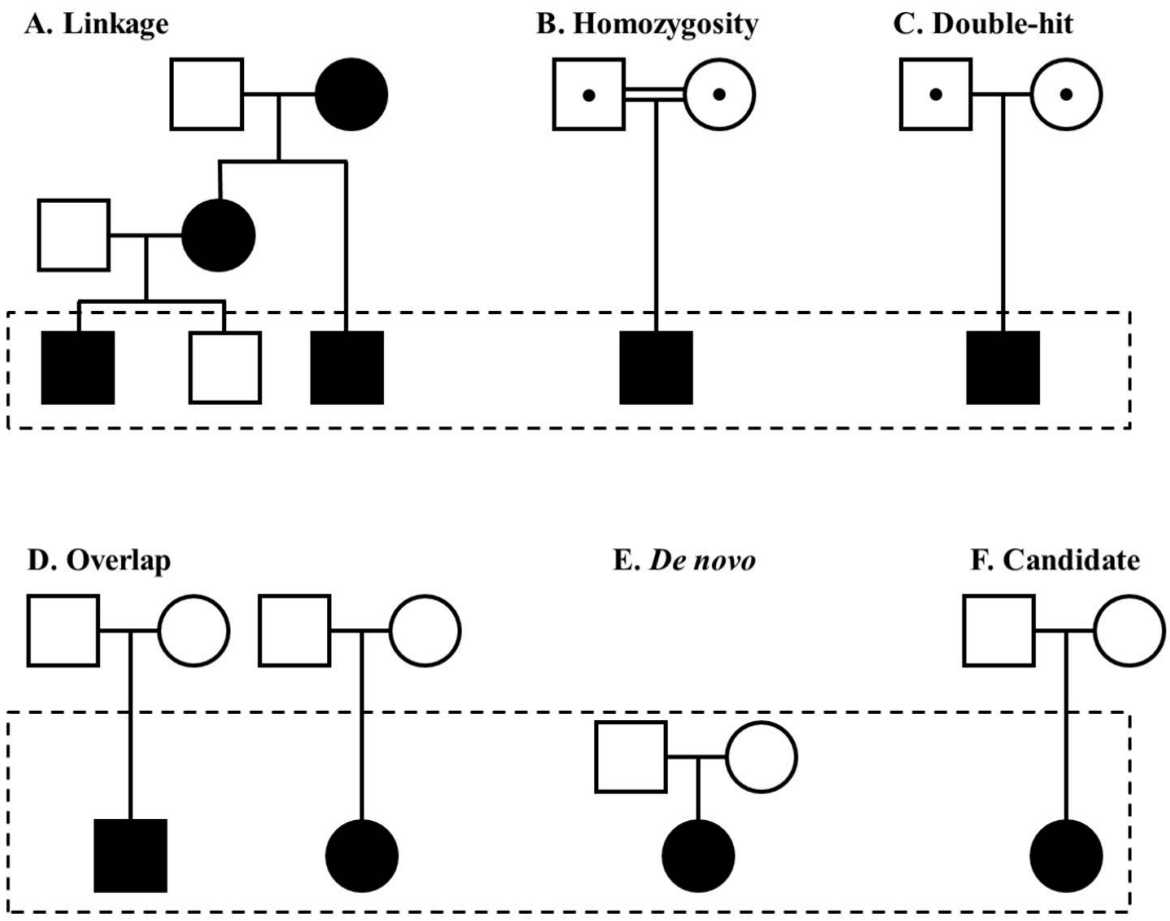

Figure 1.2. Disease gene identification strategies for exome sequencing.
Pedigrees indicate the inheritance model underlying each strategy. Squares represent male family members, circles represent female family members. Filled symbols represent affected individuals; empty symbols represent presumably healthy individuals; carriers are depicted by a symbol with a dot. Dashed rectangles encompass individuals for exome sequencing. Adapted from Gilissen et al. (2012)

In the event of a recessively inherited disorder and suspected consanguinity, a homozygosity based strategy (Figure 1.2.B) prioritizes homozygous variants present in homozygous regions of the patient's genome. In the event of a recessively inherited disorder with no consanguinity, a double-hit based strategy (Figure 1.2.C) selects for genes carrying non-synonymous homozygous and compound heterozygous variants.

As rare diseases are often sporadic, the inheritance of a disease-causing variant is unknown and affected relatives are unavailable for familial strategies. These limitations can be circumvented by an overlap based strategy (Figure 1.2.D) which sequences exomes of unrelated patients and selects for variants in a single gene present in multiple patients. On average, WES a single patient will identify novel variants in 333 genes. The addition of a second and third patient will reduce the candidate gene list from 333 genes to 33 and 8 genes, respectively (Paria et al. 2013). This approach of comparing implicated genes discovered by WES in unrelated patients has identified novel genes for Floating-Harbor syndrome, Kabuki syndrome, and Miller syndrome (Ng et al. 2010a; Ng et al. 2010b; Hood et al. 2012).

The overlap approach described above assumes that a rare disorder is monogenic as identifying unrelated patients with mutations in the same gene in genetically heterogeneous disorders is rare (Gilissen et al. 2012). However, a fraction of rare disorders that occur sporadically are thought to be caused by *de novo* mutations. As the average exome contains only 0-3 *de novo* variants, these potentially pathogenic variants can be identified by a *de novo* based strategy (Figure 1.2.E) of sequencing the exomes of a patient and the patient's parents and filtering our all inherited variants (Abecasis et al. 2010).

For many rare disorders, only a single patient is presented, limiting strategy options as family members or other affected individuals are not available. Using a candidate based strategy (Figure 1.2.F), exome data can be prioritized based on variant type (nonsense versus non-synonymous), predicted impact of the variant on protein function and structure, and conservation of the implicated nucleotide and/or amino acid. Additionally, information regarding gene function and expression in relation to the patient's phenotype may further narrow the candidate gene list. In total, application of these different strategies (Figure 1.2) for disease variant prioritization has resulted in causal variant discovery in 60-80% of studied Mendelian disorders.

IV. Congenital genitourinary disorders

Major congenital malformations are structural defects of the body or organs that impair viability and require intervention. The annual incidence of such anomalies is 6% of births worldwide and 3% of births in the US with a majority of the underlying causes unknown (Christianson et al. 2006). Congenital genitourinary disorders are the third most common congenital anomaly (1 in 135 births), behind congenital cardiovascular defects (1 in 115 births) and musculoskeletal defects (1 in 130 births) (estimated incidences by March of Dimes Perinatal Data Center, 2004). Congenital anomalies of the genitourinary system can be categorized as "internal" (pertaining to the urinary system) or "external" (pertaining to genital system). The urinary and genital systems are often grouped together as both systems develop from intermediate mesoderm and endoderm and thus share common developmental pathways. Due to their proximity and shared origin, many congenital

genitourinary disorders, such as epispadias, hypospadias, bladder exstrophy, and cloacal exstrophy, affect both the urinary and genital systems.

The primary function of the urinary tract, consisting of the kidneys, ureters, bladder, and urethra, is to produce, transport, store, and eliminate urine. Congenital anomalies of the urinary tract are both common and severe as they account for 23% of birth defects and nearly 50% of pediatric cases of end-stage renal disease (Sanna-Cherchi et al. 2009; Loane et al. 2011). More than 500 congenital disorders have been described involving renal and urinary anomalies, including prune belly syndrome, posterior urethral valves, bladder exstrophy, and polycystic kidney disease (Weber 2012). Sporadic cases are the most common manifestation of these conditions; however, a positive family history for the anomaly is observed in 10% of index patients, suggesting that many anomalies of the urinary tract are genetic in origin (Weber 2012).

The primary function of the genital system is reproduction. In males and females this system consists of the gonads, internal genitalia (duct system), and external genitalia. Congenital anomalies of the genitalia include ambiguous genitalia, cryptorchidism, hypospadias, persistent cloaca, and Müllerian agenesis, to name a few. Prevalence and severity of these anomalies range from cryptorchidism in 1:50 full-term males, hypospadias in 1:125 male births, ambiguous genitalia in 1:3000 births, Müllerian agenesis in 1:4500 births, to persistent cloaca in 1:50,000 births (Folch et al. 2000; Hughes et al. 2006; Pohl et al. 2007; Virtanen et al. 2007). Although common, a vast majority of congenital genital anomalies have no known genetic cause. For disorders of sex development (DSD), a molecular diagnosis can impact gender assignment, genital surgery,

counseling, and lifelong care. However, a molecular diagnosis is made in only 20-50% of 46,XY DSD patients (White et al. 2011; Ono & Harley 2013).

V. Genetic tools to study congenital genitourinary disorders

The availability and efficiency of both aCGH and WES have provided new insights into molecular pathways regulating genitourinary development and provided molecular diagnoses for many patients.

A common mechanism for DSD is altered gene dosage, where impaired or abnormal gonadal development is caused by gene haploinsufficiency due to copy-number losses or by gene over-expression due to copy-number gains. Thus, aCGH is a powerful tool to identify CNVs on a genome-wide scale that can cause DSD. The implementation of aCGH has allowed the identification and diagnosis of cryptic or small CNVs that were undetectable by traditional cytogenetic tools, such as karyotyping and fluorescence *in situ* hybridization (FISH). aCGH testing in three studies totaling 165 patients with varying DSD phenotypes identified known or potentially causative CNVs in approximately a third of all patients (Ledig et al. 2010; Tannour-Louet et al. 2010; White et al. 2011). Most anomalies (74% in one study) evaded detection by karyotype, thus stressing the importance of aCGH testing in DSD patients to identify causative CNVs.

While much emphasis has been placed on studying the genetic causes of renal anomalies, the genetic basis for congenital anomalies of the urinary tract is very limited (Rasouly & Lu 2013). The genetic cause of most familial and sporadic cases is unknown as mutations in genes associated with disorders of the urinary tract are detected in only 5-10% of cases (Weber et al. 2006; Thomas et al. 2011). Due to genetic heterogeneity and

infrequent and small pedigrees, urinary tract anomalies are not suited for traditional gene discovery approaches, such as linkage mapping; however, WES overcomes many of these limiting hurdles.

In a recent publication, WES of a single pedigree with congenital abnormalities of the urinary tract discovered a segregating variant in dual serine-threonine and tyrosine protein kinase (*DSTYK*) (Sanna-Cherchi et al. 2013). Subsequent screening of unrelated patients with congenital abnormalities of the urinary tract identified independent, novel *DSTYK* mutations in 7 of 311 patients (2.3%). This finding shows the effectiveness of exome sequencing to elucidate genetic defects even in small pedigrees and in cases of phenotypic and genetic heterogeneity. The fact that *DSTYK* was identified from familial exome sequencing and that *DSTYK* variants were then identified in unrelated patients reiterates the ability of exome sequencing to identify novel disease-causing genes that can account for disease pathogenesis beyond the index case.

Given the success and availability of both aCGH and WES, this research focuses on applying these genomic approaches to identify genetic causes of genitourinary disorders.

CHAPTER 2: THE GENETIC BASIS OF PRUNE BELLY SYNDROME

Summary

Prune belly syndrome (PBS) is a rare multiple congenital anomaly complex of unknown genetic cause. Assuming the cause is genetic, assessment of the basis of this rare syndrome was completed by the following approaches:

1. Identify causal variants of PBS in familial cases (Chapter 2 Part A)
2. Characterize the functional impact of discovered variants (Chapter 2 Part B)
3. Identify affected genes between sporadic PBS patients (Chapter 2 Part C)

CHAPTER 2 PART A: IDENTIFICATION OF CAUSAL VARIANTS IN FAMILIAL CASES OF PBS

Introduction

I. Incidence, Mortality, and Morbidity

Prune belly syndrome (PBS; OMIM #100100) is a multiple congenital anomaly (MCA) complex characterized by three cardinal features: 1. partial or complete lack of abdominal wall musculature resulting in a wrinkled, prune-like appearance (Figure 2.1); 2. dilation of the urinary tract, and 3. bilateral undescended testicles (cryptorchidism). The incidence of PBS is 1:35,000 to 1:50,000 live births and over 95% of patients are male (Bogart et al. 2006). An estimated 1,494 males under the age of 18 are currently living with PBS in the USA (Becknell et al. 2011). For the neonate, PBS is an extremely morbid condition, as 30% die during their initial hospitalization, 43% are born premature, and 48% require respiratory intubation and mechanical ventilation (Routh et al. 2010). Of the PBS patients that survive the neonatal period, 30% develop chronic renal insufficiency or end stage renal disease requiring dialysis or transplantation (Bogart et al. 2006). The mortality rate in PBS was estimated at 60% in 1995 with data suggesting no recent improvement despite advances in neonatal healthcare (Druschel 1995; Routh et al. 2010).

Figure 2.1. Presentation of prune belly syndrome. Patients show wrinkled "prune-like" abdomen characterized by absent or lack of abdominal wall musculature.

II. Clinical presentation of PBS

A normally developed bladder is a muscular, spherical, hollow organ that receives and stores urine from the kidneys and ureters during relaxation and contracts to expel urine during voiding. The muscular layer of the bladder is the muscularis propria, also known as the detrusor. The detrusor is a woven network of smooth muscle cells that dictate relaxation versus contraction phases. The smooth muscle cells of the detrusor are bundled into fasicles of varying size and orientation, surrounded by connective tissue carrying nerves and vessels (Figure 2.2). In PBS patients, the bladder has increased capacity (2-4X the size of a normal bladder) and poor contractility, with a diminished sensation of fullness (Kinahan et al. 1992). Histologically, PBS bladders are characterized by thickened walls (due to enlargement of the muscularis propria layer), and disorganized detrusor bundling with nearly absent fibrous strands of connective tissue (Wheatley et al. 1996).

Pathological assessment of bladders from PBS patients at the University of Texas Southwestern Medical Center is consistent with published findings (Figure 2.2). PBS bladders show dense, uniform bands of smooth muscle with no identifiable intervening connective tissue. The smooth muscle fibers are arranged haphazardly with no clear larger bundling as seen in healthy, control bladders.

In PBS patients, the ureters are often elongated, dilated, and tortuous, with the distal end more affected than the proximal portion (Sutherland et al. 1995). Histologically, the ureters show a deficiency in the number of smooth muscle cells and an increase in the ratio of collagen to smooth muscle in the ureteral muscle layer (Moerman et al. 1984; Gearhart et al. 1995).

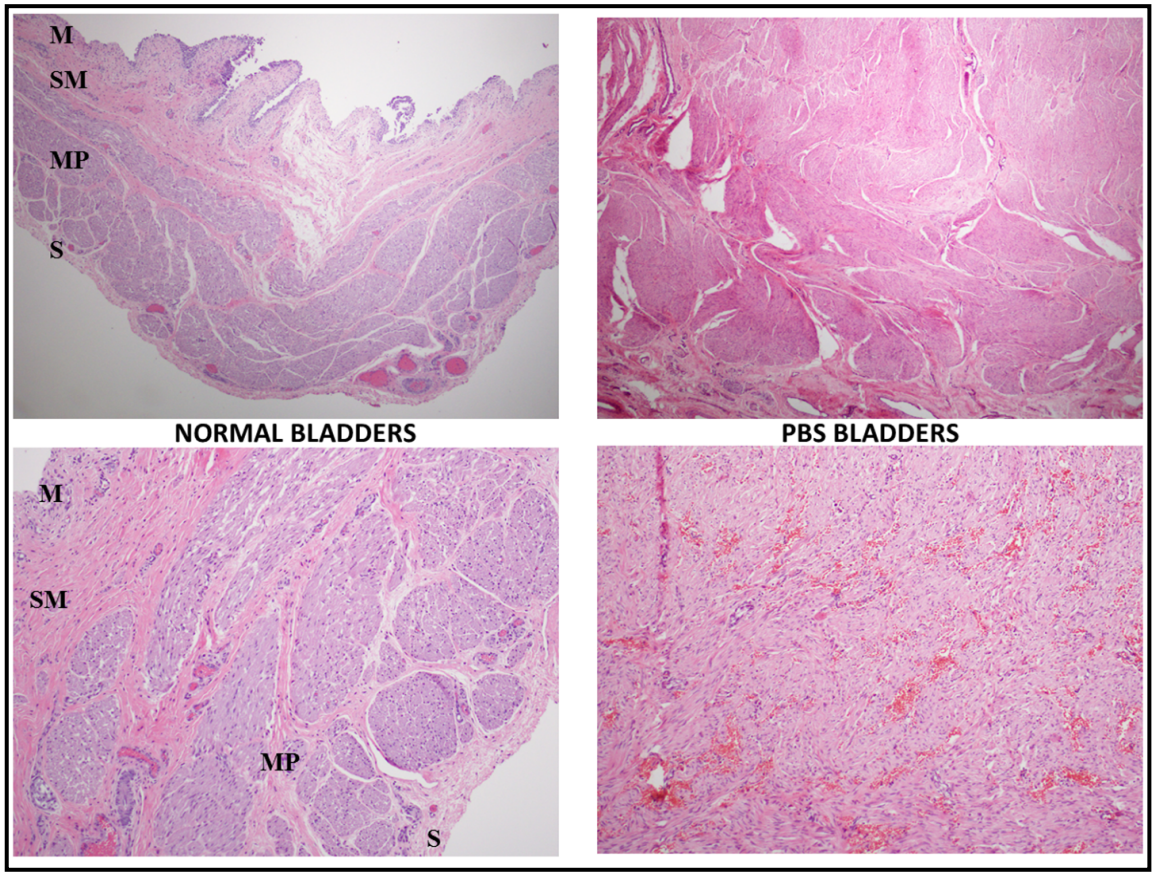

Figure 2.2 Comparison of human control versus PBS bladders. Human bladder is composed of the luminal mucosa/urothelium (M), submucosa (SM), muscularis propria (MP), and serosa/adventitia (S). Smooth muscle fibers are purple; connective tissue is pink. In normal bladder, the detrusor (MP layer) consists of variably sized and oriented smooth muscle bundles, with obvious connective tissue bands between. PBS bladders show haphazard arrangement of smooth muscle fibers with no clear larger "bundling" and no identifiable intervening connective tissue. In PBS bladders, the MP layer is grossly enlarged preventing a cross-sectional view of the full bladder wall.

Due to these defects, bladder and ureteral function are impaired and improper outflow of urine severely affects the urinary tract resulting in renal damage, ranging from hydronephrosis to bilateral renal dysplasia (Reinberg et al. 1991). As fetal urine is a major component of amniotic fluid and required for lung development, oligohydramnios (deficiency of amniotic fluid) is present in 65% of prenatally-diagnosed PBS patients, half of whom develop pulmonary hypoplasia (Shimizu et al. 1992). As such, prognosis for PBS patients depends primarily on the severity of damage to the urinary and respiratory tracts as 30% of PBS patients develop urosepsis or renal failure in the first two years of life (Sutherland et al. 1995).

The characteristic external manifestation of PBS is the wrinkled, "prune-like" skin of the abdomen. Skeletal muscle hypoplasia is seen in all three layers of the abdominal wall musculature: transversus abdominis, internal oblique, and external oblique (Mininberg et al. 1973). The upper rectus and lateral parts of the oblique muscles are typically spared. Characteristically, hypoplasia to complete absence is most evident in the infraumbilical rectus abdominis and in the right upper abdominal quadrant over the liver. Thus, the overall skeletal muscle deficiency is often asymmetric. The degree of abdominal wall wrinkling and flaccidity is variable, but in many PBS cases the muscular flaccidity may inhibit the child's ability to sit up and delay the onset of walking (Sutherland et al. 1995). The paucity of abdominal muscles contributes to chronic constipation and life-threatening respiratory infections (as these muscles are needed to strain with defecation and couching) (Holder 1989). Histological studies of the abdominal wall from PBS patients reveals normal nerve distribution and blood supply but either haphazard arrangement or absent muscle fibers (Mininberg et al. 1973).

However, the skeletal muscle hypoplasia of PBS is confined to the abdominal wall muscles. Skeletal muscles of the head, arms, and legs are unaffected, leading to no other hindrances to normal activity in these body parts. However, extra-genitourinary abnormalities are also common, as skeletal, cardiac, and gastrointestinal anomalies present in up to 45%, 25% and 30% of patients, respectively (Bogart et al. 2006; Routh et al. 2010).

III. Theories of PBS pathogenesis

There are two hypothesized theories of PBS pathogenesis: fetal bladder outlet obstruction and mesodermal arrest. The fetal bladder outlet obstruction theory suggests that bladder or urethral obstruction results in bladder distention and urethral dilation. Dilation of the bladder results in blockage of testicular descent and muscular atrophy of the abdominal wall, as the muscles directly over the bladder are the most affected. Based on the PBS phenotype and developmental timeline of the fetus, this hypothesized obstruction would occur between 13–15 weeks gestation (Wheatley et al. 1996). However, in PBS patients, a urethral obstruction is only identified in approximately 10-20% of cases, suggesting that the obstruction is either transient or only present in some cases of PBS (Wheatley et al. 1996).

The mesodermal arrest theory suggests the PBS phenotype is secondary to an unspecified defect in lateral plate mesoderm development between 6 – 10 weeks gestation (Stephens & Gupta 1994). During normal development, the mesoderm-derived lateral plate divides into a visceral and somatic layer. The somatic layer of the lateral plate mesoderm forms the abdominal wall musculature while the visceral layer gives rise to the smooth

muscles of the urinary and gastrointestinal tracts (Wheatley et al. 1996). Thus, an abnormality in the mesoderm could explain both the abdominal wall and urinary tract phenotypes of PBS.

IV. Candidate genes for PBS

Despite these mechanistic theories, the molecular basis of PBS is unknown. Several genes have been implicated in PBS pathogenesis due to rare mutations in isolated or familial reports however none are thought to be common causes of PBS (Table 2.1).

Gene OMIM	Locus/ Exons	Null mouse bladder phenotype	Human phenotypes associated with gene mutations	Variants/cases screened		
				Reported mutation	PBS cases	Non-PBS Phenotypes
HNF1β 189907	17q12; 9 exons	Embryonic lethal	Renal cysts and diabetes syndrome; Diabetes Mellitus; Renal Cell Carcinoma; Mullerian Duct Anomalies	CNV	2/2	90/173
				Sequence variations	0/32	97/452
CHRM3 118494	1q43; 5 exons	Distended bladder (males only)	Unilateral kidney dysfunction; Impaired pupillary constriction and impaired salivation	P392A*fs**43	2/21*	3/131*
				Other Mutations	0/21	0/131
ACTA2 102620	10q23.31; 9 exons	Normal bladder	Aortic aneurysm familial thoracic type 6; Multisystemic smooth muscle dysfunction syndrome	R179H	1/1	5/129
				Other Mutations	None Tested	17/129

Table 2.1. Candidate human PBS genes.
*The two PBS and the three non-PBS individuals with this CHRM3 mutation are all within the same kindred. (Barbacci et al. 1999; Matsui et al. 2000; Zimmerman et al. 2004; Edghill EL et al. 2006; Edghill et al. 2008; Murray et al. 2008; Guo et al. 2009; Chen et al. 2010; Haeri et al. 2010; Milewicz et al. 2010; Oram RA et al. 2010; Weber et al. 2011; Richer et al. 2012; Edghill et al. 2013)

IV.1. Hepatocyte nuclear factor 1β

Hepatocyte nuclear factor 1β (*HNF1β*) is a member of the homeodomain-containing superfamily of transcription factors that regulate expression of genes necessary for mesodermal and endodermal development. HNF1β is expressed in numerous tissues including kidney, prostate, mesonephric duct derivatives, pancreas, gut and liver, with a high level of expression specifically in the renal collecting duct branches during development (Coffinier et al. 1999; Kolatsi-Joannou et al. 2001). More than 40 different heterozygous mutations in *HNF1β* have been described, with the renal cysts and diabetes syndrome (#137920 also known as Maturity Onset Diabetes of the Young [MODY], type 5) representing the most common *HNF1β* phenotype (Edghill EL et al. 2006; Chen et al. 2010).

HNF1β is implicated in PBS due to two reports of male PBS patients with whole gene deletions of *HNF1β*. The first report of a PBS male with a heterozygous *HNF1β* deletion presented with the classic PBS phenotype as well as additional non-PBS features including early onset gout, type 2 diabetes, and pancreatic atrophy (Murray et al. 2008). Due to the patient's urinary tract abnormalities, he was screened for *HNF1β* CNV, identifying a *de novo* heterozygous 3.2 megabase (Mb) deletion encompassing all 9 exons of *HNF1β*. The second case presented at birth with the classic PBS phenotype, but only lived a few hours (Haeri et al. 2010). Microarray analysis detected a *de novo* heterozygous 1.3Mb deletion on 17q12 affecting 14 genes, including *HNF1β*. However, more than 90 non-PBS patients with renal disorders have also been reported with heterozygous deletions of *HNF1β*, suggesting *HNF1β* CNVs are not necessarily causal in PBS pathogenesis (Table 2.1) (Mefford et al. 2007; Aggarwal et al. 2010).

IV.2. Muscarinic acetylcholine receptor M3

A familial case of PBS was reported in which 6 brothers with congenital bladder outflow obstruction were born to consanguineous Turkish parents (Weber et al. 2011). Two of the affected brothers presented with abdominal wall distension and were diagnosed with PBS while the four other brothers were diagnosed with posterior urethral values (PUV) due the presence of urethral valve-like structures. All 6 affected brothers also presented with bilaterally impaired pupillary constriction to light and xerostomia (dry mouth); neither of which are commonly associated with PBS. Genetic analysis of this consanguineous family identified a novel homozygous loss-of-function mutation in muscarinic acetylcholine receptor M3 (*CHRM3*), resulting in a premature termination codon co-segregating with the disease (Weber et al. 2011). CHRM3 is a major detrusor smooth muscle cell receptor mediating urinary bladder contraction and is necessary for pupillary constrictors and salivary gland acini (Fowler et al. 2008). The phenotype of homozygous *Chrm3*-null mice is similar to this familial report in that mutant mice have dilated ocular pupils and only male null mice have severely distended urinary bladders resulting from impaired contractility of the detrusor smooth muscle (Matsui et al. 2000). However, *CHRM3* mutations were not identified in larger cohorts of patients with PUV and classic PBS (Table 2.1) (Weber et al. 2011).

IV.3. Alpha-smooth muscle actin

A male infant presented at birth with the classic PBS phenotype as well as abnormal pulmonary and aortic vessels, deep skin dimples, deep creases on his palms and soles, and dilated pupils unreactive to light (Richer et al. 2012). Due to pulmonary

phenotypic overlap with patients harboring mutations in α-smooth muscle actin (*ACTA2*), sequencing identified a heterozygous missense R179H variant in *ACTA2*. ACTA2 is primarily expressed in smooth muscle and is a major detrusor cytoskeletal protein. Missense mutations in ACTA2 account for 14% of familial thoracic aneurysms and have been shown to cause multisystemic smooth muscle dysfunction, early onset strokes, and coronary artery disease (Guo et al. 2007; Guo et al. 2009). Additionally, the ACTA2 R179H missense variant identified in this PBS patient has previously been reported in non-PBS patients with aortic and cerebrovascular disease and pulmonary hypertension, suggesting this ACTA2 mutation is not necessarily causal in PBS (Milewicz et al. 2010).

V. Familial reports of PBS

Initially, a genetic component to PBS was discounted due to 100% discordance in monozygotic twins (Ives 1974). However, review of the literature indicates PBS is four times more frequent in monozygotic twins than singletons, supporting a genetic component to this syndrome (Balaji et al. 2000). Multiple reports of pedigrees with a positive family history of PBS also suggest a genetic cause of PBS. A review of possible modes of inheritance in 13 familial PBS cases (Table 2.2) suggests that PBS is an X-linked recessive or sex-influenced autosomal recessive disorder (Ramasamy et al. 2005). These possible modes of inheritance correlate with the higher incidence in males (95%) as both inheritance models limit the disease state to males.

Table 2.2. Reported cases of familial prune belly syndrome

Reference	PBS Cases	Hypothesized Mode of Inheritance
Grenet P et al. (1972)	2 Brothers	Autosomal/X-linked recessive
Harley LM et al. (1972)	2 Brothers	Autosomal/X-linked recessive
Afifi AK et al. (1972)	2 Brothers	Autosomal/X-linked recessive
Garlinger P and Ott J (1974)	2 Brothers	Autosomal/X-linked recessive
Riccardi VM and Grum CM (1977)	2 Brothers	Autosomal/X-linked recessive
Ramasamy et al. (2005)	2 Brothers	Autosomal/X-linked recessive
Weber et al. (2011)	2 Brothers	Autosomal/X-linked recessive
Ibadin et al. (2012)	2 Brothers	Autosomal/X-linked recessive
Lockhart JL et al. (1979)	2 Brothers and 1 sister	Autosomal recessive
Gaboardi F et al. (1982)	2 Brothers and 1 sister	Autosomal recessive
Adeyokunnu AA and Familusi JB (1982)	1 Brother, 1 sister, 1 cousin	Autosomal recessive
Feige A (1984)	1 Brother and 1 sister	Autosomal recessive
Balaji et al. (2000)	2 Monozygotic male twins	Autosomal recessive
Chan Y and Bird LM (2004)	2 Brothers, mother, maternal grandmother	Autosomal dominant

VI. Research approach

A comprehensive analysis of the molecular cause of PBS has not previously been accomplished due to rarity and infrequent multiplex families. To delineate a genetic basis of PBS, the approach was to first study the previously identified candidate genes (*HNF1β*, *CHRM3*, *ACTA2*) in a cohort of PBS patients. Screening these candidate genes in our PBS patient cohort represents the largest genetic screen of PBS patients.

As the identified candidate genes were not expected to be common causes of PBS, the next approach was to utilize whole-genome approaches to identify causal variants of

PBS in sporadic and multiplex patients. To detect structural variations, sporadic PBS patients were tested by aCGH to determine if PBS patients harbor CNVs in genes of interest or overlapping CNVs with other PBS patients.

Next, multiplex PBS families were studied to identify sequence variations as familial cases are most supportive of PBS being a Mendelian disorder. As hypothesized modes of inheritance favor an X-linked model, PBS-affected brothers were first genotyped by microsatellite analysis to identify candidate PBS X-linked regions. Next, WES of two maternally-shared half-brothers with PBS identified an inherited, novel, likely-pathogenic variant.

Materials and Methods

Study population and recruitment

All PBS human subjects were prospectively recruited and informed consent was obtained according to a protocol approved by the Institutional Review Board at the University of Texas Southwestern Medical Center. Patients underwent phenotyping at Children's Medical Center in Dallas and at University of Texas Southwestern Medical Center. Genomic DNA from patients and available family members was extracted from peripheral blood lymphocytes via the Puregene DNA isolation kit (Gentra Systems, Minneapolis, MN) according to the manufacturer's protocols. For deceased patients, DNA was extracted from formalin fixed paraffin embedded (FFPE) tissues using RecoverALL Total Nucleic Acid Isolation kit (Ambion, Austin, TX).

Candidate gene sequencing

HNF1β and *CHRM3* were screened by sequencing coding regions and intron-exon boundaries (www.polymorphicdna.com). Detected mutations were cross-referenced to two large, multiethnic databases: NCBI dbSNP (www.ncbi.nih.gov/projects/SNP/) and 1000 Genomes Project (www.1000genomes.org/).

Multiplex ligation-dependent probe amplification analysis

Patients were screened for potential *HNF1β* CNVs using the SALSA P241-B1 MODY MLPA kit (MRC-Holland, Amsterdam, The Netherlands), per the manufacturer's protocol. This assay includes probes for all 9 exons of *HNF1β*. Amplified products were separated by size on an ABI3100 genetic analyzer (Applied Biosystems, Foster City, California, USA) and the data was analyzed using GeneMarker V2.2.0 (SoftGenetics, State College, Pennsylvania, USA). DNA from a PBS patient with a known whole-gene deletion of *HNF1β* (Murray et al. 2008) (gifted by K. Colclough) was included as a deletion control.

Chromosome X microsatellite genotyping

Chromosome X microsatellite genotyping on patient and maternal samples was performed using ABI Linkage V2.5 microsatellite markers (listed in Figure 2.6). Microsatellite markers were amplified by single or multiplex PCR and products from each sample were pooled and combined with the size standard GeneScan 500-LIZ (Applied Biosystem). The resulting products were separated on an ABI Prism 3100 Genetic Analyzer and analyzed by GeneMapper V3.7 (Applied Biosystem). For DNA extracted

from FFPE tissues, microsatellites were amplified using fluorescently-labeled primers specific for each marker and then separated on a 5% agarose gel to exclude smaller fragments resulting from insufficient amplification from degraded DNA. The larger amplified alleles were then analyzed on an ABI Prism 3100 Genetic Analyzer. The resulting microsatellite length was confirmed by comparison of each sample to the respective maternal microsatellite length and by Sanger sequencing.

Chromosome X inactivation

Ratios of X-chromosome inactivation was measured in mothers of multiplex PBS pedigrees using the androgen receptor (AR) methylation assay using methylation-sensitive restriction enzyme HpaII (Allen et al. 1992). 500 ng DNA aliquots were either digested with 10U HpaII or mock-digested in buffer containing no enzyme. Samples were digested at 37° C for 2 hours, followed by incubation at 65° C for 30 min to inactivate the enzyme. 100 ng were used as a template for PCR amplification of the AR $(CAG)_n$ repeat region using forward primer 5'-GCTGTGAAGGTTGCTGTTCCTCAT (labeled at the 5' end with 6-carboxyfluorescein) and reverse primer 5'-TCCAGAATCTGTTCCAGAGCGTGC. The forward primer was labeled at the. Products were separated on an ABI Prism 3100 Genetic Analyzer and total peak areas for both alleles in digested and undigested samples were calculated by GeneMapper V3.7.

To calculate allele inactivation, the following variables were used: signal allele 1 digested (A), signal allele 2 digested (B), signal allele 1 undigested (C), and signal allele 2 undigested (D). Signals C and D from mock-digested samples are needed to correct for unequal amplification of alleles. Inactivation of allele 1 = (A/C)/(A/C + B/D) (equation I)

and inactivation of allele 2 = (B/D)/(A/C + B/D) (equation II). A value of 0.0 equals no inactivation, 1.0 equals complete inactivation, and 0.5 is random inactivation. Inactivation values of alleles 1 and 2 always sum to 1.0 (Zitzmann et al. 2004).

Array-comparative genomic hybridization (aCGH)

Custom-designed exon-targeted aCGH was performed by the Medical Genetics Laboratories at Baylor College of Medicine using version V8.1 (180,000 oligonucleotides) and manufactured by Agilent Technologies (Santa Clara, CA). Digestion, labeling, and hybridization were completed following the manufacturer's protocols. Interpretation of the aCGH was performed by Baylor College of Medicine staff using their web-based software for genomic copy-number analysis. Confirmatory and parental FISH analyses were performed using standard procedures by Medical Genetics Laboratories at Baylor College of Medicine.

Whole exome sequencing

Exome sequencing was prepared and performed at the UT Southwestern Medical Center McDermott Center Next Generation Sequencing Core using the following protocol. Libraries from peripheral blood lymphocyte genomic DNA were prepared using the Illumina Truseq DNA Sample prep kit (San Diego, CA) and exomes were captured using the Illumina TruSeq Exome Enrichment Kit, according to the manufacturer's instructions. Enriched libraries were sequenced using Illumina HiSeq2000 sequencer, according to the manufacturer's instructions for 100-bp paired-end sequencing. Then, CASAVA (v1.8.2) was used for adapter removal and de-multiplexing; Burrows–Wheeler Aligner mapped

reads to the human genome (hg19, from UCSC) (Li & Durbin 2009); Samtools (v. 0.1.12) (Li et al. 2009) and PICARD (v. 1.41) processed mapped reads, performed sorting, removed duplicates, and added read-group names in preparation for variant calling with Genome Analysis Toolkit (GATK; v. 1.2-64) (McKenna et al. 2010). GATK calculated coverage over baited regions, performed realignment around regions containing insertions and deletions, recalibrated base qualities after this realignment, and called and filtered variants using a model-based approach. After these variant files are obtained, variants were annotated using ANNOVAR with information such as genetic function, functional impact, dbSNP rsID, and frequency.

Results

I. Patient recruitment

For this study, 93 PBS male patients of varied ethnicities (65 of European/American ancestry, 16 of Hispanic ancestry, 10 of African ancestry, and 2 of Asian ancestry) have been recruited at Children's Medical Center in Dallas, University of Texas Southwestern Medical Center, or in conjunction with the Prune Belly Syndrome Network (PBSN). DNA was extracted from peripheral blood lymphocytes from 87 living PBS males. For 6 deceased PBS males, DNA was extracted from FFPE autopsy tissue. Of the 93 recruited PBS males, 9 patients are from 4 multiplex PBS families while the remaining 84 patients have no reported family history of PBS. Additionally, 232 family members have been recruited.

Clinical data is available on 65 living PBS males in this study. In addition to the PBS cardinal features, the frequency of orthopedic (65%), gastrointestinal (63%), cardiopulmonary (49%), and neurologic abnormalities (18%) in this patient population were noted. Developmental delay was also observed in 41% of PBS patients.

II. Recruited multiplex PBS families

From the recruited PBS cases, 4 non-consanguineous multiplex kindreds have been identified (Figure 2.3). In each pedigree, black shading represents an individual diagnosed with PBS and grey shading denotes probable but unconfirmed PBS diagnosis. In family D019 (Figure 2.3.A), the mother D019M (gravida 4, para 2, spontaneous abortus 2 [$G_4P_2A_2$]), has two living sons with PBS (D019P1 and D019P2), each from a different father, as well as had one miscarriage with each father. In addition to the maternally-shared PBS half-brothers, there is familial report of PBS-affected individuals in generation II. However, these findings are not confirmed by medical records and thus are shaded grey. This pedigree is further discussed and phenotyped in Figures 2.18 and Table 2.4.

In family D040 (Figure 2.3.B), the mother D040M ($G_2P_2A_0$) has given birth to two sons, both diagnosed *in utero* with PBS and both with the same father (D040F). The first son, D040P1, was delivered at 26 weeks gestation and passed away three weeks after birth. The second son, D040P2, was delivered stillborn at 30 weeks after second attempted vesicoamniotic shunting. As both PBS sons are deceased, DNA was obtained from FFPE autopsy tissue from both individuals.

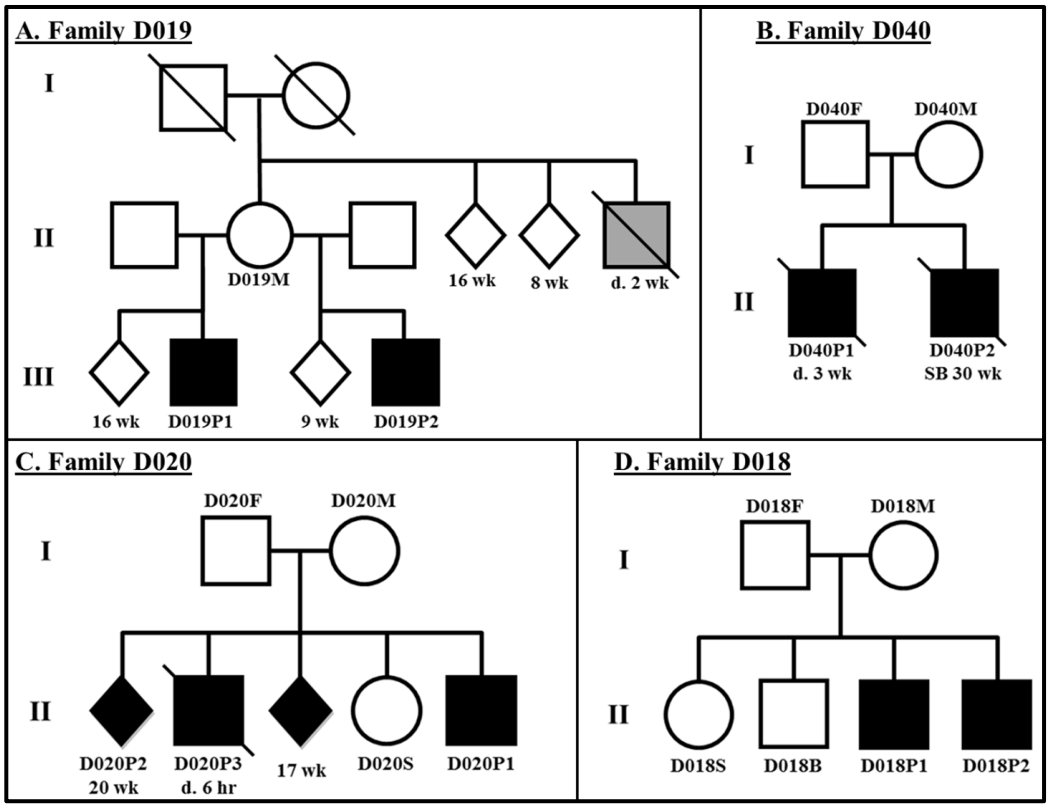

Figure 2.3. Recruited multiplex PBS pedigrees. In the pedigree, squares represent male family members, circles represent female family members, diamonds represent a miscarried or aborted pregnancy (with duration of pregnancy), and diagonal lines indicate a deceased individual (with duration of life). Black shading denotes PBS diagnoses and grey shading denotes probable but unconfirmed PBS diagnoses. SB, still-birth; d, died.

In family D020 (Figure 2.3.C), the mother D020M ($G_5P_3A_2$) has been pregnant five times, all with same father (D020F). The first pregnancy (D020P2) was diagnosed *in utero* with PBS at 20 weeks and terminated. A second pregnancy (D020P3) was diagnosed *in utero* with PBS at 17 weeks, delivered at 29 weeks, and lived 6 hours. Autopsies were performed on D020P2 and D020P3 and FFPE tissue was obtained for DNA extraction. A third pregnancy (unlabeled) was diagnosed *in utero* with PBS at 12 weeks and terminated at 17 weeks. No autopsy was performed and thus no specimen was obtained for this research study. *In vitro* fertilization with female gender selection resulted in a fourth pregnancy and a healthy daughter (D020S). Repeating the method of *in vitro* fertilization with female gender selection resulted in a fifth pregnancy (D020P1) but at 22 weeks gestation the fetus was diagnosed as male with PBS. D020P1 has a mild PBS phenotype, and is the only living PBS son in this pedigree.

In family D018 (Figure 2.3.D), the mother D018M ($G_4P_4A_0$) and father D018F have four living children: one healthy daughter (D018S), one healthy son (D018B), and two living sons diagnosed with PBS (D018P1 and D018P2).

III. Candidate gene screening

III.1. HNF1β CNV testing

Screening 42 male PBS patients for *HNF1β* CNVs was performed by MLPA, using a PBS patient with a confirmed whole-gene deletion of HNF1β as a control (Murray et al. 2008). None of the 42 PBS patients were found to have *HNF1β* CNVs (Figure 2.4).

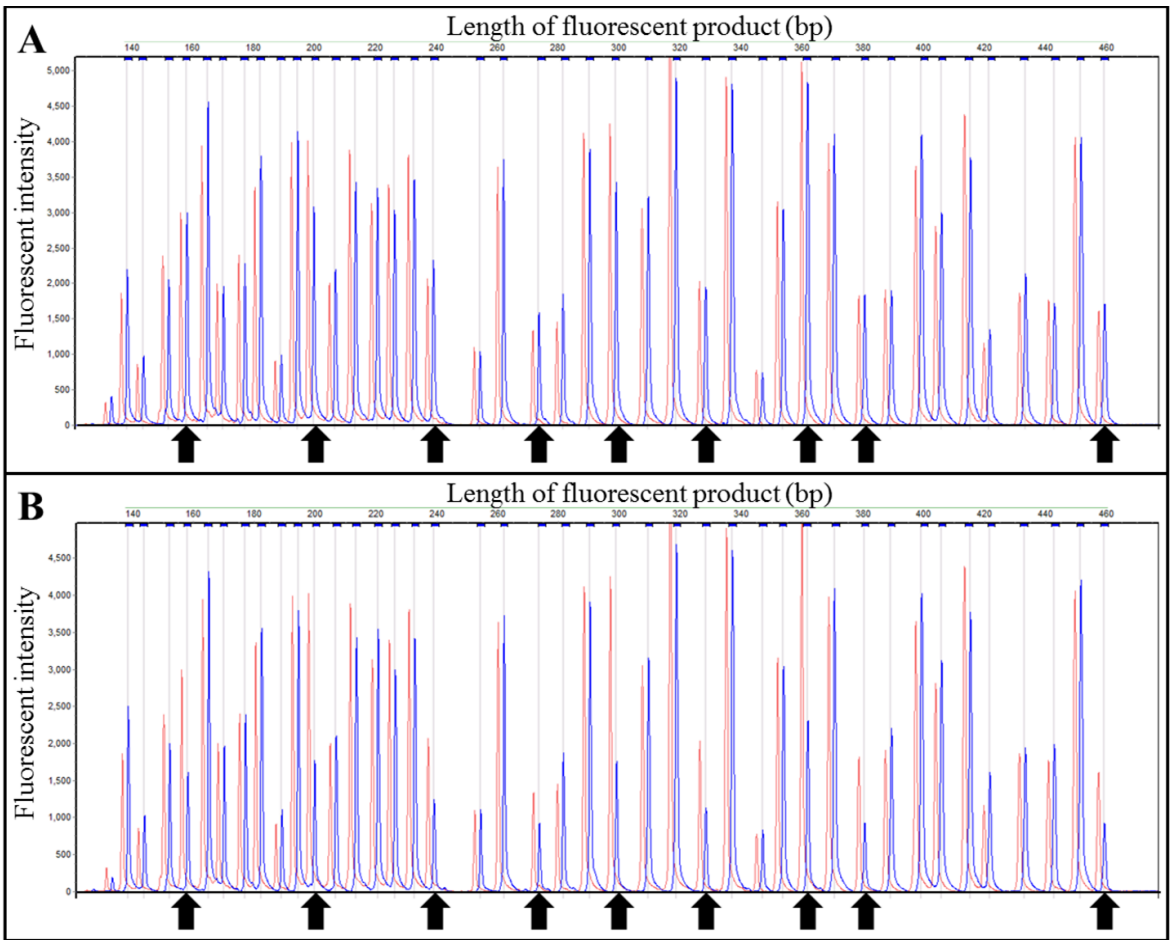

Figure 2.4. MLPA analysis did not identify HNF1β CNVs in 42 PBS patients
Arrows denote HNF1β exons while remaining peaks are addition MODY genes or control reactions. A: Results from a single PBS patient (blue peaks) compared to a normal control (red peaks). All HNF1β exons show correct copy numbers. Similar results obtained on 41 additional PBS patients. B: Results from PBS patient with a known whole gene deletion of HNF1β (blue peaks) compared to a normal control (red peaks). Each HNF1β peak is half the fluorescent intensity compared to normal control, indicative of heterozygous deletion.

III.2. HNF1β sequencing

Sequencing of all 9 exons of *HNF1β* in 30 PBS patients identified only one patient with a rare heterozygous mutation in exon 1 (rs147816724; c.182T>G) resulting in a missense mutation encoding glycine instead of valine at amino acid position 61 (V61G). Parental samples were unavailable to assess whether the mutation was inherited or *de novo*. This variant has a minor allele frequency of 0.046% according to NHLBI ESP and has previously been reported in two non-PBS patients, one with VACTERL association and one with a Müllerian anomaly and solitary kidney (Hoskins BE et al. 2008). Neither of these publications reported functional testing of the V61G missense mutation to prove causality. The V61G mutation is found in exon 1 of the *HNF1β* gene between the dimerization domain and the DNA binding domain and is conserved across multiple species. However, both *in silico* analyses predict that the V61G substitution is not functionally significant. Polyphen-2 analysis predicts V61G to be "benign" (PolyPhen-2 score = 0.000) and SIFT analysis predicts V61G is "tolerated" (SIFT score = 0.08).

In collaboration with Dr. Sachin Hajarnis from Dr. Peter Igarashi's lab, the functional significance of the V61G was tested and published (Granberg et al. 2012). Briefly, as HNF1β is known to regulate the expression of the polycystic kidney and hepatic disease 1 (*Pkhd1*) gene by directly binding to the *Pkhd1* promoter, the transcriptional activity of HNF1β encoding the V61G mutation was tested using a previously designed luciferase assay (Hiesberger T et al. 2004). Results indicate that the V61G mutation does not affect the ability of *HNF1β* to bind the *Pkhd1* promoter or encode for a dominant-negative form of *HNF1β*. These results suggest that V61G variant is not causal in PBS.

III.3. CHRM3 sequencing

The single coding exon of CHRM3 was sequenced in 43 male PBS probands. However, non-synonymous or frameshift variants were not detected.

IV. Genotyping by aCGH

aCGH testing of 12 PBS cases identified 5 (42%) patients with CNVs. Two patients have duplication CNVs: (1) a maternally inherited 0.360Mb duplication on 2q11.2 encompassing *TMEM131* and *VWA3B* and (2) a 0.324Mb duplication of unknown genetic origin on Xq23 encompassing *AFTR2*, *SLC6A14*, and *CXorf61*. Two patients have deletion CNVs: (1) a paternally inherited 0.271Mb deletion on 7q31.1 affecting *IMMP2L* and (2) a maternally inherited 0.113Mb deletion on Xq22.1 affecting *LOC442459*. Additionally, one adopted patient from Laos has two deletion CNVs (without paternal samples to determine possible genetic origin): (a) a 0.066Mb deletion on 6q23.2 affecting *TAAR9*, *TAAR8*, *TAAR6*, and *TAAR5* and (b) a 0.151 Mb deletion on 7q33.2 affecting *EXOC4*. Three CNVs were either maternally-inherited or on the X chromosome (or both), supporting but not proving the hypothesis that PBS is an X-linked or sex-influenced autosomal recessive disorder.

V. Candidate PBS X-linked regions identified by microsatellite markers

Microsatellite analysis was performed in 4 pairs of PBS-affected brothers from the identified multiplex families and their mothers: D019P1 and D019P2; D018P1 and D018P2; D040P1 and D040P2; D020P2 and D020P3. The allele lengths from 48

microsatellite markers were then compared within each pair of affected brothers to identify shared regions on chromosome X (chrX).

Samples D040P1, D040P2, D020P2, and D020P3 are deceased leaving FFPE post-mortem tissue as the sole source of DNA. Microsatellite analysis of FFPE-derived DNA is difficult due to highly fragmented DNA (100-300bp) resulting in inconsistent results in almost 50% of microsatellite markers (Farrand et al. 2002). To avoid this problem, amplified DNA from FFPE tissues was separated by an agarose gel to exclude smaller fragments resulting from insufficient amplification from degraded DNA. This size-exclusion technique allowed for confident microsatellite data from 44 of the 47 markers tested (Figure 2.5). For individuals of whom high-quality DNA was available, the size-exclusion technique was not used.

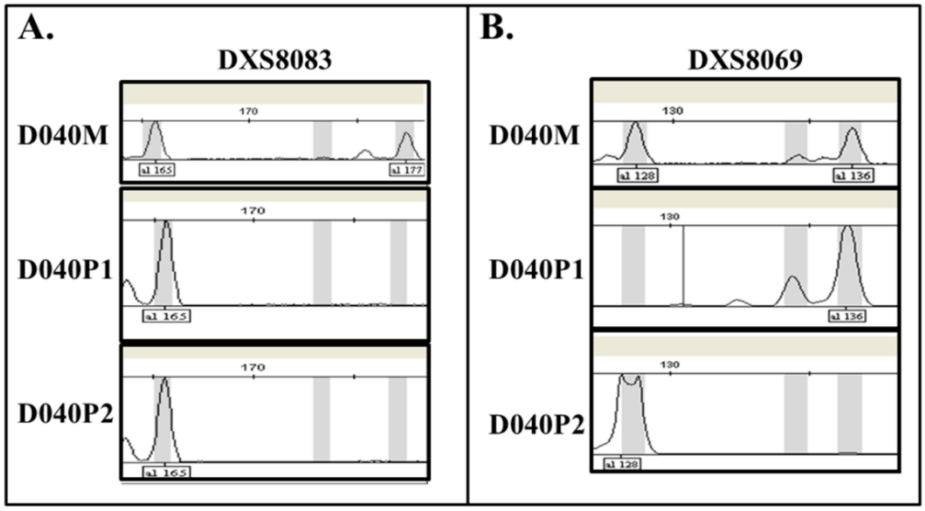

Figure 2.5. Microsatellite results from FFPE-derived DNA in D040 family Microsatellite allele lengths from PBS-affected brothers D040P1 and D040P2 were compared to maternal D040M microsatellite allele lengths to identify chromosome X markers in which both brothers inherited the same allele (A; DXS8083) versus markers in which brothers inherited different alleles (B; DXS8069).

In family D018, PBS affected brothers D018P1 and D018P2 share a single 30 Mb segment on chromosome Xp11.4 – Xq13.1. However, their unaffected brother D018B also inherited this 30 Mb segment. No regions on chromosome X (chrX) were found that were exclusively shared by the affected D018 brothers and not shared by the unaffected D018 brother suggesting either incomplete penetrance of a chrX variant or an autosomal mode of inheritance.

For the three additional PBS-affected brother pairs, two shared regions were identified within each pair (Figure 2.6). PBS sibling pair D019P1 and D019P2 inherited the same chrX between markers DXS7593 – DXS993 and DXS1106 – DXS1073. PBS sibling pair D020P2 and D020P3 inherited the same chrX between markers DXS1214 – DXS1001 and DXS1062 – DXS1073. PBS sibling pair D040P1 and D040P2 inherited the same chrX between markers DXS1223 – DXS990 and DXS8106 – DXS998.

Analysis of the shared regions between the three families identified two candidate PBS X-linked regions (Xp and Xq) in which all three PBS sibling pairs inherited the same chrX alleles (Figure 2.6). Candidate PBS Xp-linked region includes 5 markers (DXS8090-DXS993) and spans a 4.4 Mb segment on chromosome Xp21.1-p11.4 that contains 46 genes. Candidate PBS Xq-linked region includes 9 markers (DXS1062-DXS8091), spans 10.5 Mb on chromosome Xq26.3-q28, and contains 84 genes.

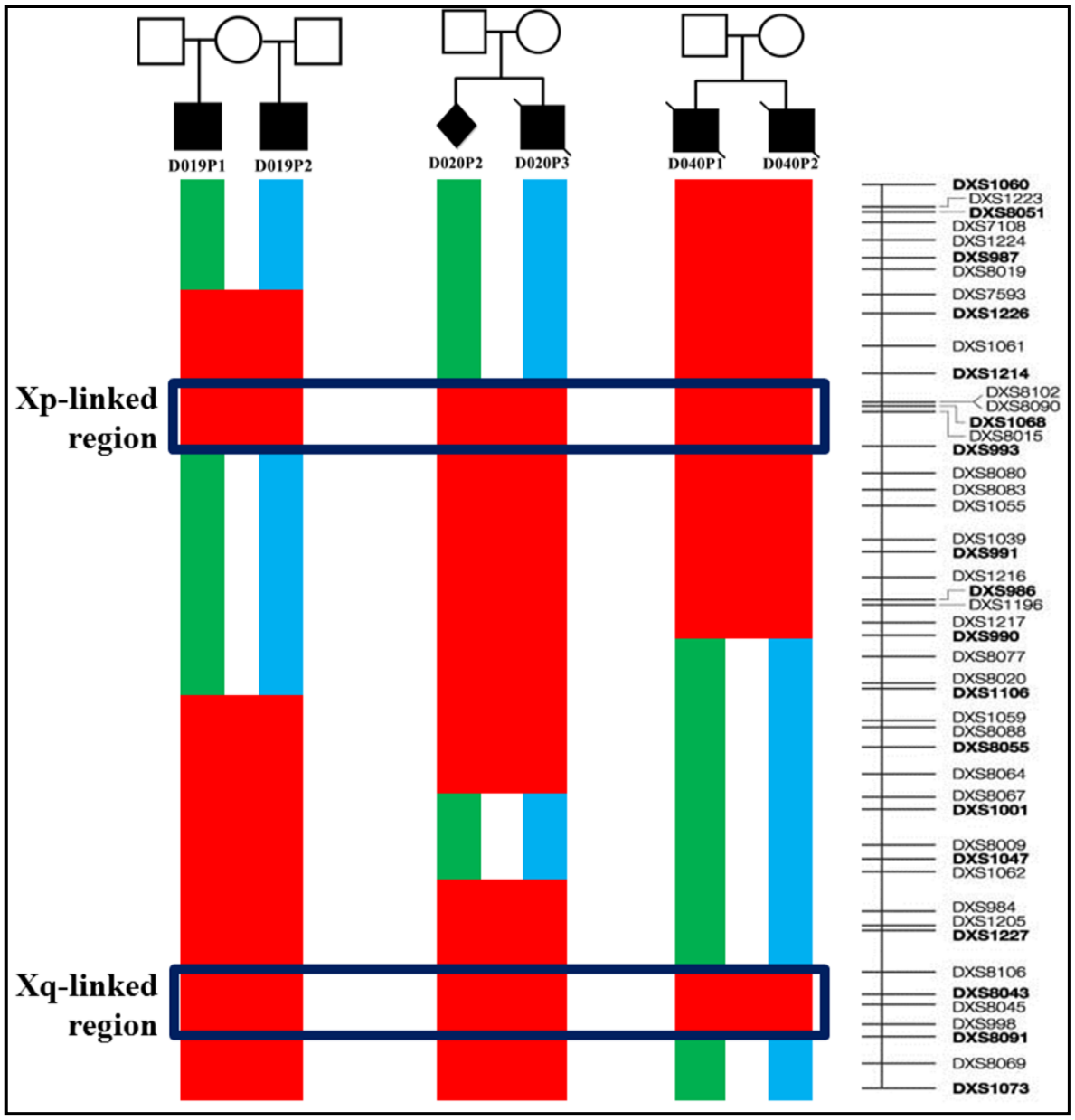

Figure 2.6. Candidate PBS X-linked regions identified by microsatelliete analysis in PBS families D019, D020, and D040

Chromosome X microsatellite markers listed on right in order from Xp22.32 (DXS1060) to Xq28 (DXS1073). Top of figure shows abbreviated pedigrees from families D019, D020, and D040. Green and blue bars denote chrX regions (corresponding length of region relative to location of markers on right) in which a sibling pair inherited different microsatellite alleles. Red segments beneath each sibling pair denote regions in which the sibling pair inherited the same microsatellite allele. For instance, D019P1 and D019P2 inherited different alleles between DXS1060 – DXS7593 (green and blue bars) and the same alleles between DXS7593 – DXS993 (combined red bars). Comparing across three pedigrees shows two candidate PBS X-linked regions (Xp and Xq).

VI. Skewed X inactivation in mothers from PBS multiplex pedigrees

Given the shared regions on chrX, mothers from the four PBS pedigrees (D018M, D019M, D020M, and D040M) were assayed to determine ratios of chrX inactivation (Figure 2.7). Results indicate highly skewed X-inactivation in D019M (95:5), moderately-skewed X-inactivation in D020M (80:20), and random X inactivation in D040M and D018M (55:45 and 50:50, respectively).

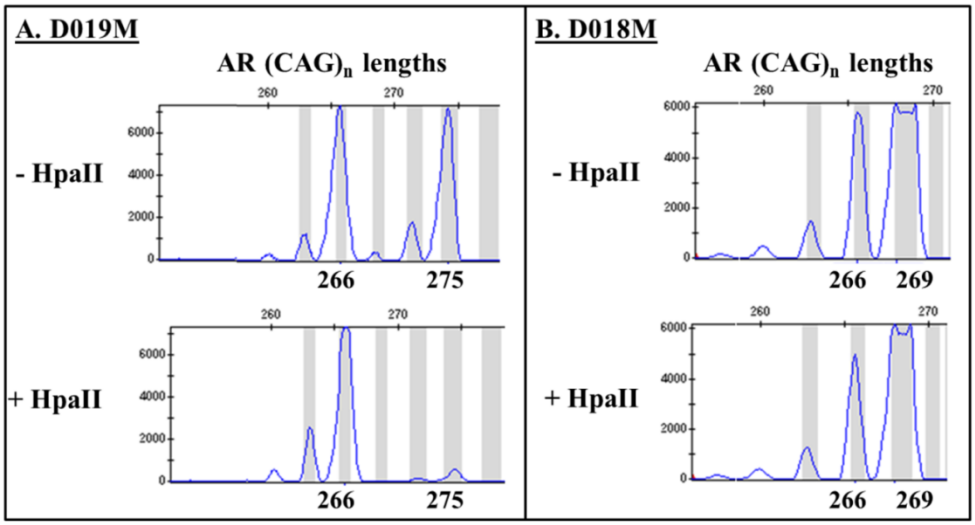

Figure 2.7. Chromosome X inactivation in D019M and D018M.
Comparing fluorescent intensity of androgen receptor (AR) allele lengths with or without methylation-sensitive restriction enzyme HpaII shows preferential methylation of 266bp allele in D019M (A) and highly-skewed X inactivation. D018M (B) shows random X inactivation evidenced by equal intensity of both alleles with or without HpaII.

VII. Whole exome sequencing D019P1 and D019P2

Maternally-shared PBS half-brothers D019P1 and D019P2 were selected for whole exome sequencing as this pedigree most strongly supports the X-linked inheritance hypothesis. Exome sequencing on D019P1 and D019P2 generated 3.57 and 4.50 gigabases (Gb) of sequence to achieve 57X and 72X coverage of the mappable, targeted exome (62 Mb), respectively. WES analysis identified 18,730 and 18,702 exonic variants in D019P1 and D019P2, respectively, of which 12,917 exonic variants were called in both samples. To identify potentially causal variants (Figure 2.8), the 12,917 shared exonic were first filtered based on variant class narrowing to 5,864 shared exonic non-synonymous variants. As D019P1 and D019P2 have different fathers, autosomal homozygous variants were removed leaving 2,821 autosomal heterozygous variants and 89 chrX hemizygous SNVs. Given the rarity of PBS (1:30,000 – 1:50,000) and that D019P1 and D019P2 are Caucasian, variants with minor allele frequency (MAF) >0.02% in 1000 Genomes Project or NHLBI ESP were excluded, as Caucasians individuals are well represented in both databases.

Only one chrX variant met these criteria: a novel hemizygous missense mutation in Filamin A (FLNA): c.6727T>C (RefSeq accession number NM_001110556.1) located on ChrX: 153,580,945 (hg19). The alternative allele was identified in 100% of the reads at this position in both D019P1 and D019P2 (47 reads and 87 reads with the alternative allele, respectively).

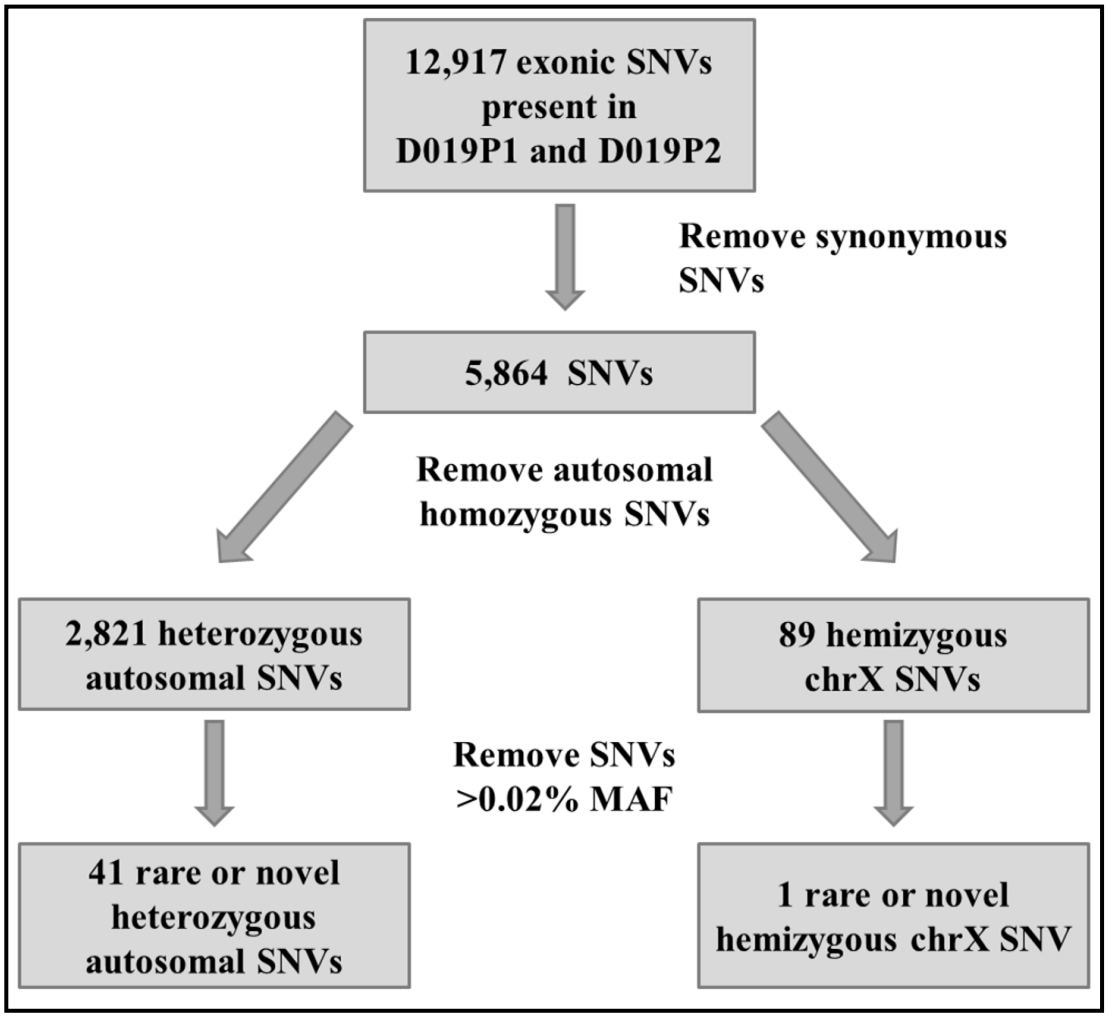

Figure 2.8. Filtering approach for exonic variants present in D019P1 and D019P2. The 12,917 exonic single nucleotide variants (SNVs) present in both D019P1 and D019P2 were filtered based on variant class, genotype, chromosome location, and minor allele frequency (MAF) to identify 41 rare or novel heterozygous autosomal SNVs and one rare or novel hemizygous chromosome X SNV.

This single nucleotide change results in a cysteine to arginine substitution at amino acid position 2160 (C2160R). This cysteine residue is highly conserved across species (Figure 2.9), with a Genomic Evolutionary Rate Profiling (GERP) score of 5.58 (range -12.3 to 6.17; 6.17 being the most conserved) (Cooper et al. 2005). Polyphen-2 analysis predicts C2160R to be "probably damaging" (PolyPhen-2 score = 0.999) and SIFT analysis predicts C2160R is "damaging" (SIFT score = 0.00).

Sanger sequencing confirmed that both PBS half-brothers are hemizygous for this FLNA variant (Figure 2.10) and their mother, D019M, is heterozygous for this variant. There is unconfirmed maternal family history of PBS in this family (Figure 2.3.A), however there are no living blood relatives available for testing nor FFPE tissue from deceased family members.

G. gallus	2094	TRRRRAPPEAHVGTACDLSLKMPEPTAHDVTAQVTAPSGTSMAAQVLEGE	2143
B. Taurus	2137	TRRRRAPSVANIGSHCDLSLKIPEISIQDMTAQVTSPSGKTHEAEIVEGE	2186
C. lupus	2137	TRRRRAPSVANVGSHCDLSLKIPEISIQDMTAQVTSPSGKTHEAEIVEGE	2186
R. norvegicus	2145	TRRRRAPSVANVGSHCDLSLKIPEISIQDMTAQVTSPSGKSHEAEIVEGE	2194
M. musculus	2145	TRRRRAPSVANVGSHCNLSLKIPEISIQDMTAQVTSPSGKTHEAEIVEGE	2194
M. mulatta	2145	TRRRRAPSVANVGSHCDLSLKIPEISIQDMTAQVTSPSGKTHEAEIVEGE	2194
H. sapiens	2145	TRRRRAPSVANVGSHCDLSLKIPEISIQDMTAQVTSPSGKSHEAEIVEGE	2194

Figure 2.9. Conservation of cysteine residue in FLNA across species
Cysteine residue at position 2160 in Homo sapiens is conserved across species (yellow)

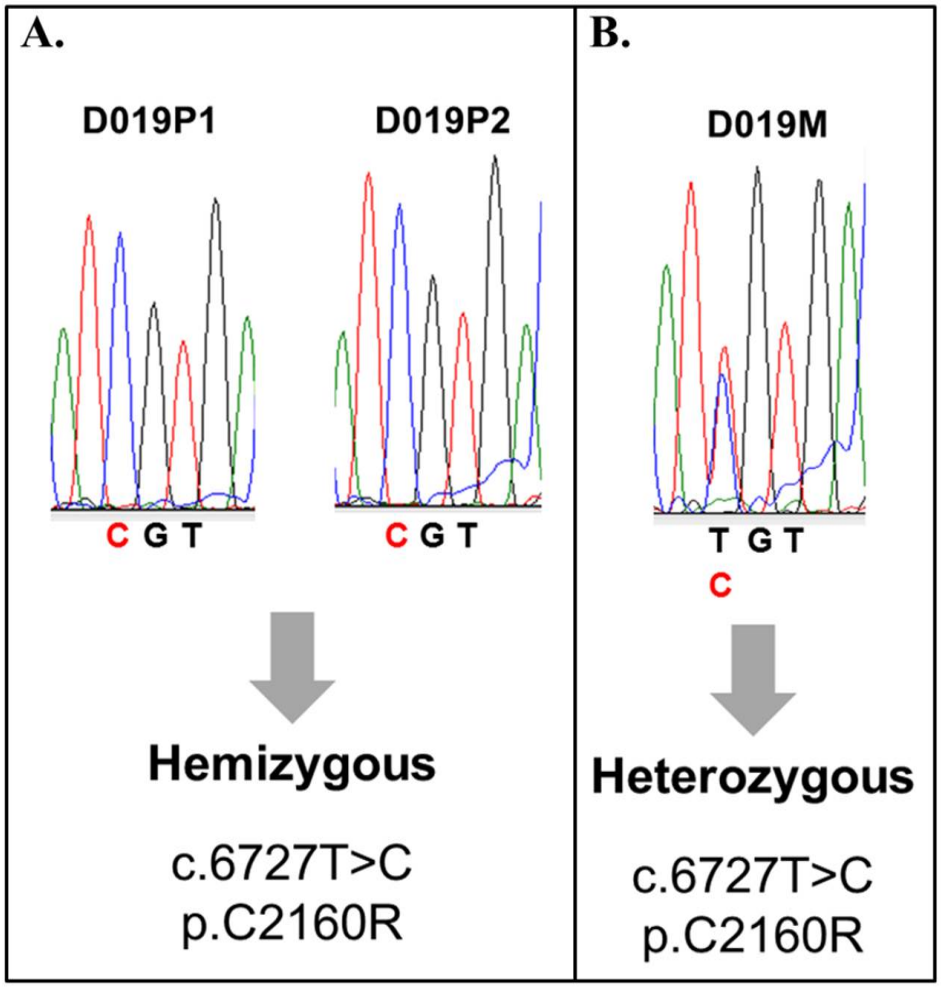

Figure 2.10. Confirmation of c.6727T>C variant in D019 family
A. Sanger sequencing of D019P1 and D019P2 confirmed the whole exome sequencing detection of FLNA hemizygous missense variant c.6727T>C; C2160R. B. D019M is heterozygous for FLNA variant.

Discussion

PBS is lethal in 60% of affected individuals and highly morbid in the survivors, with a high prevalence of renal and cardiovascular complications. The etiology of PBS is currently unknown however case reports of familial PBS, of which affected brothers is the most common occurrence, coupled with a higher incidence in males (95%) suggests a genetic component to PBS which is likely X-linked recessive or sex-influenced autosomal recessive.

I. Candidate PBS genes

Three candidate genes have been suggested for PBS: *HNF1β*, *CHRM3*, and *ACTA2*. *HNF1β* is candidate PBS gene due to two reports of PBS patients with chromosome 17q12 deletion CNVs encompassing *HNF1β* (Haeri et al. 2010). Both CNV testing and Sanger sequencing of *HNF1β* in 42 and 30 PBS patients, respectively, did not identify any causal variants (Granberg et al. 2012). These findings suggest that *HNF1β* is not a common cause of PBS and that the reported *HNF1β* CNVs in PBS patients account for the additional non-PBS phenotypic features. Additionally, of the reported 90 patients with *HNF1β* CNVS, clinical features matching the PBS phenotype have not been described (Chen et al. 2010; Edghill et al. 2013).

Sequence-level variations of *CHRM3* and *ACTA2* have been identified only in a single PBS family or single PBS case report, respectively. The *CHRM3* mutation was discovered in a familial case of six brothers from a consanguineous union that were diagnosed with PBS or a "PBS-like phenotype" (Weber et al. 2011). Sequencing of *CHRM3* in 43 PBS patients in our recruited cohort did not identify any causal variants

suggesting that *CHRM3* is not a common cause of PBS and that the clinical presentation in the reported consanguineous family is not classic PBS but a similarly presenting phenotype.

Lastly, a variant (R179H) in *ACTA2* has been previously described in a single sporadic PBS patient that also presented with non-PBS features (Richer et al. 2012). Our PBS cohort was not screened for variants in *ACTA2* as the R179H variant has been identified in five additional non-PBS patients and missense *ACTA2* variants account for 14% of familial thoracic aneurysms suggesting that *ACTA2* is not a strong candidate gene for PBS (Guo et al. 2007; Milewicz et al. 2010).

Together, the results from this study and the fact that previously identified variants in PBS candidate genes are not specific to, nor phenocopy PBS, suggest that *HNF1β*, *CHRM3*, and *ACTA2* are not strong candidate genes for PBS and that the genetic cause of common PBS remains unknown.

II. Identification of novel candidate regions and genes

After ruling out the proposed candidate PBS genes, the next approach was to utilize familial cases to discover novel candidate regions or genes that may be causal in PBS. Focusing on multiplex PBS families, which are most supportive of both a genetic component and X-linked hypothesis for PBS, can circumvent the problem of genetic heterogeneity as related affected patients primarily inherit an identical disease-causing mutation.

As seen in Figure 2.3, each pedigree supports an X-linked hypothesis as only males are affected. To test the hypothesis that PBS is an X-linked recessive disorder,

microsatellite analysis was performed on 4 pairs of PBS-affected brothers from the identified multiplex families to determine if the PBS-affected brother inherited shared regions on chrX and if the familial X-regions overlapped between families. As PBS-affected individuals from two of the four multiplex families (D020 and D040) are deceased, FFPE post-mortem tissue was the sole source of DNA. As microsatellite analysis of FFPE-derived DNA is problematic due to DNA fragmentation, I took advantage of the fact that the microsatellite markers of interest are on the X chromosome thus only a single allele length should be present in each male sample. Gel separation of the desired amplicon resulted in confident microsatellite data from 44 of the 47 markers tested, as determined by the ability of the size-exclusion allele to match one of the mother's allele lengths.

For PBS-affected brother pairs from families D019, D020, and D040, each pair was found to have shared two inherited regions on chrX. Comparing the shared regions across all three PBS-affected pairs identified two PBS candidate regions on chrX. While this finding supports the hypothesis of a causal variant on chrX, the candidate regions encompass 130 genes. Thus sequencing selected candidate genes within these regions is not cost or time effective.

Combining X-linkage with X-inactivation studies gives further insight into an X-linked hypothesis for PBS. In females, the choice of which X chromosome to silence can result in a range of X inactivation ratios from 50:50 (random inactivation) to 100:0 (non-random inactivation). Skewed X-inactivation (ratio >80:20) and highly skewed X-inactivation (ratio >95:5) can be indicative of one X chromosome harboring a deleterious allele resulting in non-random inactivation (Van den Veyver 2001). This favorably skewed X-inactivation may protect female carriers of X-linked recessive mutations from the

phenotypic consequences of the mutation (Desai et al. 2011). As highly-skewed X inactivation occurs in only 0.8% of the female population, finding highly-skewed inactivation deserves increased scrutiny as the event is highly unlikely and indicative of female carrier status of an X-linked disorder (Van den Veyver 2001; Amos-Landgraf et al. 2006). In this study, two of the mothers, D019M and D020M, exhibit moderately (80:20) and highly skewed (95:5) X-inactivation, respectively. Thus skewed inactivation in two mothers of PBS multiplex pedigrees also supports an X-linked hypothesis.

Results of X-linkage from affected brothers and maternal X-inactivation from the fourth PBS multiplex pedigree (D018; Figure 2.3.D) do not support an X-linked hypothesis suggesting not all PBS pedigrees are X-linked. These findings, together with previous publications of multiple PBS candidate genes, suggest that PBS is a genetically heterogeneous disease in which different genes or loci may be causal in PBS.

III. Whole exome sequencing D019P1 and D019P2

Maternally-shared half-sibs were selected for WES as this pedigree is most supportive of a genetic cause of PBS as multiple family members are affected (or thought to be affected) in multiple generations. Additionally, by sequencing two related individuals, challenges that arise from genetic heterogeneity are nearly eliminated as all affected family members are thought to have inherited the identical disease-causing variant.

In the event that the disease-causing variant is not on chrX for family D019, but is instead a sex-limited or reduced penetrant autosomal dominant disorder, the entire exome was sequenced, as opposed to sequencing only chrX. Even though PBS family D019

strongly supports an X-linked hypothesis of PBS, not all PBS pedigrees support this hypothesis, thus by focusing only on chrX an autosomal disease-causing variant could be missed. Given this consideration, autosomal variants identified in D019P1 and D019P2 may require additional studies to determine plausible PBS pathogenesis.

To identify candidate disease-causing variants, WES results from each of the PBS half-sibs (D019P1 and D019P2) were compared to identify shared variants. The highest reported incidence of PBS is 1:30,000 births and the largest accessible human genetic database (NHLBI ESP) contains exomes from 6,500 individuals. If a single PBS patient was represented in NHLBI ESP, the MAF frequency of this alternative allele would be 0.015%, thus variants with MAF frequency >0.02% were excluded. A missense variant in FLNA was the only chrX variant that met the aforementioned criteria. Additionally, FLNA is located between chrX microsatellite markers DXS8069 and DXS1073, a region shared in both D019 and D020 PBS brothers (Figure 2.6). The remaining heterozygous autosomal variants were all missense changes; no nonsense mutations met the aforementioned criteria. Given the D019 pedigree structure, highly-skewed X inactivation, and predicted damaging effects of the C2160R variant, FLNA emerged as a PBS candidate gene.

CHAPTER 2 PART B:

CHARACTERIZATION OF THE FILAMIN-A VARIANT C2160R

Introduction

I. Summary of FLNA

Filamin A (*FLNA*) is located on chromosome Xq28 (between markers DXS8069 and DXS1073; Figure 2.6) and is composed of 48 exons spanning 26 kb. FLNA is a widely expressed actin-binding protein that regulates several key cellular functions, including cell shape, migration, and contraction, by binding both the actin cytoskeleton and multiple transmembrane receptors. Mutations in human FLNA, ranging from whole gene CNVs to missense variations, are associated with multiple human disorders characterized by defects in neuronal migration, impaired vascular function, and skeletal dysplasia.

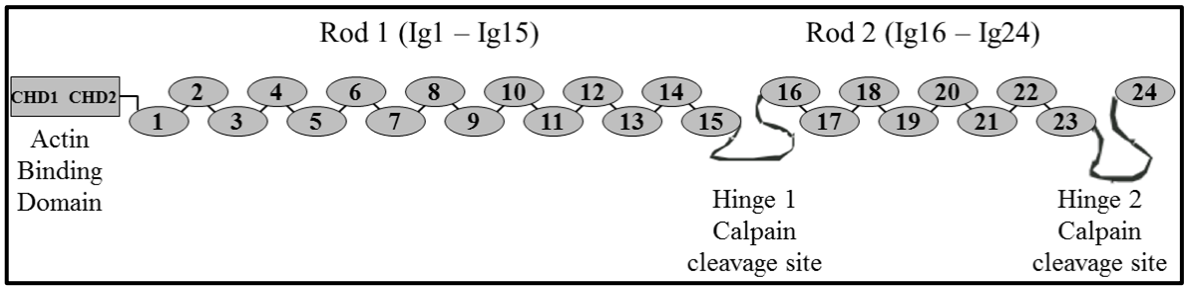

Figure 2.11. Structure of FLNA monomer

II. Structure and domains of FLNA protein

Each FLNA monomer contains an N-terminal actin binding domain (ABD) consisting of two calponin homology domains (CHD1 and CHD2), followed by 24 immunoglobulin-like (Ig) β-sheet pleated repeat domains (Ig1 – Ig24), each with ~96 amino acids (Figure 2.11). Two calpain-sensitive hinges separate the repeat domains into rod 1 (Ig1 - Ig15), rod 2 (Ig16 – Ig23), and a C-terminal dimerization domain (Ig24) which

allows FLNA to form a homodimer (Figure 2.12). A FLNA homodimer results in a V-shape configuration of the dimeric molecules and perpendicular branching of F-actin (Nakamura et al. 2007).

Each FLNA Ig-repeat domain contains eight β-sheet strands (β-strand A – β-strand H) resulting in a β-barrel structure. The 24 Ig-repeat domains are categorized into classes A, B, C, and D, based on sequence homology. Class A Ig-repeat domains are characterized as the ligand-binding domains as these domains are configured such that β-strands C and D (C/D face) form a binding groove utilized by binding partners (Ithychanda et al. 2009b).

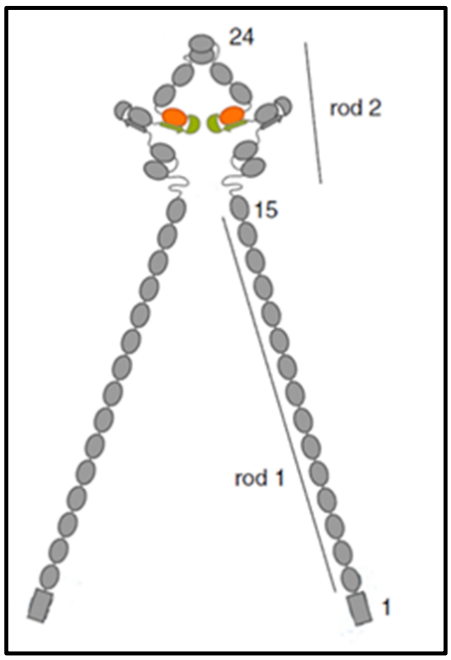

Figure 2.12. Structure of FLNA homodimer
Dimerization of FLNA at Ig24. Ig repeats 20 and 21 are seen in green and orange, respectively. Rod 1 forms a straight, extended structure while rod 2 forms a more compact, globular structure due to intramolecular interactions. Adapted from Rognoni et al. (2012)

In rod 1, repeats Ig9–Ig15 contain an actin binding site that, in addition to the N-terminal ABD, facilitates high-affinity FLNA/actin binding. The flexible structure of repeats Ig1–Ig8 allows repeats Ig9–Ig15 to configure optimal alignments of filamentous-actin (f-actin) monomers with FLNA downstream from the initial N-terminal binding site. Aside from f-actin, only a few other proteins are known to bind rod 1 (Ithychanda et al. 2009b).

Rod 2 (Ig16–Ig23) does not bind f-actin and instead has a prominent role regulating FLNA binding to numerous receptors and scaffolding proteins. More than 70 proteins are known to bind or interact with the repeat domains on rod 2 (Zhou et al. 2007; Zhou et al. 2010). In contract to the rod 1 FLNA extended chain (58 nm long), rod 2 forms a compact, folded structure (19 nm long) that is the result of intramolecular interactions between adjacent paired Ig-repeat domains (Figure 2.12). On rod 2, even-number Ig-repeat domains 16, 18, and 20 pair with neighboring odd-number Ig-repeat domains 17, 19, and 21 resulting in a nonlinear, spring-like globular structure.

III. FLNA interactions regulate cell morphology, migration, and contraction

The actin cytoskeleton structure is essential for regulating cell shape, morphology, migration, and contraction, as dictated by external stimuli and signals. Proper cellular response and actin remodeling depends upon the ability of transmembrane receptors to transmit signals to the underlying actin cytoskeleton (Zhou et al. 2010).

Within a functional group of smooth muscle cells that are held together by the extracellular matrix (ECM), like the bladder detrusor, each individual muscle cell can relax or contract via its intracellular actin-myosin contractile machinery (actomyosin units).

However, proper actomyosin-mediated contraction in smooth muscle cells must be accompanied by force transduction to the ECM and cell stiffening via actin cytoskeleton reorganization.

As seen in Figure 2.13 (Gunst & Zhang 2008), a relaxed smooth muscle cell contains actomyosin units disbursed within the cytosol and attached to each other by cytosolic dense bodies. The smooth muscle cell membrane contains adhesion complexes consisting of cytoskeletal proteins and transmembrane integrin receptors that bind to the ECM and detect mechanical strain. Upon mechanical strain or neurotransmitter-mediated contraction stimulus, activated CHRM3 or the purinergic receptor (P2X1R) results in an influx of intracellular calcium via the sarcoplasmic reticulum or plasma membrane channels (Figure 2.14). Upon myosin light chain phosphorylation, the cytosolic actin-myosin motor units contract.

Simultaneously but independently, cytoskeletal remodeling creates a stabilized, reinforced cortical actin motor which links the contracting actomyosin motor units to the membrane adhesion complexes (Figure 2.13). Linking actomyosin motor units to membrane adhesion complexes allows for both cell stiffening in response to stimuli and mechanical transduction of cellular internal tension to the extracellular matrix. As FLNA binds transmembrane receptors and actin (Figure 2.14), FLNA provides a physical link between transmembrane receptors and the actin cytoskeleton thus facilitating bidirectional transmission between the cell and the ECM.

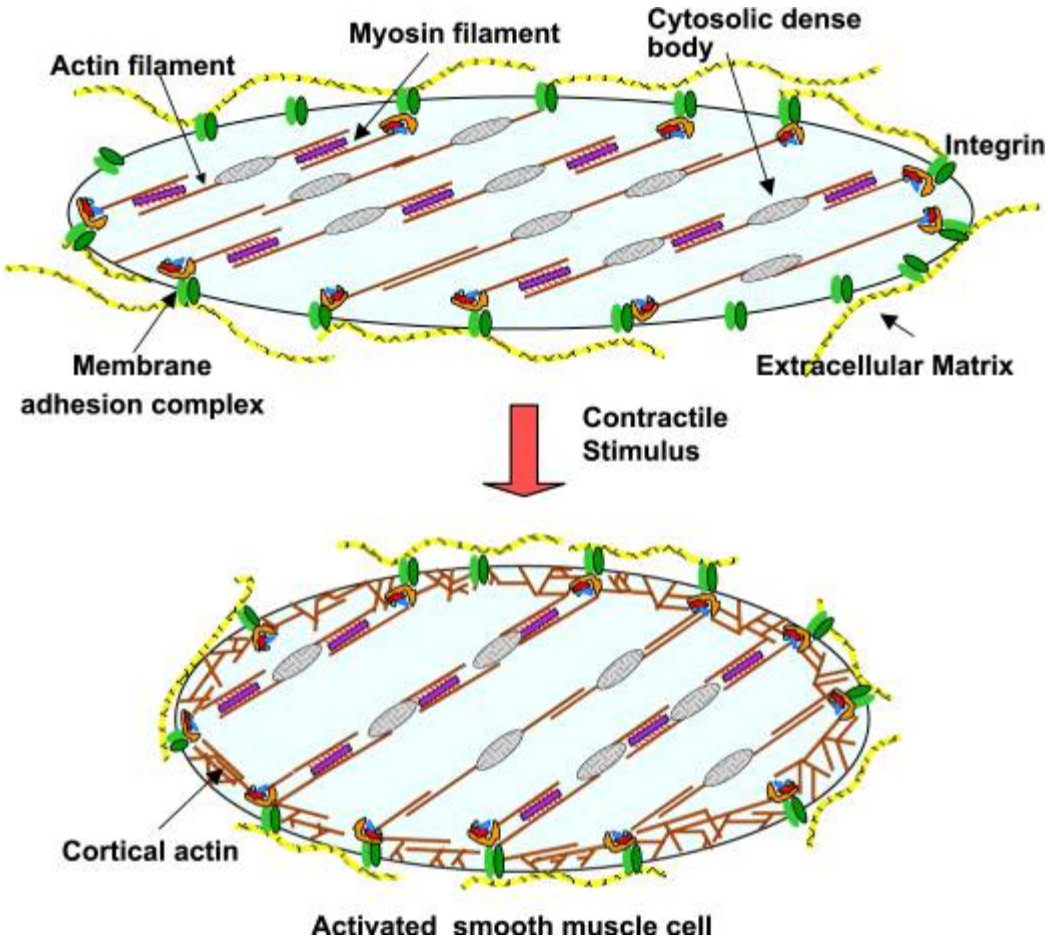

Figure 2.13. Model of cytoskeletal dynamics in smooth muscle contraction.
Activation of a smooth muscle cell stimulates the assembly of macromolecular protein complexes at cell membrane/ECM adhesion junctions (focal adhesions) that regulate the formation of actin networks and fortifies connections between actin and integrins. The formation of actin networks strengthen the membrane for the transmission of force generated by the actomyosin system and enables adaptation of the smooth muscle cell to external forces. Figure from Gunst and Zhang (2008)

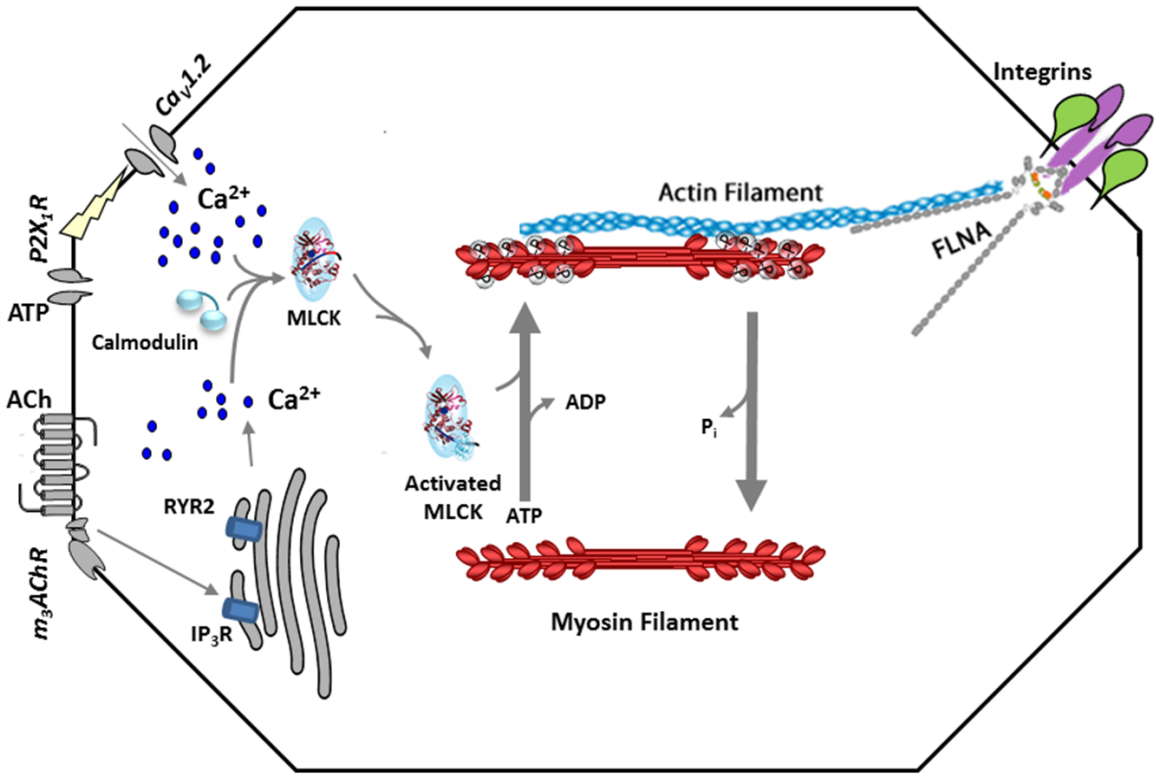

Figure 2.14. Role of FLNA in smooth muscle cell contraction
In a smooth muscle cell, ATP binding to the P2X1R purinergic receptor opens the voltage-gated calcium channel, Cav1.2, leading to a large calcium influx. Ryanodine receptor 2 (RYR2) and inositol trisphosphate receptor (IP_3R) release smaller amounts of calcium from the sarcoplasmic reticulum. Cytosolic calcium binds to calmodulin, which then activates myosin light chain kinase (MLCK) for phosphorylation of myosin. Phosphorylated myosin interacts with actin filaments leading to force development or shortening through actin filaments anchored indirectly at the extracellular matrix. Filamin A (FLNA) provides the physical link between actin filaments and the ECM by binding both actin and integrins. Adapted from Tsai et al. (2012)

This role of FLNA in bidirectional signaling is supported by studies of FLNA involvement in both cell migration and contraction. Cell migration depends upon FLNA-mediated f-actin cross-linking at the leading edge of migrating cells as loss of FLNA results in impaired cell migration upon extracellular signals (Cunningham et al. 1992). Similarly, external signals of stiffness or force rely upon FLNA to direct and transduce changes on the intracellular actin cytoskeleton as mechanical tension results in FLNA recruitment to adhesion complexes where FLNA regulates the accumulation and tension of actin (Glogauer et al. 1998; D'Addario et al. 2002). Consequently, loss of FLNA is associated with a strong decrease in internal contractile tension and results in more fluid cells that cannot regulate their own stiffness (Kasza et al. 2009). These findings suggest FLNA is a necessary component of the signaling machinery that couples the ECM to intracellular actomyosin contractility. Thus, FLNA serves as a mechanosensor, an actin-crosslinking protein that receives mechanical cues and transforms them into biochemical signals.

IV. FLNA interactions with β-integrins regulate cellular functions

Transduction of signals from the ECM to the actin cytoskeleton is mediated by membrane adhesion complexes (Figures 2.13 and 2.14), also known as focal adhesions. Within focal adhesions are numerous transmembrane receptors, including integrins. Integrins are heterodimeric (α/β) adhesion receptors that link extracellular and intracellular systems by attaching the cell to the ECM and bi-directionally transducing mechanical force and regulatory signals between the ECM and the cell.

Structurally, integrins are composed of extracellular loops utilized in ligand binding and a C-terminal intracellular tail with numerous competing intracellular interacting partners. Extracellular binding to integrins is regulated by the intracellular integrin tail, a process called "inside-out signaling." Binding of talin, an intracellular cytoskeleton protein, to integrin intracellular tails results in a structural change that is transmitted through the transmembrane domain to the extracellular domain. This process converts integrin from a low-affinity state to a high-affinity state (integrin activation) (Tadokoro et al. 2003). Many cellular processes, including cell migration and cell polarity, are dependent on integrin activation and focal adhesion complexes.

FLNA binds the cytoplasmic tails of many β-integrins (including β1, β2, β3, and β7), thus providing a mechanical and biochemical link through which the actin cytoskeleton can respond to external cues. Binding of FLNA to β-integrin tails is an important component of cell migration as FLNA/β7 and FLNA/β1 interactions support moderate and high levels of cell migration, respectively (Calderwood et al. 2001). The extent of FLNA/β-integrin binding is highly regulated as excessive FLNA/β-integrin interactions impair cell migration by inhibiting membrane protrusion and cell polarization.

FLNA/β1 binding is also essential for cell contraction and remodeling of collagen matrices (Gehler et al. 2009). In response to mechanical force, β1 integrin recruits both FLNA and actin to focal adhesions containing β1-integrin, suggesting a role for FLNA in cellular stabilization and response to mechanical force (Glogauer et al. 1998). These findings suggest that FLNA/β1-integrin complexes play a significant role in both mechanosensing of matrix tension and as an effector of cellular contraction against the ECM.

V. FLNA Ig20 inhibits integrin binding at Ig21

The C/D faces of FLNA ligand-binding domains on rod 2 (Ig17, 19, 21, and 20) are utilized by interacting partners or adjacent even number FLNA Ig-repeat domains (Ithychanda et al. 2009b). The primary binding site for cytoplasmic β-integrin tails is the C/D face of Ig21 however this site is occupied by β-strand A of Ig20 (Figure 2.15). The binding mode of Ig20-Ig21 mimics Ig21-intergrin binding, thus Ig20 blocks integrin interactions with Ig21, suggesting an auto-inhibitory mechanism regulating FLNA/integrin binding. Structural analyses show that intramolecular interactions between Ig20 and Ig21 are less optimal than Ig21/integrin binding suggesting that inhibition of Ig20 upon Ig21/integrin binding is only partial (Lad et al. 2007b).

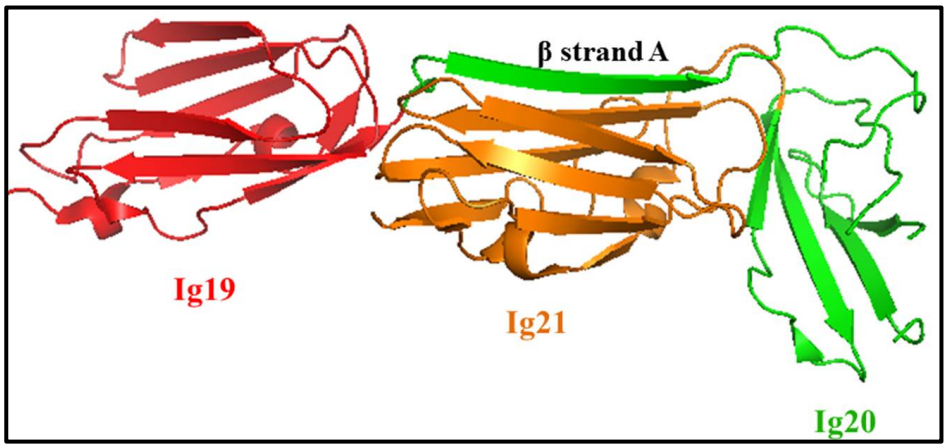

Figure 2.15. Structure of FLNA Ig19-21
Ribbon diagram of FLNA Ig19 (red), Ig20 (green), and Ig21 (orange). β-strand A (denoted above) of Ig20 interacts with Ig21.

Binding of integrins to the cryptic FLNA Ig21 site requires conformational changes that will alter interactions between neighboring repeat pairs in rod 2 (Figure 2.16). A hypothesized mechanism for up-regulation of integrin binding sites of FLNA is force-induced exposure of the binding sites as physiological forces are sufficient to expose the cryptic integrin binding site on Ig21 (Chen et al. 2009; Pentikainen & Ylanne 2009). Mechanical stretching of FLNA removes Ig20 from Ig21 without disrupting the C/D face of Ig21, thus exposing the Ig21 site and enhancing integrin binding (Pentikainen & Ylanne 2009). Binding of integrin tails to the stretched FLNA structure is also thought to stabilize stretched FLNA as the integrin tail covers a hydrophobic domain of Ig20 that is exposed by stretching (Pentikainen & Ylanne 2009). Once force is released, β-strand A of Ig20 will refold back onto Ig21, displacing integrin.

Up-regulation of integrin binding sites in FLNA has been demonstrated *in vitro* by introducing sequence variations in Ig20, either by whole domain deletion (ΔIg20) or substitution of a single Ig20 residue (I2144E) that facilitates Ig20-Ig21 binding. Variations ΔIg20 and I2144E result in enhanced FLNA binding to β-integrin tails resulting from exposure of the C/D binding face of Ig21 (Lad et al. 2007b). These results indicate that FLNA variants ΔIg20 or I2144E form FLNA proteins that assume the "open" configuration allowing enhanced FLNA/integrin interactions without regulation from a force-induced signal.

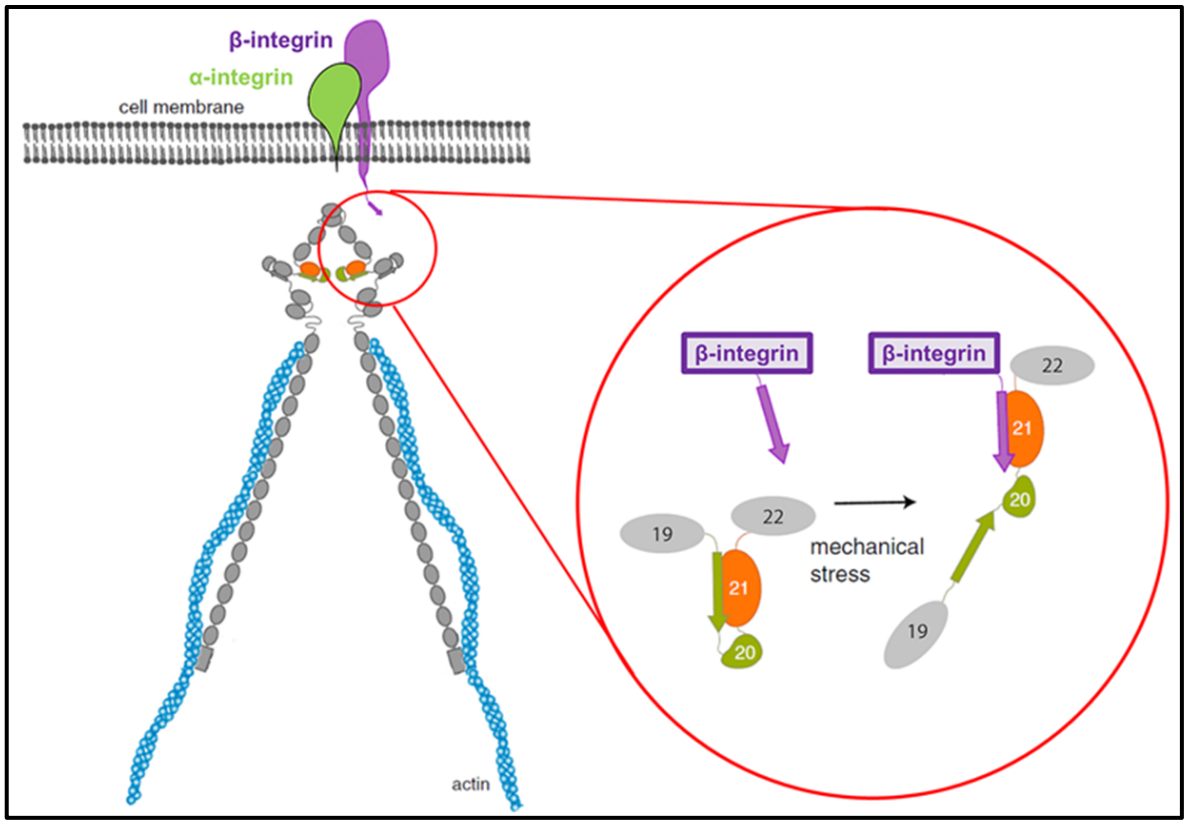

Figure 2.16. FLNA binding to integrin tails requires conformational change
Intramolecular interactions between FLNA (grey) repeat domains Ig20 and Ig21 (green and orange, respectively), prevent β-integrin tails (purple) from binding Ig21. Mechanical force is sufficient to remove Ig20 from Ig21, allowing β-integrin to bind at Ig21. Adapted from Rognoni et al. (2012)

VI. Balance of FLNA/integrin interactions regulate integrin activation

Regulating the quantity of FLNA/interactions is necessary as a sufficient degree of FLNA/integrin binding stabilizes membrane adhesion complexes while excessive binding of FLNA prevents efficient actin remodeling and cell motility (Kim et al. 2008). Previously, increased binding of FLNA to β-integrin tails was shown to impair cell migration suggesting that tight interactions between FLNA and β-integrin tails are associated with a blockade of cell polarization and transient membrane protrusion, the first steps in cell migration (Calderwood et al. 2001). Numerous cellular functions depend on the activation of integrins by talin; however talin and FLNA binding sites on cytoplasmic integrin tails overlap (Kiema et al. 2006). Thus competition between FLNA and talin regulate the activation of integrins and subsequent dependent cellular functions.

Talin associates with integrin tails only when FLNA/integrin interactions are diminished (Calderwood et al. 2001). As explained above, the structure of FLNA domains Ig20 and Ig21 results in Ig20-mediated inhibition on integrin binding at Ig21. This inhibition is released by mechanical stress which up-regulates FLNA/integrin binding. Once force is released, Ig20 folds back onto Ig21, displacing integrin and allowing talin to freely bind with integrin. This force-induced mechanism prevents excessive FLNA/integrin binding and promotes talin-induced integrin activation.

The balance of FLNA/integrin interactions is regulated by the affinity of FLNA and talin for the integrin binding site and the affinity of FLNA for migfilin, a widely expressed component of actin-cytoskeleton membrane junctions. Migfilin binds to FLNA Ig21 at the identical site of β-integrin tail binding thus dissociating integrin from FLNA (Ithychanda et al. 2009a). Migfilin-induced dissociation between integrins and FLNA facilitates talin-

mediated activation of integrin and actin cytoskeleton remodeling, as evidenced by impaired actin assembly upon disruption of FLNA/migfilin interactions (Tu et al. 2003). FLNA binding to integrin is thought to function as an "off switch" by inhibiting integrin activation and ECM-cytoskeleton focal adhesion communications. Migfilin binding to FLNA then alleviates this repression by promoting integrin activation and cellular processes dependent on integrin activation, such as cell adhesion junctions, migration, and contraction.

VII. Alternative splicing of FLNA

Regulation of FLNA/integrin binding can also be achieved through alternative splicing. Alternative splicing of FLNA has been shown to remove exon 40, generating isoform "FLNA var-1" which lacks 41 amino acids from the C-terminal of IgFLNa19 and N-terminal of IgFLNa20 (residues 2127-2167) (van der Flier et al. 2002). These residues encompass the β-strand A of repeat Ig20, which interacts with the C/D face of IgFLNa21. Thus FLNA var-1 translation results in loss of inhibitory function and increased integrin binding (van der Flier et al. 2002). FLNA-var1 mRNA has a weak but widespread distribution; however, the mechanisms regulating this alternative splicing are unknown (van der Flier et al. 2002).

VIII. FLNA regulates transcriptional activity

Cytoplasmic FLNA also regulates transcriptional activity by either retaining transcription factors in the cytoplasm or activating transcription factors for nuclear localization (Sasaki et al. 2001; Yoshida et al. 2005; Kim et al. 2007). Full-length FLNA

also regulates transcription by mediating the trafficking of transcriptional regulators into the nucleus. Transcription factor FOXC1 regulates neural crest and mesenchymal mesoderm cell fate in the absence of PBX1. FLNA down-regulates FOXC1 activity by mediating nuclear and subnuclear localization of PBX1 which facilitates formation of FOXC1-PBX1 complexes that are unable to recruit coactivator complexes and are targeted to transcriptionally inactive, HP1a-rich heterochromatin regions of the nucleus (Berry et al. 2005).

A small fraction of full-length FLNA localizes to the nucleus and evidence suggests that FLNA calpain-cleavage-induced C-terminal rod 2 fragment (90 kDa) also has a nuclear presence and regulates transcriptional activity (Loy et al. 2003). FLNA rod 2 is necessary for nuclear localization of the androgen receptor (AR), a nuclear transcription factor that mediates male sexual differentiation. By competing with AR coactivator transcriptional intermediary factor-2 (TIF2), FLNA represses AR transactivation, disrupts AR interactions, and disrupts TIF2-activated AR function (Ozanne et al. 2000). Additionally, in hypoxic conditions, the C-terminal rod 2 FLNA fragment facilitates nuclear localization of hypoxia-inducible factor 1α (HIF-1α). In the nucleus, FLNA rod 2 is recruited to HIF-1α target gene promoters, resulting in up-regulation of HIF-1α target gene expression in a hypoxia-dependent-manner (Zheng et al. 2014).

IX. Human phenotypes associated with mutations in FLNA

FLNA structural and sequence-level variations are associated with many disorders with non-overlapping phenotypes. Given the large size of FLNA and numerous interacting partners, differences in FLNA disease phenotypes are caused by gain- or loss-of-function variations that alter the roles of specific FLNA domains.

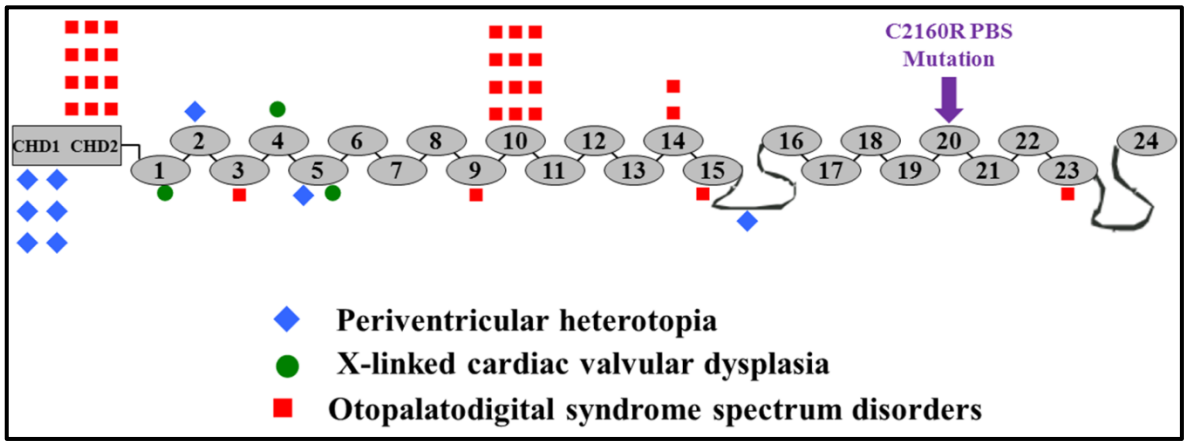

Figure 2.17. Location of FLNA missense mutations associated with clinical disorders FLNA missense mutations are primarily clustered in actin-binding domains CHD1 and CHD2 and rod 1.

Mutations in FLNA were first associated with periventricular heterotopia (PVNH; #300049), a condition characterized by epileptic seizures and brain malformations. In PVNH, morphologically normal, heterotopic neurons fail to migrate from the subventricular zone to the cerebral cortex and instead persist as nodules in the ventricular surface of the brain (Eksioglu et al. 1996; Fox et al. 1998). X-linked PVNH, caused by mutations in FLNA, is predominately found in females and has been described in PVNH families with an under-representation of males, indicative of prenatal lethality in hemizgyous males. FLNA mutations associated with PVNH are distributed throughout the

gene and are typically loss-of-function frameshift and nonsense mutations, resulting in nonsense-mediated RNA decay. Clustered missense mutations in the CDH1 region of the actin-binding domain have also been identified (Sheen et al. 2001; Moro et al. 2002; Robertson 2005). There are two reports of surviving male PVNH patients, both of whom were found to have Xq28 duplications encompassing FLNA (Fink et al. 1997; Fox et al. 1998). This finding suggests that FLNA dosage is critical for neuronal migration and altering this dosage impairs normal neuronal migration as FLNA relays the signals needed for reorganization of the neuronal shape and position. This hypothesis is supported by a study in rats that revealed changing the dosage of FLNA within the periventricular zone affects neuronal polarity and orientation (Nagano et al. 2004).

FLNA mutations are also associated with a broad range of congenital malformations known as the otopalatodigital syndrome spectrum disorders (OPD-spectrum disorders), which include otopalatodigital syndrome types I (OPD1; #311300) and II (OPD2; #304120), frontometaphyseal dysplasia (FMD; #305620), and Melnick-Needles syndrome (MNS; #309350). These disorders are characterized by skeletal dysplasia along with craniofacial, cardiac, genitourinary, and intestinal anomalies in both sexes. The most severe phenotype, MNS, is characterized by severe malformations in the hindbrain, heart, intestines, and kidneys and prenatal lethality in males (Melnick & Needles 1966; Donnenfeld et al. 1987). ODP-spectrum disorders are associated with recurrent missense mutations that cluster in four specific FLNA regions: the actin-binding domain and repeat domains Ig3, Ig10, and Ig14/15. All cases of MNS are accounted for by FLNA mutations, with >90% occurring within Ig10. All males with OPD1 and OPD2 have missense mutations in the CH2 region of the actin-binding domain (Robertson 2005).

In females with OPD-spectrum disorders, the degree of disease severity is correlated with skewed X-inactivation that favors expression of the normal allele. MNS females exhibit near-complete skewing against the mutated FLNA allele suggesting that mutations in Ig10 are the most severe (Robertson et al. 2003). FLNA missense mutations associated with ODP-spectrum disorders are gain of function mutations whereas PVNH is associated with loss-of-function variations, thus providing a hypothesis for the non-overlapping disease phenotypes primarily associated with FLNA.

X-linked recessive forms of chronic idiopathic intestinal psuedoobstruction (CIIP) and congenital short bowel syndrome (CSBS) are also associated with FLNA. In a study of 10 families in which male patients presented with CIIP, all were found to have Xq28 duplications encompassing FLNA (Clayton-Smith et al. 2009). Another study of familial X-linked CIIP detected a 2-bp deletion (c.65-66delAC) in exon 2 of FLNA that was heterozygous in all female carriers and hemizygous in an affected male (Gargiulo et al. 2007). This 2-bp deletion frameshift causes a premature stop codon resulting in loss-of-function of full-length FLNA; however, a shorter FLNA isoform is translated using a second methionine downstream of the 2-bp deletion. This shorter FLNA isoform is missing the first 27 amino acids which are part of the N-terminal ABD. Another 2-bp deletion (c.16-17delTC) in exon 2 of FLNA was identified in 3 male patients (2 related; 1 isolated) with X-linked CSBS (van der Werf et al. 2013). This 2-bp deletion frameshift also results in a premature stop codon and is hypothesized to function similarly to the 2-bp deletion in CIIP in that the long FLNA isoform is absent and only the shorter FLNA isoform missing the first 27 amino acids is present.

Lastly, analysis of three multiplex X-linked cardiac valvular dysplasia families identified 3 different FLNA missense mutations segregating with the disease, occurring in FLNA repeat domains Ig1, Ig4, and Ig5. In all three families, the disease was inherited with complete penetrance in males and incomplete in female carriers, due to different X-inactivation patterns.

In summary, the literature on FLNA variations and clinical diseases suggests that loss-of-function mutations (either deletions or nonsense mutations) are lethal in males and result in PVNH in females; gain-of-function missense mutations in the ABD or repeat domains 3, 10, or 14/15 result in the OPD-spectrum disorders; missense mutations in repeat domains 1, 4, or 5 result in cardiac valvular dysplasia; and frameshift mutations causing translation of only a shorter FLNA isoform results in CIIP or CSBS. These genotype-phenotype correlations suggest very specific functions for each domain of FLNA.

X. Animal models of FLNA loss-of-function

Male hemizygous *Flna*$^{k/y}$ mice die mid-gestation by embryonic day (E) 14.5 with severe cardiac structural defects, widespread hemorrhaging from abnormal vessels, and additional skeletal and palate defects (Feng et al. 2006; Hart et al. 2006). However, migration and motility of many cell types, including neural crest cells, was not affected. Instead, the most striking defect in *Flna*-null male mice was abnormal adherens junctions and defects in cell-cell contacts, suggesting that loss of cell motility-independent *Flna* functions are the primary cause of lethality in these mice. Phenotypes of female heterozygous *Flna*$^{k/w}$ mice vary as 20% died in the first 3-4 months with many anomalies,

including lung edema, liver thrombi and necrosis, and cardiac dilation (Feng et al. 2006). Additionally, lower than expected numbers of female *Flna*$^{k/w}$ mice are birthed, suggested embryonic lethality in some female heterozygotes. Additionally, knockdown of FLNA orthologue "actin-binding protein 280" in zebrafish results in brain and body axis defects, cardiac adema, hydrocephalus, and eye defects (Adams et al. 2012).

Materials & Methods

FLNA and β-integrin expression

For mouse expression studies, tissue from male wild-type E13 and E15 or postnatal day 1 was collected and stored in RNA-later (Ambion, Austin, TX). For human expression studies, surgical tissue from male patients was collected and stored in RNA-later. Total RNA was isolated using TRIzol reagent (Invitrogen, Carlsbad, CA) followed by purification using Aurum Total RNA Mini Kit (Bio-Rad, Hercule, CA), both according to manufacturers' instructions. RNA was used for reverse transcription using the SuperScript® VILO™ cDNA Synthesis Kit (Invitrogen, Grand Island, NY) and real-time PCR was performed using an iCycler real-time PCR machine (Bio-Rad, Richmond, CA). Commercially available TaqMan Gene Expression Master Mix (Applied Biosystems, Carlsbad, CA) was utilized with probes for the following genes: FLNA (Mm01187533_m1), ITGB1 (Mm01253233_m1), ITGB7 (Mm01296188_m1), and CDKN1B (human: Hs00153277_m1 or mouse: Mm00438168_m1). Probes for FLNA, ITGB1, and ITGB7 were verified by Applied Biosystems to detect both human and mouse gene expression. Mean relative gene expression was calculated after normalization to

cyclin-dependent kinase inhibitor 1B (CDKN1B) using the ΔΔCt method (Livak & Schmittgen 2001). Three independent experiments were performed in triplicate.

Expression of FLNA var-1 was detected by RT-PCR of cDNA from human surgical tissue, obtained as described above. Primers were designed to encompass 41 residues in Ig20 to generate a 285bp fragment in full-length FLNA and 162bp fragment in FLNA-var1 when 41 residues are removed (Table 2.3).

Table 2.3. FLNA PCR primers

FLNA Regions	Forward primer	Reverse primer
Ex38	AGAAAGGAGGCAGCCTGTG	TGTGTTGATGTCCACCTTGC
Ex39-40	GAGGCTCAGGGGTATCCATC	GATGGGCTAGTGAGCAGCAG
Ex41	CCAAGAGGAGGGGTGGAG	CTGCCGGCTCTTTCCTC
Ex42-43	TCTACCTTGGCTATGCCTGG	CACTGAACACAGGGCCAAG
Ex40a	GCAGCCCCTTCTCTGTGA	AGGGATTTTCAGGCTGAGGT
Ex40b	GCAGCCCCTTCTCTGTGA	GATGGGCTAGTGAGCAGCAG
Var1	CACAGAGCCAGGCAACTACA	ACAAAGCGGATGCAGTAGGT

FLNA and β-integrin binding assay

Recombinant integrin tail (β7, β1A, and β1A Y788A) model proteins, consisting of an N-terminal His-tag sequence followed by a thrombin cleavage site, a cysteine-residue linker, and the specific integrin cytoplasmic domain, were produced, purified, and generously supplied by the Calderwood lab (Pfaff et al. 1998). The β1A Y788A mutation was previously shown to inhibit FLNA binding to β1A and served as a control for specific binding (Pfaff et al. 1998).

Binding assays using recombinant integrin tail model proteins were performed as previously described using GFP-fusion proteins (Lad et al. 2007a). A plasmid encoding human FLNA_GFP in pcDNA3 was generously supplied by the Calderwood lab. Point mutations C2160R and I2144E were introduced by QuikChange site-directed mutagenesis (Stratagene, La Jolla, CA). Chinese hamster ovary (CHO) cells were transfected with GFP-fusion constructs containing full-length human FLNA or FLNA mutants using Lipfectamine were harvested 48 hours later. Cell lysates were then incubated with integrin cytoplasmic tail model proteins bound to His-Bind® Resin (Novagen, Madison, WI). Bound proteins were fractionated by SDS-PAGE and analyzed by immunoblotting with anti-FLNA mAB1680 (Chemicon, Temecula, CA). Both binding of recombinant integrin tails to the resin and equal loading of coated resin was verified by Coomassie Blue staining of the SDS-PAGE-fractionated eluted proteins.

FLNA variant screening in PBS patients

Additional DNA sources from D081P

To test for possible mosaicism of an FLNA variant in PBS patient D081P, additional DNA was obtained from buccal swabs, urine, and duodenum biopsy (FFPE). DNA was extracted from the FFPE biopsy tissue using RecoverALL Total Nucleic Acid Isolation kit (Ambion). A fragment library from preparation of whole exome sequencing was obtained. The fragment library was produced from lymphocyte DNA that was fragmented, had universal adaptors annealed to each fragment, and had undergone seven rounds of amplification.

FLNA PCR and Sanger sequencing

Screening for mutations in FLNA was carried out by allelic discrimination and Sanger sequencing. For the allelic discrimination assay, Taqman probes for the FLNA c.6727T>C mutation was designed by Applied Biosystems. For mutation screening in sporadic PBS patients, PCR primers for FLNA exons 38 – 43 (coding for repeat domains 19 – 21) were designed using ExonPrimer (accessed through UCSC; Table 2.3). Primer pairs for only exon 40 (as the primer pair from ExonPrimer amplifies exons 39 and 40 in one product) are also listed in Table 2.3. PCR products were purified using Wizard SV Gel and PCR Clean-Up System (Promega) and Sanger sequenced at the McDermott Center Sequencing Core at UT Southwestern Medical Center.

Cloning FLNA exon 40 PCR product

A 216-bp amplicon of FLNA exon 40 was produced using corresponding FLNA Ex40b primers (Table 2.3) and isolated by gel extraction using Wizard SV Gel and PCR Clean-Up System (Promega). Next, pGEM-T Easy Vector System I (Promega) was used to clone the PCR product and DNA was extracted from isolated clones using Wizard Plus SV Minipreps DNA Purification System (Promega). Plasmid DNA was Sanger sequenced using the universal T7 primer at the McDermott Center Sequencing Core.

Results

I. D019P1 and D019P2 phenotyping

As FLNA variations are associated with specific clinical disorders, further phenotyping was performed on the PBS half-brothers D019P1 and D019P2 to determine overlap with other FLNA-associated disorders and additional family history of any clinical features (Figure 2.18).

Patient D019P1 (IV:2 in Figure 2.18), was diagnosed with bilateral hydronephrosis and renal dysplasia at 12 weeks gestation. At birth (32 weeks gestation), he presented with the cardinal features of PBS: abdominal muscle hypoplasia, ureteral dilation, an enlarged bladder, and bilateral cryptorchidism. His brother, patient D019P2 (IV:4 in Figure 2.18), was diagnosed with PBS in utero at 16 weeks gestation due to detection of a grossly enlarged bladder via ultrasound. At birth (32 weeks gestation), patient D019P2 also presented with abdominal muscle aplasia, ureteral dilation, an enlarged bladder, and bilateral cryptorchidism. In addition to the PBS features, both brothers also exhibit multiple facial and skeletal anomalies, including: ocular hypertelorism, micrognathia, camptodactyly, scoliosis and bowed limbs.

The D019 pedigree is also positive for a family history of both PBS and skeletal and facial anomalies. The affected probands had a maternal uncle (III:6) that died two weeks after birth with long digits, renal dysplasia, and features similar to PBS. According to family members, a maternal great uncle (II:6) also exhibited PBS features at birth. While many of the female family members do not have PBS features, facial and skeletal dysplasia phenotypes segregate within the pedigree. The mother D019M (III:2), maternal grandmother (II:2), maternal great aunt (II:3), and maternal great-grandmother (I:2) of PBS

probands D019P1 and D019P2 share many skeletal and facial dysplastic phenotypes, including camptodactyly, micrognathia with small facial features, and bilateral cleft palate. Although these relatives were unavailable for testing, recurrence of these FLNA-associated traits suggests segregation of the FLNA variant in this family. Comparing the non-PBS features identified in D019P1 and D019P2 to the OPD-spectrum disorders demonstrates overlap with many of the associated OPD phenotypes (Table 2.4). This comparison suggests that the PBS brothers exhibit a significant amount of overlap with MNS, a lethal disorder in males.

	D019P1	D019P2	OPD1	OPD2	FMD	MNS
Hearing loss	+	+	++	+++	++	N/A
Cerebellar hypoplasia	-	-	-	+	-	-
Cardiac anomalies	-	-	+	++	+	++
Omphalocele	-	-	-	++	-	+
Cleft palate	+	-	+	++	-	-
Developmental delay	-	-	-	++	-	N/A
Craniofacial anomalies	+	+	+++	+++	+++	+++
Prominent supraorbital ridges	+	+	++	++	+++	++
Downslanting palpebral fissures	+	-	++	++	+++	+/-
Ocular hypertelorism	+	+	++	++	+++	+/-
Full cheeks	-	+	-	-	-	+++
Micrognathia	+	+	-	++	-	+++
Facial asymmetry	+	-	-	-	-	+++
Skeletal dysplasia	+	+	+++	+++	+++	+++
Limited joint movement	+	+	++	++	++	N/A
Limb bowing	+	+	+	++	+/-	++
Long digits	+	+	+/-	+/-	+/-	++
Scoliosis	+	+	-	+/-	++	+++
Camptodactyly	+	+	-	++	-	-

Table 2.4. Overlap of phenotypes present in PBS D019 brothers and OPD-spectrum disorder males. Symbols in D019P1 and D019P1 denote presence (+) or absence (-) of phenotypic trait. For columns of otopalatodigital syndrome types I (OPD1) and II (OPD2), frontometaphyseal dysplasia (FMD), and Melnick-Needles syndrome (MNS), symbols denote the frequency with which phenotypic traits are associated with the diagnosis in males: not associated (-); rarely reported (+/-); common (+); frequent (++); and invariant component of the phenotype (+++). N/A in MNS denotes not applicable as MNS is embryonic lethal in males.

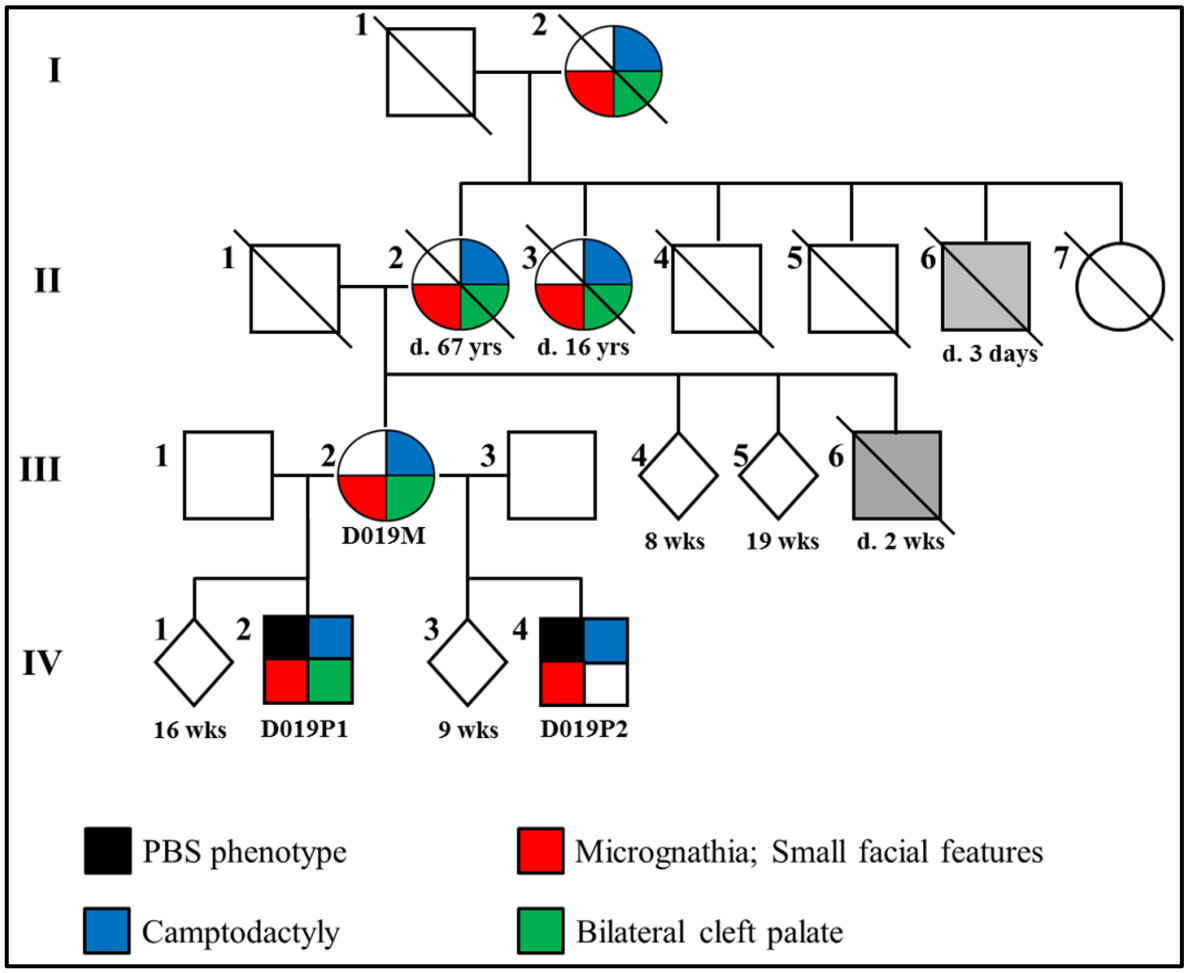

Figure 2.18. Expanded D019 pedigree showing additional anomalies. In family D019, black shading represents PBS phenotype; blue shading camptodactyly; red shading micrognathia and small facial features; green shading bilateral cleft palate. Grey shading represents unconfirmed PBS phenotype.

II. FLNA is highly expressed in human and mouse bladder

Expression of FLNA in human and mouse tissues was accessed by online databases and quantitative PCR (qPCR). According to GenePaint, an atlas of expression patterns determined by in situ hybridization, *Flna* is highly expressed in the developing bladder, abdominal wall musculature, and intestinal muscles in an E14.5 C57BL/6 mouse embryo. To verify this finding, qPCR was performed in the developing (E13 – P1) male mouse bladder, ureters, and kidneys (Figure 2.19). The results indicate enhanced expression during ureteric and bladder development as compared to the developing kidney.

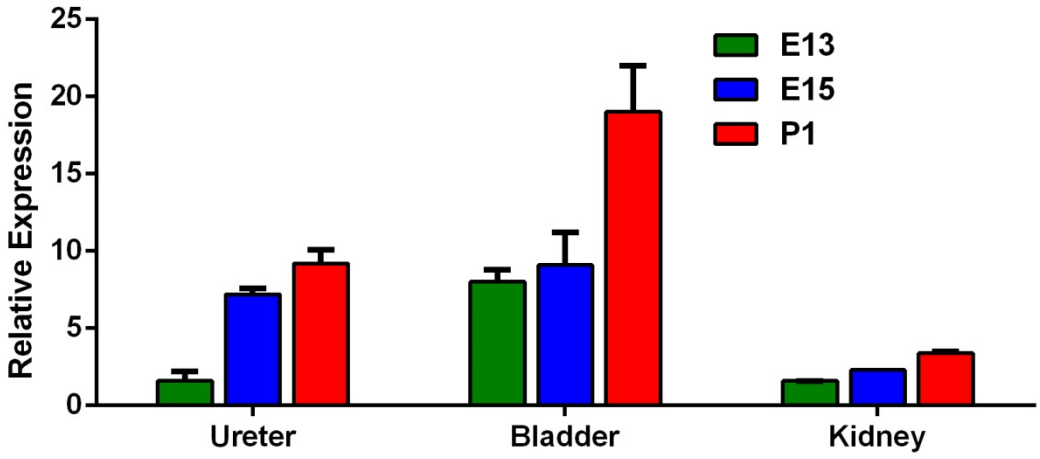

Figure 2.19. Flna mRNA is highly expressed in developing mouse bladder and ureter
Expression of Flna mRNA by qPCR in ureters, bladders, and kidneys from E13, E15, and P1 male mice. Flna expression was normalized to Cdkn1B.

Surgical tissues from the bladder, ureters, and abdominal wall of a human male 1.5 year old patient were assayed for FLNA expression via qPCR (Figure 2.20). FLNA was present in all three organs with the highest expression in the bladder. Due to limited tissue availability, additional negative control tissues, such as kidney, were not available.

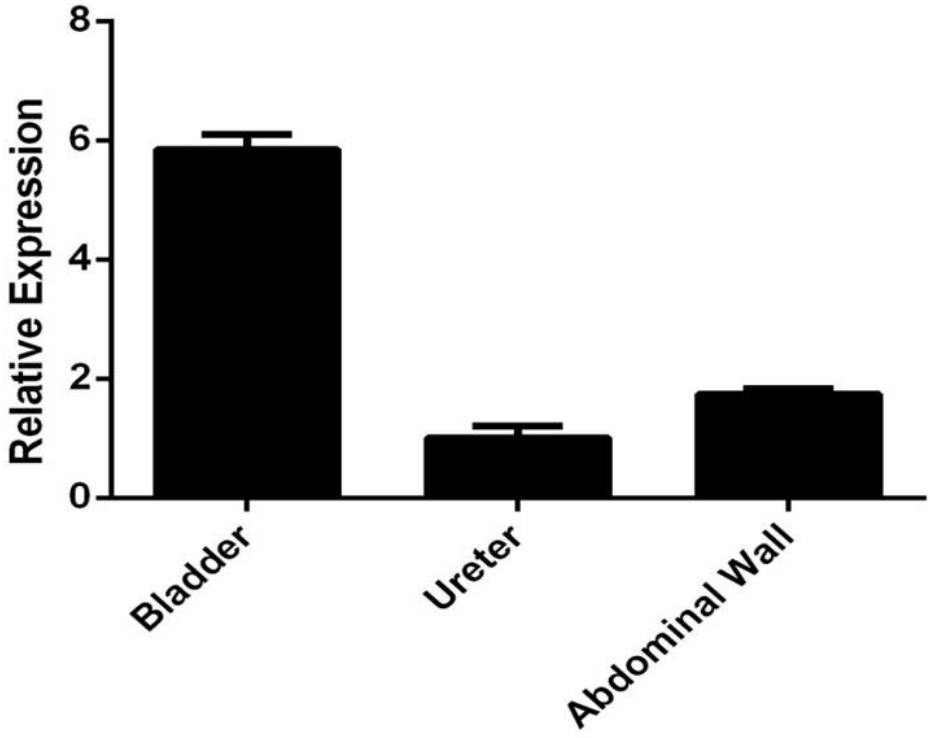

Figure 2.20. FLNA mRNA is highly expressed in human male bladder
Expression of FLNA mRNA by qPCR in surgical tissues from a human male 1.5 year old patient. FLNA expression was normalized to CDKN1B.

III. ITGB1 is highly expressed in PBS-affected human tissues

As FLNA is known to bind β-integrin 1 (ITGB1) and β-integrin 7 (ITGB7), the expression of both integrins were assayed in the bladder, ureters, and abdominal wall from a human male 1.5 year old patient. According to the results, ITGB7 is near absent in all tissues while enhanced expression of ITGB1 is observed in all three organs (Figure 2.21). These results suggest that the predominant FLNA binding partner in the PBS-affected organs (bladder, ureters, and abdominal wall) is ITGB1 and not ITGB7.

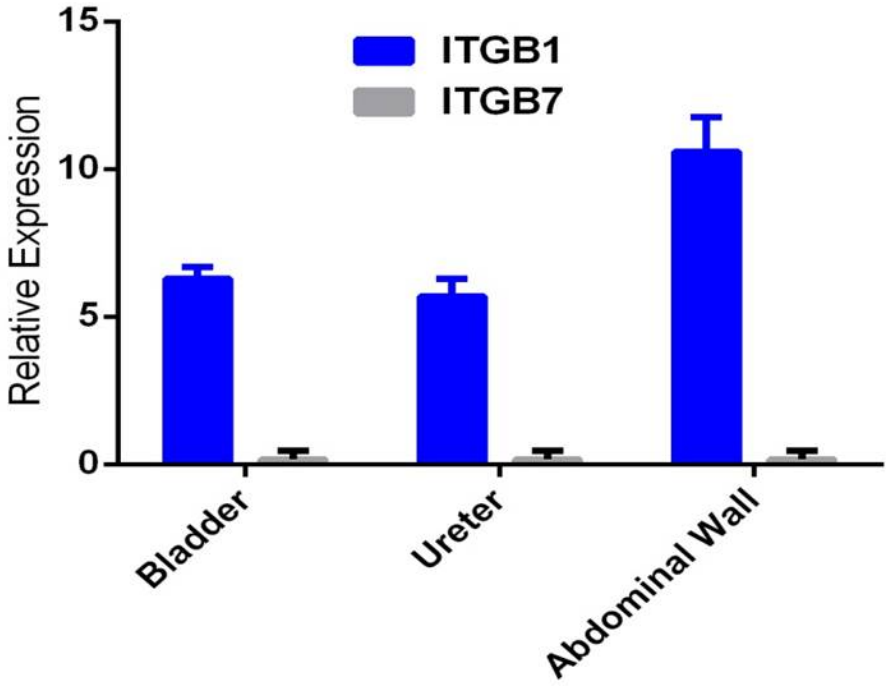

Figure 2.21. ITGB7 mRNA is highly expressed in human male PBS-affected tissues. Comparison of ITGB7 and ITGB1 mRNA expression by qPCR in surgical tissues from a human male 1.5 year old patient. Expression was normalized to CDKN1B.

IV. Full-length FLNA is the predominate isoform in human tissue

Expression of both full length FLNA and the splice variant FLNA-var1, which lacks 41 amino acids in Ig20, were compared in human tissue from a PBS patient and an age- and sex-matched control using RT-PCR. Only full-length FLNA, containing Ig20, was detected in the bladder, ureter, and abdominal wall musculature in both PBS and control human tissue (Figure 2.22).

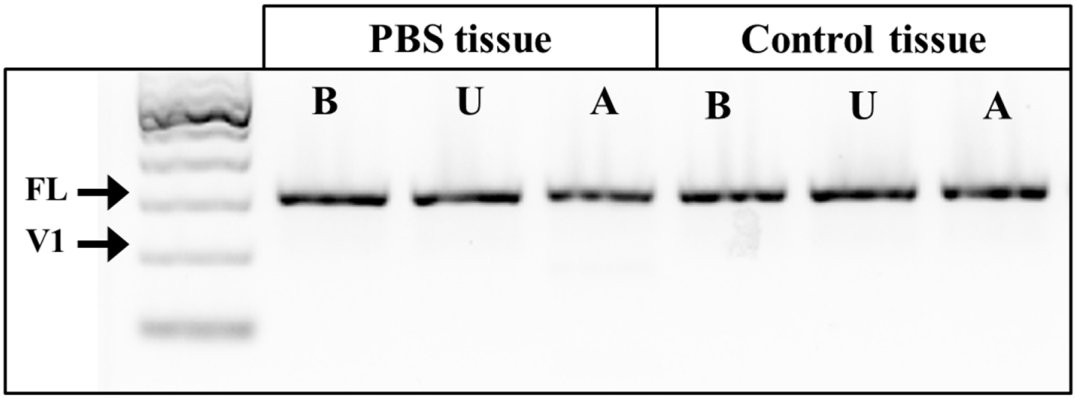

Figure 2.22. Full-length FLNA is the predominate isoform in human tissue. Expression of full-length FLNA (FL) or FLNA var-1 (V1) compared across bladder (B), ureter (U), and abdominal wall musculature (A) in human male tissue from a PBS patient and normal male control (both 1.5 yr at time of tissue collection).

V. FLNA variant C2160R enhances FLNA binding to β-integrins

The ability of β-integrin tails to bind FLNA was compared across cell lysates collected from CHO cells transfected with human full-length wild-type (WT), C2160R (mutation identified in PBS half-sibs), or I2144E FLNA. I2144E was included in this assay as previously reports indicate that this substitution destabilizes the Ig20-21 interaction and results in enhanced β-integrin binding compared to WT FLNA (Lad et al. 2007b).

Binding of human FLNA-WT, FLNA-I2144E, and FLNA-C2160R to β-integrin tails was assessed in pull-down assays with several β-integrin tails as bait (Figure 2.23). FLNA-C2160R exhibited enhanced binding to β7 integrin tails as compared to FLNA-WT (Figure 2.23.A). This finding was not limited to β7 integrins as C2160R also enhanced binding to β1A tails (Figure 2.23.B). Binding was accessed by comparisons of C2160R to FLNA-WT, FLNA-I2144E, and untransfected CHO cell lysates. Detection of equal loading of β-integrin tail coated resin in all lanes verifies that changes in FLNA/integrin binding are not due to differences in the amount of β-integrins in pull-downs. Additionally, immunoblotting for FLNA in whole cell lysates indicated near equal levels of FLNA production in all transfected cells (Figure 2.23.D). β1A Y788A did not pull down WT, C2160R, or I2144E FLNA, indicating that binding between FLNA and β7 or β1A integrins is specific (Figure 2.23.C).

The quantity of FLNA-C2160R binding to β-integrins is similar to binding assays with the previously studied FLNA-I2144E, suggesting that the C2160R point mutation is sufficient to destabilize Ig20-21 interactions, expose the integrin-binding site on Ig21, and enhances FLNA/integrin interactions.

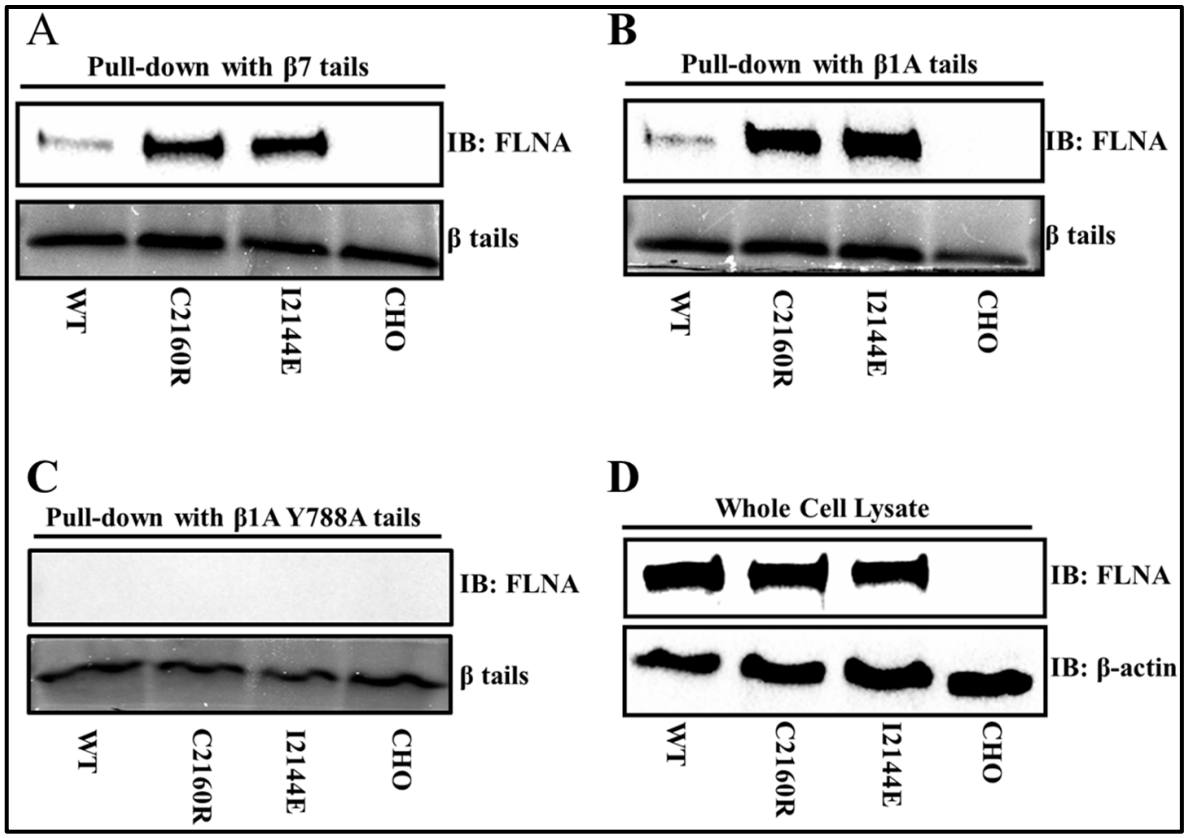

Figure 2.23. C2160R enhances FLNA binding to β-integrins

Pull-down assays were performed with β-integrin tails using lysates from CHO cells transfected with human FLNA-WT, FLNA-C2160R, FLNA-I2144E, or untransfected CHO cells; bound proteins were detected by immunoblotting with anti-human FLNA antibody. C2160R enhanced FLNA binding to both β7 (A) and β1A (B) integrin tails. Binding was abolished with β1A Y788 tails (C). Whole cell lysate (D) shows equal FLNA expression between transfected cells.

VI. FLNA variant testing in additional PBS patients

VI.1. Allelic Discrimination

To determine if FLNA variant c.6727T>C, coding for the C2160R missense mutation, is present in additional PBS patients, 73 PBS males and 2 mothers from PBS multiplex pedigrees (D020M and D040M) were screened by an allelic discrimination assay. Samples D019P1 and D019P2 were included as hemizgyous positive controls and D019M as a heterozygous control. All assayed male and female samples were hemizgyous or homozygous wild-type, respectively.

VI.2. Sanger sequencing

As allelic discrimination only assays for the single nucleotide change c.6727T>C, additional screening was required to detect other potential FLNA mutations in PBS patients. Given the auto-inhibitory structure of FLNA repeats Ig19–21 and the finding that C2160R or I2144E disrupts this structure, missense mutations in repeats Ig19–21 could have a similar effect. To identify potential mutations, exons 38–43 (encoding Ig19-21) were PCR and Sanger sequenced in 41 PBS males however non-synonymous variants were not identified.

VI.3. Exome Sequencing

To further delineate the genetic cause of PBS, whole exome sequencing was performed in 19 sporadic male PBS patients and the results analyzed to detect commonly implicated genes in this cohort (further explanation and results in Chapter 2 Part C). Whole exome sequencing identified the FLNA c.6727T>C; p.C2160R variant in one additional

PBS patient (D081P). However, the results indicate that the FLNA variant in D081P is not hemizygous as 110 reads at this locus contain the reference allele while only 32 reads contain the alternative allele (mutation frequency of 22.5%). This odd frequency suggests either D081P is mosaic for this variant or that this variant is a false positive due to errors in WES. Thus further studies are required to determine the validity of this variant in D081P.

VII. Assessment of potential mosaicism in D081P patient

VII.1. Sanger sequencing in multiple DNA sources from D081P

To determine if the FLNA C2160R variant in D081P was called due to errors in mapping or aligning reads from exome sequencing, exon 40 was amplified from the prepared fragment library from lymphocyte-derived DNA using either FLNA primer pair Ex40a or Ex40b (Table 2.3). Sanger sequencing of either amplicon identified an alternative peak at c.6727 (Figure 2.24.B). This peak of lower intensity, as compared to the WT "T" allele peak, is the alternative "C" allele detected by exome sequencing. These results suggest that the c.6727T>C variant was not called due to an error in variant calling or read mapping, as both primer pairs are specific to FLNA exon 40. However, these results do not rule out incorrect introduction of this variant during fragment library preparation.

Sanger sequencing from lymphocyte-derived genomic DNA did not detect a peak corresponding to the alternative "C" allele (Figure 2.24.A). PCR and Sanger sequencing of additional DNA sources (buccal cells, duodenal biopsy tissue, and epithelial cells from urine) also did not detect a peak corresponding to the alternative "C" allele. Additionally, the patient's mother (D081M) was found to be homozygous WT c.6727T.

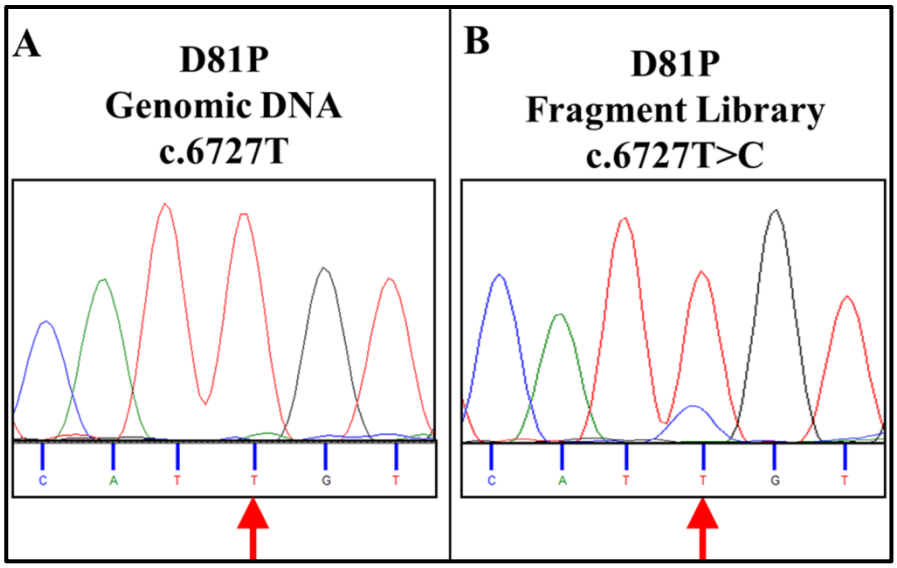

Figure 2.24. Sequencing D081P indicates FLNA variant c.6727T>C is present in fragment library but not genomic DNA. Sanger sequencing of genomic DNA from D081P lymphocytes (A) does not detect the c.6727T>C variant. A smaller peak corresponding to alternative "C" allele is present in D081P fragment library.

VII.2. Cloning FLNA exon 40 amplicon from D081P

Whole exome sequencing on lymphocyte-derived DNA from patient D081P identified the FLNA c.6727T>C variant. If patient D081P is mosaic for the FLNA c.6727T>C variant, then a population of lymphocytes should harbor the mutation as whole exome sequencing on the lymphocyte-derived DNA identified the variant. However, Sanger sequencing lymphocyte-derived DNA from patient D081P did not detect this variant (Figure 2.24.A). To determine if the variant was undetectable by Sanger sequencing genomic DNA due to low frequency of cells containing the variant, clones generated by cloning an amplicon containing exon 40 from D081P lymphocyte-derived DNA were screened. In total, 30 clones containing the FLNA exon 40 insert were tested by Sanger sequencing, however none were found to have the c.6727T>C variant.

Discussion

I. C2160R is the only human FLNA variant in Ig20 domain

Exome sequencing two PBS half-brothers identified a novel c.6727T>C; C2160R missense mutation in FLNA, an actin-binding protein that regulates the actin cytoskeleton response to external and internal cues. Aberrations to FLNA are associated with a series of human disorders with high genotype-phenotype correlation depending on the FLNA domain-specific functions. The identified novel PBS variant (C2160R) is significant as this variant not only occurs on FLNA rod 2 but also in Ig20, a well-studied domain hypothesized to play a major regulatory role in FLNA interactions but not associated with any prior identified human disorders (Figure 2.17).

More than 44 missense variants, 30 nonsense variants, 17 splicing variants, 35 indels, and 10 whole gene CNVs have been described in patients with FLNA-associated phenotypes. Aside from missense variants, the remaining changes are predicted to cause loss of function, shortened isoforms, and incorrectly translated FLNA. 44 missense mutations have been identified in patients with OPD-spectrum disorder or cardiac valvular dysplasia and 98% of these variants occur in the actin-binding domain and rod 1. Previously, only one FLNA missense variant has been identified on rod 2: a F2345S heterozygous change in Ig22 in an OPD-spectrum disorder female patient. The fact that 98% of FLNA missense variants occur in the actin binding domain and rod 1 suggests that the disease-causing variants in these locations impact physical interactions between FLNA and actin. In contrast, regulatory rod 2 (Ig16–Ig23) does not bind actin and instead has a prominent mediating actin cytoskeletal remodeling by receiving internal and external signals; suggesting that human mutations in rod 2 are more likely to be embryonic lethal.

II. Assessment of possible mosaicism in D081P

WES of 19 sporadic PBS cases identified the FLNA c.6727T>C; p.C2160R variant in a third, unrelated patient (D081P). The results from this sample are confounding as the c.6727T>C variant was only detected in 23% of the reads. As D081P is male with a single chrX, the frequency of an identified variant should be 0% or 100% suggesting either D081P is mosaic or the variant calling is due to errors in WES. Contamination of the D081P sample with D019P1 or D091P2 DNA can be ruled out as DNA extraction, exome library preparation, and exome sequencing were carried out years apart.

False positives in WES can occur when contigs are mapped to incorrect genomic coordinates if the contig has high homology to an off-target genomic region. Exon 40 of FLNA, including both the c.6727T nucleotide and p.C2160 residue, is highly conserved among the filamin family (filamin A, B, and C). Thus, calling of the variant is not due to sequence variation among the filamin family and no other homologous regions were identified. Additionally, sequencing the fragment library (both pre- and post-capture) with two sets of primers specific for this locus confirms the presence of the variant in the library preparation stage. However, the inability of Sanger sequencing to detect the variant in lymphocyte DNA or 30 clones of FLNA exon 40 from D081P lymphocyte DNA suggests D081P is not mosaic. If exome sequencing detected the variant in lymphocyte-derived DNA at an estimated 23% occurrence then the variant should be present in multiple clones.

The above data suggest that PBS patient D081P does not harbor the same FLNA variant identified in D019P1 and D019P2; however, this FLNA mutation c.6727T>C; p.C2160R is absent from all known human genetic databases, included dbSNP, 1000 genomes, NHLBI EVS (~6500 samples), the Human Gene Mutation Database (HGMD),

and all known published literature. The fact that this identical variant has only been identified in other PBS patient supports the hypothesis that D081P is mosaic for this variant; however further studies are required to confirm this hypothesis.

Theoretically, if patient D081P has PBS due to mosaicism of FLNA variant c.6727T>C, then this variant should be present in DNA extracted from PBS-affected organs, such as abdominal wall, bladder, and ureters. Currently, the only sources of DNA from PBS patient D081P are lymphocytes, buccal cells, duodenal biopsy tissue, and epithelial cells from urine. If the mosaic hypothesis is correct, none of these cell types are necessarily expected to harbor the FLNA variant, except possibly the epithelial cells within the urine samples. Epithelial cells in urine are primarily shed from renal tubular cells or bladder urothelium, which have a different embryonic origin compared to muscle cells, which may explain why the variant is absent in this DNA source. To truly confirm the presence or absence of the FLNA c.6727T>C variant, muscle biopsy from the bladder, ureters, or abdominal wall is needed. At present, these tissues are unavailable, but D081P will undergo bladder reconstruction and an abdominoplasty in the near future. Once these sources are available, DNA derived from the PBS-affected organs can be assayed for presence of this variant.

III. C2160R results in enhanced FLNA/integrin binding

The identified novel missense mutation C2160R occurs in FLNA rod 2 in Ig20. While no human mutations have been published in repeat domains Ig19, 20, or 21, these regions have been heavily studied as they form an auto-inhibitory structure that regulates β-integrin binding at FLNA Ig21.

Functional characterization of the identified C2160R variant in FLNA Ig20 (Figure 2.23) indicates that C2160R likely results in an "open" FLNA Ig20-Ig21 structure, exposing Ig21 to freely bind β-integrins without regulation. Impaired cellular properties are associated with enhanced FLNA/integrin interactions as FLNA and talin binding sites overlap on β-integrin tails (Calderwood et al. 2001; Kim et al. 2008). Talin binding activates integrin, which is necessary for focal adhesion formation and ECM-cell signaling; however talin only associates with β-integrin when FLNA/integrin interactions are diminished. These findings suggest that enhanced FLNA/integrin binding results in loss of cellular mechanosensing properties and may account for the PBS phenotype in patients hemizygous for the C2160R FLNA variant.

In healthy cells, regulation of FLNA/integrin binding at Ig21 is accomplished by two mechanisms: alternative splicing of FLNA and force-induced exposure. Alternative splicing of FLNA removes exon 40 (exon of C2160R variant), generating FLNA-var1, an isoform lacking 41 amino acids from Ig20 (van der Flier et al. 2002). The identified PBS mutation C2160R occurs within the 41 amino acids absent from FLNA-var1. If FLNA-var1 is the predominate isoform detected in PBS-affected organs (bladder, ureters, abdominal wall musculature), the functional impact of C2160R would be attenuated as this residue would be absent from the organs of interest. However, only full-length FLNA was detected in human organs of interest (Figure 2.22), supporting the hypothesis that FLNA C2160R is the PBS-phenotype causal variant.

These observations suggest that FLNA binding to integrin functions as a cellular brake to inhibit integrin activation which in turn inhibits ECM-cytoskeleton communication. This cellular brake is alleviated by inhibiting FLNA/integrin interactions

which promotes integrin activation and cellular processes dependent on integrin activation, such as cell adhesion junctions, migration, and contraction. Functional testing indicates that C2160R variant enhances FLNA/integrin binding, which according to the above hypothesis inhibits ECM-cell signaling, and thus may explain the PBS phenotype in PBS patients with the FLNA variant.

IV. Hypothesized modes of PBS pathogenesis due to C2160R FLNA variant

As C2160R occurs on rod 2, the rod characterized by protein-protein interactions and signal transduction, this variant is hypothesized to disrupt the role of FLNA in mechanosensing. Through interactions with integrins, FLNA induces changes in cell morphology or contractility by perceiving changes in ECM stiffness or force generation and enacting the corresponding changes on the actin cytoskeleton. FLNA variant C2160R may impair the ability of the cell to sense the stiffness of the ECM or external forces and correctly regulate its own stiffness or response. Thus, the perturbed muscle phenotype associated with PBS (absent abdominal wall musculature and disorganized, non-functional detrusor smooth muscle in the bladder) may be caused by disruptions in the mechanosensing role of FLNA in cell differentiation, protection, and contraction.

IV.1. Differentiation

Lineage commitment of naive mesenchymal stem cells (MSCs) is partly determined by stiffness of the surrounding ECM. Soft matrices that mimic brain environments result in neurogenic cells, stiffer matrices that mimic muscle result in myogenic cells, and rigid matrices that mimic collagenous bone result in osteogenic cells

(Engler et al. 2006). Thus proper differentiation requires functional focal adhesion networks to sense the stiffness of the microenvironment. A previous study found that culturing cells in increasing matrix densities increases the quantity of FLNA/integrin binding suggesting that the quantity of FLNA/integrin binding provides a mechanism by which a cell determines the stiffness of the ECM (Gehler et al. 2009). Due to variant C2160R, FLNA/integrin binding is enhanced which may result in the cell incorrectly ECM stiffness during embryonic development. Altered mechanosensing may in turn change cell commitment and result in incorrect cell differentiation, proliferation, and organization of skeletal/smooth muscle layers within the developing organs. This altered cell fate may explain the perturbed function of bladder detrusor smooth muscle cells and the absence of abdominal wall musculatures in PBS patients. This hypothesis that FLNA dictates normal patterning of muscular layers within organs is supported by evidence of abnormal lamination of the small intestinal muscularis propria in chronic idiopathic intestinal psuedoobstruction (CIIP) patients with FLNA mutations (Kapur et al. 2010).

IV.2. Protection

Upon application of force, intracellular cytoskeletal remodeling is necessary to maintain membrane integrity and shape. Failure to adapt to applied mechanical stimuli can induce apoptosis and loss of normal tissue function, as described in skeletal and cardiovascular tissues (Cheng et al. 1995; Clements et al. 2001). FLNA is known to protect against force-induced cell depolarization and death by enhancing formation and maturation of focal adhesions (Pinto et al. 2014). In the absence of FLNA, force application results in irreversible cell depolarization and cell death (Kainulainen et al. 2002).

Focal adhesion recruitment and strengthening is largely dependent on talin-induced β-integrin activation as talin binding converts integrin from a low-affinity state to a high-affinity state. In the high-affinity state, preferential binding of ECM ligands to specific integrins initiates signaling pathways regulating cell growth, division, survival, and differentiation. Variant C2160R results in enhanced FLNA/integrin binding which in turn presumably inhibits integrin/talin binding and subsequent integrin activation. Thus, by inhibiting integrin activation, C2160R may prevent proper cell-ECM adhesion complexes which in turn inhibits the cell's ability to protect against force-induced apoptosis. A characteristic feature of PBS is the absence (or significant lack) or abdominal skeletal muscles. Perhaps in the case of FLNA C2160R, the mutant protein is incapable of this cytoprotective role due to inhibition of integrin activation. Thus, abdominal skeletal muscles are unable to correctly adapt to applied mechanical force, thus causing apoptosis of abdominal skeletal muscle cells.

A similar mechanism may also account for the bladder detrusor smooth muscle cell phenotype observed in PBS patients. When the bladder is unable to void urine, as seen in patients with PBS or bladder outlet obstruction, the detrusor muscle is chronically stretched, resulting in increased oxygen consumption and decreased contractile function (Arner et al. 1990; Gosling et al. 2000). As a result of bladder outlet obstruction and resulting hypoxia, levels of hypoxia-inducible factor 1α (HIF-1α) increase and full-length FLNA is cleaved to FLNA rod 2 (Ekman et al. 2014). FLNA rod 2 facilitates nuclear localization of HIF-1α, thereby activating HIF-1α-dependent target genes (Zheng et al. 2014). As variant C2160R occurs on FLNA rod 2, perhaps this variant results in loss of hypoxia–induced cytoprotection of bladder detrusor smooth muscle cells.

IV.3. Contractility

In response to nerve-generated neurotransmitter stimulation for detrusor contraction, smooth muscle cells generate internal contractile tension to exert force on the ECM or neighboring cells, resulting in myosin-mediated contractility (Giannone & Sheetz 2006). A cell's ability to "pull or push" upon a substrate largely depends on FLNA as a mechanosensor to sense the stiffness of the environment and regulate cell tension against the environment in response. The buildup of cellular tension requires cross-linking of actin by FLNA as loss of FLNA results in a strong decrease in internal contractile tension and fluid cells that cannot regulate their own stiffness (Kasza et al. 2009).

Cytoskeletal reorganization upon myosin-generated internal force is largely dependent on FLNA/β-integrin interactions. Overexpression of FLNA Ig21 (which will freely bind β-integrin without inhibition by Ig20) reduces contractile function and myosin activation suggesting that enhanced FLNA/integrin binding is detrimental to contractility (Gehler et al. 2009). In the context of PBS, the C2160R variant may prohibit generation of internal forces needed for detrusor cells to contract against the ECM to facilitate complete expulsion of urine with voiding.

Another hypothesized mechanism for detrusor underactivity in PBS patients with FLNA C2160R variant is excessive local concentration of actin. β1-integrin recruits both FLNA and actin to focal adhesions containing β1-integrin in a force-induced manner (Glogauer et al. 1998). Without regulation, enhanced FLNA/integrin binding also enhances the local concentration of cross-linked actin. The amount of actin is an important determinant of both contraction and actomyosin activity as increased actin results in a slower and incomplete contraction (Janson et al. 1991). In PBS patients, enhanced

FLNA/integrin binding due to C2160R variant may result in excessive actin localization and inhibition of detrusor muscle contraction.

V. FLNA as a candidate PBS gene

Both the known functions of FLNA and results from this study strongly support FLNA as a candidate PBS gene and C2160R as the casual variant in PBS pathogenesis in D019P1, D019P2, and possibly D081P (pending further studies). Iterative phenotyping of D019P1 and D019P2 found phenotypic overlap with OPD-spectrum disorders (Table 2.4). Additionally, the patient possibly mosaic for FLNA C2160R (D081P) also exhibits skeletal anomalies, including bilateral hip dysplasia and scoliosis. The absence of variants in FLNA Ig19–21 in an additional 57 PBS patients (by either WES or Sanger sequencing regions of interest) suggests that FLNA variants are not a common cause of PBS. Instead, FLNA variants may account for severe cases of PBS or PBS patients that also present with skeletal and facial anomalies. Additionally, PBS patients may harbor CNVs altering FLNA Ig20; however, the entire PBS cohort has not been tested by aCGH or MLPA, thus the frequency of FLNA CNVs remains to be determined.

Identification of FLNA as a candidate PBS gene also uncover molecular pathways that when perturbed may account for additional PBS patients. The FLNA C2160R variant is hypothesized to impair the mechanosensing machinery of the cell however integrins, talin, migfilin, and other proteins mediated membrane adhesion complexes are also necessary for this function. Thus variants in these additional genes may also disturb cellular functions by a similar mechanism as C2160R and result in a similar PBS

phenotype. In addition, as FLNA rod 2 has transcriptional functions, continued studying of this FLNA C2160R rod 2 variant may uncover additional regulatory pathways.

CHAPTER 2 PART C: IDENTIFICATION OF CANDIDATE GENES BY WHOLE EXOME SEQUENCING SPORADIC PBS PATIENTS

Introduction

Familial cases of PBS were initially selected for candidate gene identification via chrX linkage and WES as familial recurrence significantly increases the likelihood that a disease is monogenic and nearly eliminates the problems of genetic heterogeneity (Boycott et al. 2013). Related individuals will have presumably inherited an identical disease-causing variant which facilities variant filtering to identify a causal variant. However, familial recurrence of PBS is very rare, with less than 20 multiplex kindreds documented worldwide (Balaji et al. 2000; Ramasamy et al. 2005). Of the 93 male PBS patients recruited to this study, only nine patients have a familial recurrence of PBS, which limits the availability of sequencing the exomes of only familial PBS cases.

As the remaining 84 non-familial PBS patients in this study are sporadic, the inheritance of a disease-causing variant is unknown as the mutation could be *de novo*, dominant with reduced penetrance or sex bias (as 97% of PBS patients are male), or recessive. In sporadic cases, affected related family members are unavailable to facilitate variant filtering or for segregation analysis of causal variants. These hurdles can be overcome by sequencing the exomes of multiple unrelated PBS patients and first compiling a list of candidate genes in each patient. Next, candidate gene lists are compared to identify genes implicated in multiple patients in this cohort as identification of variants

in the same gene in unrelated patients is highly suggestive that the candidate gene is causal in disease pathogenesis (Boycott et al. 2013; Paria et al. 2013).

On average, WES of a single patient will identify novel variants in 333 genes. The addition of a second and third unrelated patient (with the same phenotype) and comparing implicated genes across all patients will reduce the candidate gene list from 333 genes to 33 and 8 genes, respectively (Paria et al. 2013). This approach of comparing implicated genes discovered by sequencing only the exomes of unrelated patients has identified novel genes for Freeman-Sheldon syndrome, Floating-Harbor syndrome, Kabuki syndrome, and Miller syndrome (Ng et al. 2009; Ng et al. 2010a; Ng et al. 2010b; Hood et al. 2012). To further delineate the genetic cause of PBS, the exomes of 19 sporadic males patients were sequenced to identify candidate PBS genes.

Methods

Exome sequencing was prepared and performed at the UT Southwestern Medical Center McDermott Center Sequencing Core following the same protocol as outlined in Chapter 2 Part A (pg 30).

Results

The exomes of 19 sporadic, unrelated PBS male patients of varied ethnicity (15 Caucasian patients and 4 African-American) were sequenced. On average, 4.14 Gb of sequence was generated per sample to achieve an average 67X coverage of the mappable, targeted exome (62 Mb) (Table 2.5). Anticipating that synonymous variants are less likely to be pathogenic, each of the 19 sporadic PBS samples was filtered to focus on exonic non-

synonymous variants and frameshift indels. As inheritance in sporadic PBS patients in unknown, both homozygous and heterozygous variants were included. Given the rarity of PBS (1:30,000 – 1:50,000) variants with MAF >0.02% in 1000 Genomes Project or NHLBI ESP were excluded, as Caucasian and African-American individuals are represented in both databases. On average, 229 rare (MAF <0.02%) non-synonymous or frameshift variants were identified in each PBS sample (Table 2.5).

PBS ID	Ethnicity	Gb of sequence	Ave. coverage	Number of rare NS or FS variants
D006P	AA	4.40	71X	310
D017P	C	3.68	59X	222
D026P	C	3.77	60X	324
D050P	C	6.55	106X	373
D058P	C	3.23	52X	176
D060P	C	2.77	44X	208
D061P	C	2.88	46X	134
D062P	C	3.05	49X	131
D065P	C	3.37	54X	172
D066P	C	3.19	51X	173
D068P	C	4.71	76X	188
D069P	C	4.28	69X	171
D071P	C	3.31	53X	156
D074P	C	3.44	55X	215
D075P	AA	3.93	63X	257
D076P	AA	4.80	77X	341
D078P	C	4.21	68X	149
D081P	C	6.43	103X	341
D082P	AA	6.74	108X	305

Table 2.5. Results from whole exome sequencing 19 sporadic male PBS patients
WES of 19 sporadic PBS patients of varied ethnicities (AA African-American; C Caucasian) generated between 2.77 – 6.74 gigabases (Gb) of sequence. On average, the 62 Mb targeted exome had between 44X – 108X coverage. Each of the 19 samples were filtered to identify rare (MAF <0.02%) non-synonymous (NS) or frameshift (FS) variants.

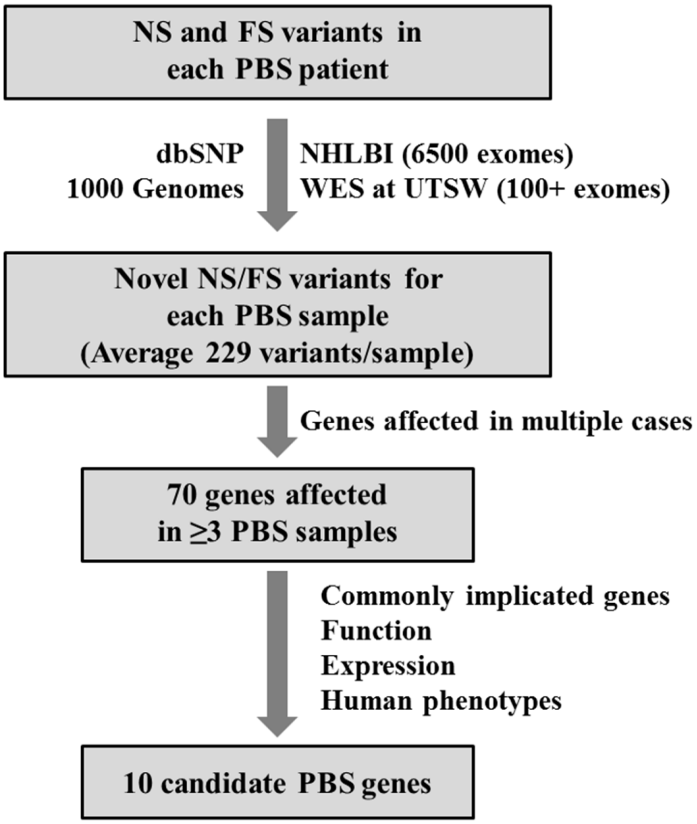

Figure 2.25. Filtering approach to identify candidate genes from whole exome sequencing 19 sporadic PBS patients

Non-synonymous (NS) and frameshift (FS) variants were identified in each of the 19 sporadic PBS samples. Next, only rare or novel NS and FS, defined as ≤0.02% MAF in dbSNP, 1000 Genomes, NHLBI, or any exomes sequenced at UTSW were selected. This filtering approach identified on average 229 rare NS or FS variants per sample. Next, genes containing variants that meet the above criteria were compared across all 19 samples; identifying 70 genes with rare variants in ≥3 PBS samples. The 70 punitive candidate genes were next filtered based on function, expression, known human phenotypes associated with variants in the gene, and frequency of variants identified within the gene, revealing 10 strong candidate PBS genes.

Next, genes containing rare (MAF <0.02%) non-synonymous or frameshift variants in each PBS sample (Table 2.5) were compared across samples to determine the number of PBS patients containing a variant in each gene (Figure 2.25). This candidate gene approach identified 70 genes implicated in ≥3 PBS samples. No candidate genes were shared across all 19 exomes. Candidate genes with the highest count in PBS patients (6 patients each) were immunoglobulin-like and fibronectin type III domain containing 1 (*IGFN1*), mucin 4 (*MUC4*), axonemal central pair apparatus protein (*HYDIN*), and titin (*TTN*).

The 70 punitive candidate PBS genes were further filtered based on known function, expression (specifically focusing on bladder expression), and phenotypes associated with each gene. Filtering also excluded commonly implicated genes as determined by variant frequency from published databases and occurrence of variants in published exome sequencing projects of unrelated individuals. *TTN* was excluded due to size (>109,000 nucleotides and >35,000 amino acids in length), high incidence of variants (2753 non-synonymous and frameshift variants according to NHLBI ESP), and frequent identification of novel variants by exome sequencing (Lilleoja et al. 2012). Based on the above criteria, *MUC4* and *HYDIN* were also excluded from the PBS candidate gene list (Ng et al. 2010a). Filtering based on function, expression, human phenotypes, and frequency of gene variants identified 10 strong candidate PBS genes (Table 2.6).

.

Count	Gene	Gene name	Chr	Expressed in human bladder	Variants predicted damaging
6	IGFN1	immunoglobulin-like and fibronectin type III domain containing 1	1q32.1	Yes	5/6
5	HSPG2	heparan sulfate proteoglycan 2	1p36.12	Yes	4/5
3	RYR2	ryanodine receptor 2	1q43	Yes	3/3
3	ITPR2	inositol 1,4,5-trisphosphate receptor, type 2	12p12.1	Yes	2/3
3	ITGB2	integrin beta 2	21q22.3	Yes	1/3
3	PLCE1	phospholipase C epsilon 1	10q23.33	Yes	3/3
3	MLL2	myeloid/lymphoid or mixed-lineage leukemia 2	12q13.12	Unknown	1/3
3	LRP2	low density lipoprotein receptor-related protein 2	2q31.1	Unknown	1/3
3	SYNE2	spectrin repeat containing nuclear envelope 2	14q23.2	Yes	3/3
3	MYO9B	myosin IXB	19p13.11	Yes	1/3

Table 2.6. Candidate PBS gene list from exome sequencing 19 sporadic PBS patients
Count represents the number of sporadic PBS patients with a rare variant in each candidate gene (n=19). 'Variants predicted damaging' column represents the number of variants predicted damaging by PolyPhen2 or SIFT out of the total number of variants in this gene in this cohort.

Discussion

I. PBS sporadic case selection

This study represents the first attempt to identify candidate PBS genes by sequencing the exomes of unrelated PBS patients. Familial PBS cases have been recruited and are ideally suited for WES (Figure 2.3) as sequencing the exomes of D019P1 and D019P2 identified a novel, hypothesized-causal FLNA variant and WES is currently underway on PBS family D018 (two PBS brothers, one unaffected brother). PBS multiplex families D020 and D040 are not suited for WES as the affected individuals are deceased leaving FFPE tissue as the only source of DNA. While the exomes from biopsy FFPE specimens has been successfully sequenced, biopsy specimens are formalin-fixed and embedded in paraffin for short periods of time as degradation of nucleic acids by fixation occurs in a time-dependent manner (Menon et al. 2012). Conversely, DNA from FFPE autopsy specimens is highly degraded due to delays in tissue fixation postmortem and prolonged formalin exposure (Okello et al. 2010). For these reasons, sporadic PBS exomes were selected for exome sequencing instead of the two remaining multiplex PBS kindreds.

Of the 84 sporadic PBS patients in this study, patients were selected for WES based on ethnicity and availability of additional family members. To facilitate filtering of novel or rare variants identified by WES, public databases with large numbers of ethnically matched individuals are needed to determine the MAF of each variant. European-American and African-American individuals are well represented (4300 and 2203 unrelated individuals, respectively) in the most recent NHLBI ESP data release (ESP6500) while Asian and Hispanic ethnicities are underrepresented or absent. Due to underrepresentation, common ethnicity-specific variants may be incorrectly categorized as novel or rare,

confounding filtering approaches to narrow variants. For these reasons, PBS patients of European or African descent were selected for WES.

In sporadic cases with no familial history, inheritance is unknown, thus PBS patients with recruited family members were selected for WES to facilitate inheritance or segregation analysis of an identified variant. Of the 19 sporadic PBS patients selected for WES, both paternal and maternal DNA samples are available on 15 patients. Additionally, six of the sporadic PBS patients have an unaffected brother, the inclusion of which may be utilized in determining penetrance or causality of inherited variants.

II. Filtering approach

The approach of this study was to compare multiple PBS sporadic cases to identify candidate PBS genes. This approach assumes that a single variant is sufficient to cause PBS, that the variant is rare and private to PBS patients, and that the variant is likely coding and highly penetrant. Failure to comply with any of these assumptions may incorrectly exclude a PBS causal variant. This approach also assumes that variants must be present in multiple (≥3) PBS patients for a gene to be categorized as a candidate PBS gene. As seen previously in this study, WES D019P1 and D019P2 identified a novel FLNA variant but additional FLNA variants were not detected in sporadic PBS patients (not including a potential mosaicism in PBS patient D081P). Thus, excluding genes implicated in less than three sporadic PBS patients may discount a potential PBS candidate gene.

Narrowing the PBS candidate gene list from 70 to 10 genes by excluding commonly implicated genes, such as *TTN* and *HYDIN*, may also incorrectly exclude a potential PBS causal gene as novel variants in both *TTN* and *HYDIN* are causal in

cardiomyopathy and primary ciliary dyskinesia pathogenesis (Olbrich et al. 2012; Toro et al. 2013). Given these considerations, candidate genes identified from PBS sporadic WES should be viewed as a preliminary candidate gene list as further studies are needed to validate the inclusion (or exclusion) of identified candidate genes. As this approach only considers 19 of the 84 sporadic PBS patients, subsequent Sanger sequencing of candidate genes in the remaining 65 sporadic PBS patients may identify additional rare variants and increase the ranking of a PBS candidate gene. In the instance of Kabuki syndrome, a similarly applied overlap strategy identified *MLL2* as a candidate gene from exome sequencing 10 sporadic patients (Ng et al. 2010a). *MLL2* variants were identified in seven patients by WES but subsequent Sanger sequencing identified *MLL2* indels in two of the three remaining patients that were missed by WES. By this logic, counts of sporadic PBS patients with variants in a specific candidate gene may be underestimated, requiring re-sequencing of select candidate genes within these 19 sporadic PBS patients.

III. Candidate PBS gene list

Filtering the initial 70 candidate genes implicated in ≥3 PBS sporadic patients, identified 10 strong PBS candidate genes (Table 2.6). Interestingly, many of these candidate genes, along with FLNA, support a hypothesis of perturbed muscle cell function (Figure 2.26; first introduced in Figure 2.14). *IGFN1* is the highest ranked PBS candidate gene on this list as six PBS patients harbor rare variants in *IGFN1*. IGFN1 interacts with filamin C, is expressed in skeletal muscles, and contains five Ig-like domains (Beatham et al. 2004). Additionally, three PBS patients each were found to have rare variants in ryanodine receptor 2 (*RYR2*) and inositol 1,4,5-trisphosphate receptor, type 2 (*ITPR2*), both

of which are required for the release of calcium from the sarcoplasmic reticulum. RYR2 and ITPR2 are necessary for muscle cell contraction as an influx of intracellular calcium is needed for activation of the myosin light chain kinase (MLCK) which in turn phosphorylates myosin. Perhaps variants in *RYR2* and *ITPR2* in PBS patients cause incomplete cell contraction. Rare variants in integrin beta 2 (*ITGB2*) were also identified in three PBS patients. All three variants occur in the extracellular domain of ITGB2 suggesting that *ITGB2* variants in PBS patients may perturb cellular mechanosensing of the extracellular environment.

Identification of an FLNA variant in familial PBS and additional candidate genes by sporadic WES suggest that PBS is a genetically heterogeneous syndrome caused by variants affecting cellular contraction or mechanosensing functions. PBS cardinal features are present in all patients in this cohort; however, the frequencies of orthopedic, cardiopulmonary, and neurologic abnormalities vary. The differences in clinical presentations may be explained by the range of candidate PBS genes identified. To further validate these genes as potentially causal in PBS pathogenesis, iterative phenotyping of PBS patients is required to determine if presented abnormalities overlap with phenotypes described for each candidate gene, as detailed with D019P1 and D019P2 to compare abnormalities associated with FLNA variants. Correlations of genotype and phenotype within this small but well phenotyped patient population will assist in the validation of PBS candidate genes. Additionally, segregation analysis within these families will determine if the variant is *de novo* or suggest noncausality or variants present in unaffected brothers of PBS patients.

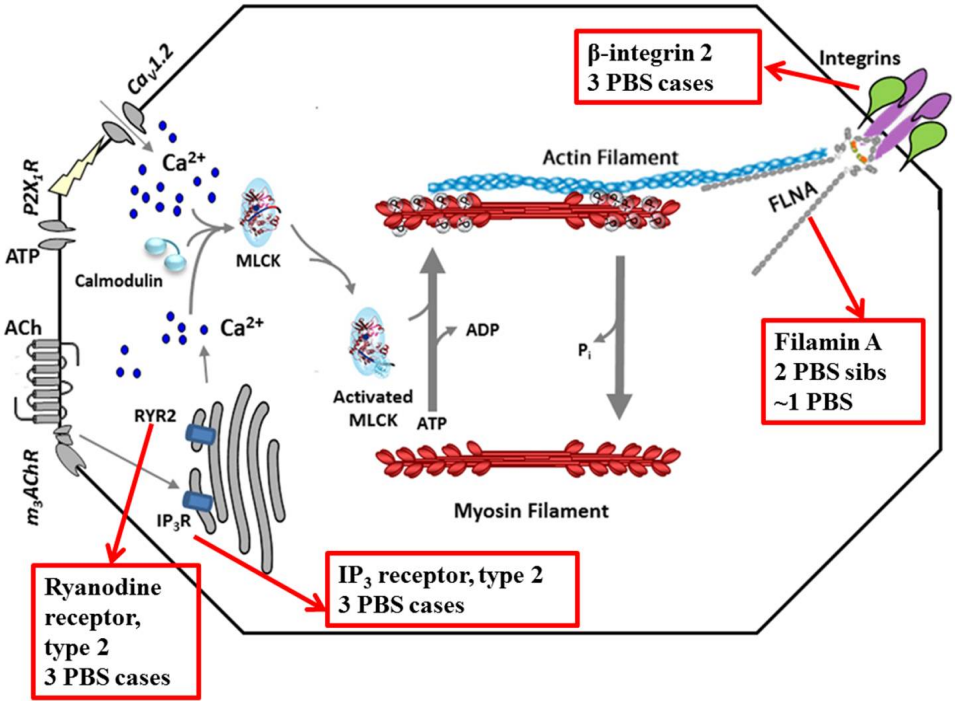

Figure 2.26. PBS candidate genes in cell contraction model
Model of cell contraction first described in Figure 2.14. In addition to the FLNA variant identified in two PBS half-brother (and possible third mosaic patient), sporadic PBS exome sequencing identified rare non-synonymous variants in: ryanodine receptor 2 (RYR2), 3 PBS patients; inositol 1,4,5-trisphosphate receptor, type 2 (ITPR2), 3 PBS patients; and integrin beta 2 (ITGB2), 3 PBS patients.

CHAPTER 2: CONCLUSIONS

Prune belly syndrome (PBS) is a rare multiple congenital anomaly complex with high morbidity as 30% of PBS patients die during their initial hospitalization (Routh et al. 2010). As PBS patients have lifelong complications, including renal insufficiency or renal failure in 30% of patients, delineating the etiology and possible genetic basis of PBS becomes more important. Different mechanisms and candidate genes for PBS have been suggested, but none account for the entire spectrum of features (including additional skeletal, cardiac, and gastrointestinal anomalies), variations in severity, distinct predominance in males, and familial recurrences.

While PBS is often hypothesized to be an X-linked disorder, no candidate chrX genes have been suggested as a stillborn PBS fetus with a ring X chromosome is the only report of PBS due to an X-linked variation (Guillen et al. 1997). Thus, discovery of a FLNA variant in PBS half-brother D019P1 and D019P2 is the first report of a likely causal chrX variant in a PBS patient or multiplex pedigree. Additionally, confirmation of the FLNA C2160R mutation in the possible-mosaic PBS patient D081P would be significant as this report would be the first instance of a PBS causal mutation identified in unrelated PBS patients.

Sequencing the exomes of 19 sporadic PBS patients identified additional candidate PBS genes, which along with FLNA, support a hypothesis that variants in genes regulating muscle cell contraction or mechanosensing may be causal in PBS pathogenesis. This implication that a common pathway, as opposed to a single gene, is causal in PBS pathogenesis suggests PBS heterogeneity on two levels: phenotypic and genetic. In addition to the classic PBS features, patients in this study also present with orthopedic

(65%), gastrointestinal (63%), cardiopulmonary (49%), and neurologic abnormalities (18%). Thus, genetic heterogeneity may explain the differences in both clinical severity and phenotypic spectrum by allowing for different mechanistic causes of PBS. As all identified candidate genes from WES 19 sporadic PBS cases (Table 2.6) are autosomal, variations in autosomal genes are more likely to be causal in sporadic PBS patients while X-linkage may only account for some familial cases. However, genetic heterogeneity does not account for male predominance or presentation of classic PBS presentation in all patients. Thus, continued efforts in prioritizing identified candidate PBS genes, screening addition sporadic patients, and continued recruitment of familial PBS families, may uncover candidate PBS genes that account for multiple patients and provides genotype-phenotype correlations.

Scientific information regarding genetic components of PBS can guide diagnosis, treatment, and counseling. Genotype-phenotype correlative studies may improve pregnancy outcome prognosis and lead to better suited *in utero* interventions on a case-by-case basis. Additionally, the creation of a PBS sequencing panel may permit noninvasive prenatal testing of fetal DNA in maternal blood, IVF pre-implantation genetic diagnosis, and detection of PBS gene carriers for family counseling.

In addition, this research has the potential to impact clinical disorders beyond PBS. Detrusor underactivity is a major clinical problem and common in patients with lower urinary tract symptoms, but receives little scientific attention. Although PBS is a rare cause of detrusor underactivity, studying the genetic etiology of PBS may identify novel mediators of detrusor muscle development, signaling, and function. From this information, novel drugs may be designed to improve therapeutic options of detrusor underactivity.

CHAPTER 3: COPY-NUMBER VARIATIONS IN CONGENITAL ANOMALIES OF THE GENITALIA

Introduction

One in 4,500 infants is born with congenital anomalies of the genitalia, include abnormalities of the gonads, internal genitalia (duct system), and/or external genitalia, and for most the molecular basis is unknown (Hughes et al. 2006). Understanding the genetic cause of genital anomalies can impact decisions regarding sex assignment, genital surgery and lifelong management. Before human sex determination and subsequent gonadal, ductal, and genital development, the two sexes develop in an identical fashion for the first six weeks of gestation, called the indifferent stage. Next, during the sex determination stage, bipotential gonads commit to developing into testes or ovaries, as dictated by the genetic sex. Then, during sex differentiation, gonad-specific hormones act on the internal and external genitalia resulting in either a male or female sexual phenotype. The indifferent, sex determination, and sex differentiation stages are highly regulated by large genetic networks and both sequence variants and CNVs in genes necessary in these stages are sufficient to cause a wide-range of genital anomalies (Ono & Harley 2013).

During the indifferent stage a common single perineal opening for the genital, urinary and gastrointestinal tracts (or cloaca) persists until week five of gestation. At this point, development of the urorectal septum divides the cloaca into a urogenital sinus anteriorly and a hindgut/anorectum posteriorly. Persistent cloaca is a female anomaly in which the cloaca dos not divide into the proper genital, urinary and gastrointestinal tracts

and instead persists beyond five weeks gestation. Both the etiology and genetic components of persistent cloaca are unknown.

During the sex determination or sex differentiation stages, disruption of the genetic networks regulating genital development cause disorders of sex development (DSD), defined as congenital conditions in which development of chromosomal, gonadal, or anatomical sex is atypical (Hughes et al. 2006). The DSD phenotype can range from external and internal genital abnormalities to complete sex reversal. Mutations in known DSD-causal genes account for only 20-50% of 46,XY DSD cases, meaning the genetic basis for the remaining patients is unknown (White et al. 2011; Ono & Harley 2013).

Karyotypes are a standard test for DSD to determine the genetic sex but many DSD-causal variants remain undetected by karyotyping, such as microdeletions or microduplications <3Mb in size (Miller et al. 2010). Altered gene dosage undetectable by karyotyping is a common mechanism for DSD since many of the sex determining genes occur on sex chromosomes. Both copy-number losses resulting in haploinsufficiency and copy-number gains resulting in gene over-expression result in abnormal sex development in males and females (Jordan et al. 2001; Sutton et al. 2011).

Only recently have newer genomic tests been applied to cases of DSD. aCGH is capable of identifying cryptic or small CNVs that were undetectable by traditional cytogenetic tools, such as karyotyping and FISH. Due to higher resolution, aCGH offers a higher diagnostic yield (15%-20%) for congenital anomalies. In a study of 116 patients with idiopathic DSD, aCGH testing identified clinically relevant CNVs in 21.5% of patients (Tannour-Louet et al. 2010). Of the clinically relevant CNVs, 74% evaded detection by karyotyping, stressing the power of aCGH to detect disease-causing variants.

The objective of this study was to identify novel candidate genes or loci for persistent cloaca and novel variations or genes for DSD by patient phenotyping and CNV genotyping via aCGH.

CHAPTER 3 PART A:

DNA COPY-NUMBER VARIATIONS IN PERSISTENT CLOACA PATIENTS

Steven M. Harrison[1], Casey Seideman, MD[1], and Linda A. Baker, MD[1,2]

[1]Department of Urology, University of Texas Southwestern Medical Center, Dallas, TX

[2]McDermott Center for Human Growth and Development, University of Texas Southwestern Medical Center, Dallas, TX

Accepted

Journal of Urology, 2014, Vol 191

Epub ahead of print

Abstract

Purpose: Persistent cloaca is a devastating female anomaly associated with renal insufficiency/failure, urinary and fecal incontinence, and Mullerian dysfunction. Genetically engineered murine models of persistent cloaca suggest that this anomaly could have a genetic component in humans. Genomic copy-number variations (CNV) have been shown to account for previously unexplained genetic diseases by identifying candidate genes in various disorders. The purpose of this study was to assess if novel CNVs are present in persistent cloaca patients.

Materials and Methods: With IRB approval, we performed retrospective chart review identifying patients with persistent cloaca. Lymphocyte DNA was prospectively tested by whole genome array-comparative genomic hybridization (aCGH). Hedgehog acyltransferase (*HHAT)* was Sanger sequenced from genomic DNA.

Results: 17 females with cloaca had mean age 12 years [0.5-23yrs] at recruitment. 7(41%) females have a solitary functioning kidney and 2 patients each have renal insufficiency and renal replacement therapy. The length of the common cloaca channel ranged from 1.5-6cm in 6 newborn cases. Six (35%) had vaginal duplication; four patients had spinal anomalies. aCGH identified 7(41%) patients with CNVs, including 5 gains and 2 losses. Two CNVs were novel: a paternally-inherited duplication on 16p13.2 and a *de novo* deletion on 1q32.1q32.3. Sequencing of a candidate gene, *HHAT*, identified no causal mutations.

Conclusions: Persistent cloaca is a rare but morbid birth defect and CNVs are common in these females. *HHAT* mutations are not common in cloaca females. Further investigation of these genomic rearrangements may lead to the identification of genetic causes of persistent cloaca.

Introduction

Persistent cloaca is a congenital anomaly limited to females in which the rectum, vagina, and urinary tract typically converge into a common channel, resulting in a single perineal opening. The incidence of persistent cloaca is between 1:20,000 and 1:50,000 (Forrester & Merz 2004; A & MA 2006) with some phenotypic variability resulting anatomically in several cloacal variants. Persistent cloaca is associated with additional anomalies, most commonly urinary tract and spinal abnormalities. Previous reports shows 27% of persistent cloaca patients have renal dysplasia, 14% ectopic kidney, and 13% solitary kidney (Warne et al. 2002). Patients with urinary tract abnormalities are more likely to develop chronic renal failure, with an overall mortality rate of 6% from renal failure (Warne et al. 2002). Spinal abnormalities occur between 34–50% with tethering of the spinal cord being the most common spinal abnormality seen in 27% of persistent cloaca patients (Hendren 1992; Rink et al. 2005).

In normal development, the cloaca persists until 5 weeks' gestation at which point this transient structure is partitioned by the cranial to caudal urorectal septum and the lateral to medial Tourneaux folds surrounding the cloaca (Qi et al. 2000), resulting in a urogenital sinus anteriorly and a hindgut/anorectum posteriorly (Warne et al. 2011). Some have hypothesized a primary developmental field defect as a cause for combined neural tube and cloacal anomalies.

Sonic hedgehog (SHH), is a signaling protein that regulates growth and patterning during embryonic development, and has been implicated in the development of the hindgut. Knock-out mice lacking *Shh* (*Shh*$^{-/-}$) recapitulate the anorectal malformation spectrum, specifically the presence of a cloaca (Ramalho-Santos et al. 2000). Mutant

female mice lacking *Gli2* or *Gli3*, two zinc-finger transcription factors necessary in Shh signaling, also exhibit the anorectal malformation spectrum. However persistent cloaca is only observed in the double mutant female mice deficient in *Gli2 and Gli3* (Mo et al. 2001). Female mice deficient in *Bmp7* or *Efnb2* also exhibit persistent cloaca (Dravis et al. 2004; Wu et al. 2009). However, none of these murine genes have been implicated in human patients with persistent cloaca.

A single patient with persistent cloaca and renal dysplasia was found to have mutation in Uroplakin IIIA (*UPIIIA*) (Jenkins et al. 2005). This gene is expressed in the human embryonic urogenital sinus, implicating *UPIIIA* as a candidate gene for persistent cloaca. However, subsequent sequencing of *UPIIIA* in 20 persistent cloaca patients did not reveal any mutations (Jenkins et al. 2007). Additionally, persistent cloaca has been associated with isolated reports of chromosome rearrangements of 7p and 8q and mutations in *DHCR7,* however persistent cloaca in these patients occurred in conjunction with a syndrome, such as Langer-Giedion syndrome, Prune Belly Syndrome, and Smith-Lemli-Opitz syndrome (Miller et al. 1979; Ramos et al. 1992; Kelley & Hennekam 2000).

The cause of persistent cloaca is unknown, however the occurrence of mouse cloaca models resulting from genetic engineering and reports of rare persistent cloaca patients with single gene defects, suggest a genetic component to this anomaly. Small deletions or duplications of DNA, called copy-number variations (CNVs), have been used to identify candidate loci or genes for previously unexplained genetic anomalies (Vissers et al. 2004; Henrichsen et al. 2009). Array-comparative genomic hybridization (aCGH), also known as chromosome microarray analysis or cytogenomic microarray analysis, is a convenient microarray-based genomic copy-number analysis test capable of testing for

CNVs throughout the genome. The objective of this study was to identify candidate genes or loci for persistent cloaca by patient phenotyping and CNV genotyping via aCGH. Based on the aCGH results, an identified candidate gene, hedgehog acyltransferase (*HHAT*), was then studied in additional persistent cloaca patients.

Materials and Methods

Study population

All human subjects were identified by retrospective chart review and recruited after informed consent was obtained according to a protocol approved by the Institutional Review Board at the University of Texas Southwestern Medical Center. Patients underwent phenotyping at Children's Medical Center in Dallas and at University of Texas Southwestern Medical Center. Genomic DNA from patients and available parents was extracted from peripheral blood lymphocytes via the Puregene DNA isolation kit (Gentra Systems, Minneapolis, MN) according to the manufacturer's protocols.

Array-comparative genomic hybridization

Custom-designed exon-targeted aCGH was performed using versions V8.1 (180,000 oligonucleotides) or V8.3 or V9.1.1 (both 400,000 oligonucleotides) designed by the Medical Genetics Laboratories at Baylor College of Medicine and manufactured by Agilent Technologies (Santa Clara, CA). Digestion, labeling, and hybridization were completed following the manufacturers' protocols. Baylor College of Medicine web-based software was used for genomic copy-number analysis. Confirmatory and parental FISH

analyses were performed using standard procedures by Medical Genetics Laboratories at Baylor College of Medicine.

HHAT sequencing

After identifying a *de novo* deletion encompassing the *HHAT* gene, genomic DNA was screened for mutations by sequencing coding regions and intron-exon boundaries of *HHAT* (www.polymorphicdna.com). For normal controls, detected *HHAT* mutations were cross-referenced to two large, multiethnic databases: NCBI dbSNP (www.ncbi.nih.gov/projects/SNP/) and the 1000 Genomes Project (www.1000genomes.org/).

Results

I. Phenotype

We identified 17 female persistent cloaca patients age 0.5 to 23 years old (mean age 12) at the time of the study (Table 3.1). Subjects were of varied ethnicity (9 Hispanics, 5 Caucasians, 3 African-American). The length of the common cloaca channel ranged from 1.5 – 6.0 cm (mean 3.7 cm) in 6 newborn cases. Of the 17 persistent cloaca patients, 8/32 kidneys are dysplastic/atrophic, 7 patients (41%) have a solitary functioning kidney, 2 patients (12%) have renal insufficiency, and 2 patients (12%) have renal replacement therapy. Six (35%) have vaginal duplication and 8(47%) have uterus didelphys. Spinal anomalies were found in 4/17 patients (24%), including 2 tethered cords (12%), 1 fatty filum terminale (6%), and 1 vertebral fusion anomaly (6%). Additionally, 2 patients (12%) have mild-moderate mental retardation and 1 patient (6%) had hydrops fetalis.

II. Genotype

Screening for CNVs via aCGH identified 7 patients (41%) with CNVs, including 5 patients with DNA duplications and 2 patients with DNA deletions (Table 3.1). Four of the discovered duplications and one of the deletions occur in regions that have been observed in normal individuals (Database of Genomic Variants [DGV]), leaving 1 novel duplication and 1 novel deletion. The novel duplication CNV is paternally inherited and results in a 0.497 Mb duplication of 16p13.2, affecting a single gene: *A2BP1*. The novel deletion CNV is *de novo* and results in a 7.245 Mb deletion of 1q32.1q32.3, affecting over 100 genes, including hedgehog acyltransferase (*HHAT*). As *HHAT* is a necessary component of the Shh pathway, we decided to sequence this gene in persistent cloaca patients.

III. Sequencing HHAT

The 11 coding exons and intron-exon boundaries of *HHAT* were sequenced in 14 of the 17 identified patients with persistent cloaca. No mutations were detected in the exons and all detected intronic mutations have previously been reported in normal individuals in dbSNP.

Table 3.1. Phenotypes and aCGH genotypes of 17 females with persistent cloaca

Case	Cloaca length	# uteri/ vaginas	# funct. kidneys	aCGH version	aCGH result	Chr. region	Min. CNV Size	CNV In DGV
1	6cm	1 / 1	2	V9.1.1	Duplication; Maternally-inherited	12q14.2	0.053 Mb	Yes
2	N.D.	1 / 1	0	V8.1	Duplication; Unknown origin	16p11.2	0.206 Mb	Yes
3	N.D.	1 / 1	1	V8.1	Duplication; Paternally-inherited	16p13.2	0.497 Mb	No
4	N.D.	1 / 1	1	V8.1	Duplication; Unknown origin	21q22.3	0.240 Mb	Yes
5	N.D.	2 / 2	1	V8.3	Duplication; Unknown origin	3p26.3	0.267 Mb	Yes
6	N.D.	2 / 2	0	V8.3	Deletion; *De novo*	1q32.1	7.245 Mb	No
7	2.5cm	2 / 2	2	V9.1.1	Deletion; Unknown origin	2q21.3	0.056 Mb	Yes
8	N.D.	1 / 1	1	V8.1	Normal			
9	N.D.	2 / 2	1	V8.1	Normal			
10	1.5cm	1 / 1	2	V8.3	Normal			
11	2.5cm	2 / 2	2	V8.1	Normal			
12	N.D.	1 / 1	2	V8.1	Normal			
13	4.2cm	1 / 1	2	V8.1	Normal			
14	5.5cm	2 / 2	1	V9.1.1	Normal			
15	N.D.	2 / 1	1	V8.3	Normal			
16	N.D.	2 / 1	2	V8.1	Normal			
17	N.D.	1 / 1	2	V8.1	Normal			

N.D., not determined

Discussion

To our knowledge, this is the first study investigating the role of CNVs in persistent cloaca. Phenotypically speaking, our cohort of patients is similar to cloaca cohorts in prior publications. However, of the two females with mild-moderate mental retardation, one harbors a novel CNV deletion and has dysmorphic facies and digits accompanying her genitourinary anomalies. Thus, females with mental retardation and persistent cloaca should undergo CNV genetic testing.

When available, familial cases of congenital anomalies or discordance in monozygotic twins can greatly aid in detection of candidate genes or genomic loci by comparing genetic variations between affected and healthy family members. In the absence of familial cases of persistent cloaca or candidate genes for this anomaly, we chose to genotype unrelated females with persistent cloaca by aCGH. Of the 41% of our cohort with a CNV, in only two patients was the CNV not previously reported in the normal control databases, thus making them noteworthy and worth pursuing. First, the paternally inherited novel 0.497 Mb duplication CNV on 16p13.2 caused partial duplication of *A2BP1*. The A2BP1 gene encodes the akinesin-2 binding protein 1, a tissue-specific mRNA splicing protein most expressed in the murine heart, skeletal muscle, and brain. In humans, this gene has been implicated in seizures, ataxia, and autism. It is not readily clear how this gene would generate a persistent cloaca phenotype nor does this patient manifest the additional phenotypes seen in humans. Second, the *de novo* novel 7.245 Mb deletion CNV on 1q32.1q32.3 caused a deletion of over 100 genes, including *HHAT*. The HHAT protein catalyzes the N-terminal palmitoylation of SHH, a post-translational modification that is critical for SHH signaling (Buglino & Resh 2008). Mice deficient in

Hhat synthesize non-palmitoylated *Shh* and share phenotypic overlap with *Shh* mice, specifically defects in neural tube and limb development (Chen et al. 2004). However, the presence of a persistent cloaca is not noted in the $Hhat^{-/-}$ mice. As $Shh^{-/-}$ mice and double mutant mice deficient in the Shh signals *Gli2* and *Gli3* exhibit persistent cloaca, *HHAT* seemed a likely causal gene for persistent cloaca as *HHAT* is also necessary in SHH signaling and thus warranted further study. The coding region of *HHAT* was sequenced in 14 persistent cloaca patients but did not discover any mutations. However, sequencing of the coding region does not rule out mutations in the regulatory regions of *HHAT* that can dictate expression. Lastly, many other genes in this large genomic deletion could be causal but remain untested at this time.

The occurrence of mouse genetically engineered models of persistent cloaca and isolated persistent cloaca human case reports with gene mutations suggests a genetic component to this anomaly. As persistent cloaca is typically found in patients with no family history of cloacal anomalies, this disorder is likely caused by either *de novo* dominant mutations or inherited dominant mutations with reduced penetrance (Jenkins et al. 2007). Interestingly, of the 7 identified patients with CNVs, the 2 novel CNVs are: a *de novo* deletion on 1q32.1q32.3 and a paternally-inherited duplication on 16p13.2. Both novel CNVs support the genetic inheritance models, as a *de novo* mutation occurs sporadically and a paternally-inherited mutation suggests a sex-influenced dominant inheritance which is why the father is unaffected.

Following this line of logic, it is conceivable that since cloaca is a sex-limited phenotype, discounting the 5 CNVs as not causal could be erroneous. In four of these cases, parental DNA samples were not available to test inheritance. The normal control

databases do not routinely record sex and race. Thus, it could be that an unaffected father could have the CNV, passing it on to affect his daughter. This could cause us to underestimate the importance of our CNV findings.

To better understand these genomic rearrangements and the potential impact of these rearrangements of cloacal pathogenesis, we recommend continued screening of persistent cloaca patients by aCGH followed by parental testing if abnormal. Identification of overlapping CNVs in multiple cloaca patients would identify the strongest candidate regions for containing cloacal-causing genes. Additionally, further study of the genes within these identified CNVs, with regards to gene function, expression, and known disorders associated with the gene, can potentially narrow down these regions to a few candidate cloaca-causing genes.

On a case by case basis, the identification of causal variants could lead to improved genetic counseling, thereby aiding family planning for the parents, unaffected carrier siblings, and patients. In the case of suspected cloaca during pregnancy, a prenatal genetic diagnosis might in the future be correlated with severity of cloaca and impact prenatal care and outcomes. In addition, prenatal confirmation of cloaca permits planned delivery and postnatal care at a qualified tertiary care facility with pediatric specialists experienced in the complex care of cloaca. As reproductive outcomes and overall patient outcomes improve, it becomes more important to assess and delineate the possible genetic basis of cloaca.

Persistent cloaca is a rare but morbid birth defect and CNVs are common in these females. While one patient was found to have a heterozygous deletion of *HHAT*, subsequent analysis found no sequence mutations in this persistent cloaca cohort,

suggesting that *HHAT* sequence variations are not a common cause of persistent cloaca. Further investigation of these genomic rearrangements may lead to the identification of genetic causes of persistent cloaca, thereby aiding prenatal diagnosis and genetic counseling.

CHAPTER 3 PART B:

SCREENING AND FAMILIAL CHARACTERIZATION OF COPY-NUMBER VARIATIONS IN *NR5A1* IN 46,XY DISORDERS OF SEX DEVELOPMENT AND PREMATURE OVARIAN FAILURE

Steven M. Harrison[1], Ian M. Campbell[2], Melise Keays[1], Candace F. Granberg[1], Carlos Villanueva[1], Grace Tannin[3,7], Andrew R. Zinn[4,5], Diego H. Castrillon[6], Chad A. Shaw[2], Paweł Stankiewicz[2], and Linda A. Baker[1,5,7]

[1]Department of Urology, [3]Department of Pediatrics, [4]Department of Internal Medicine, [5]McDermott Center for Human Growth and Development, [6]Department of Pathology
University of Texas Southwestern Medical Center, Dallas, TX

[7]Children's Medical Center at Dallas, Dallas, TX

and

[2]Department of Molecular and Human Genetics, Baylor College of Medicine, Houston, TX

Published in the American Journal of Medical Genetics, Part A, 2013

161(10): 2487-2494

Abstract

The *NR5A1* gene encodes for steroidogenic factor 1, a nuclear receptor that regulates proper adrenal and gonadal development and function. Mutations identified by *NR5A1* sequencing have been associated with disorders of sex development (DSD), ranging from sex reversal to severe hypospadias in 46,XY patients and premature ovarian failure (POF) in 46,XX patients. Previous reports have identified four families with a history of both 46,XY DSD and 46,XX POF carrying segregating *NR5A1* sequence mutations. Recently, three 46,XY DSD sporadic cases with *NR5A1* microdeletions have been reported.

Here, we identify the first *NR5A1* microdeletion transmitted in a pedigree with both 46,XY DSD and 46,XX POF. A 46,XY individual with DSD due to gonadal dysgenesis was born to a young mother who developed POF. Array CGH analysis revealed a maternally inherited 0.23 Mb microdeletion of chromosome 9q33.3, including the *NR5A1* gene. Based on this finding, we screened patients with unexplained 46,XY DSD (n=11), proximal hypospadias (n=21) and 46,XX POF (n=36) for possible *NR5A1* copy-number variations (CNVs) via multiplex ligation-dependent probe amplification (MLPA), but did not identify any additional CNVs involving *NR5A1*. These data suggest that *NR5A1* CNVs are an infrequent cause of these disorders but that array CGH and MLPA are useful genomic screening tools to uncover the genetic basis of such unexplained cases. This case is the first report of a familial *NR5A1* CNV transmitting in a pedigree, causing both the male and female phenotypes associated with *NR5A1* mutations, and the first report of a *NR5A1* CNV associated with POF.

Introduction

The nuclear receptor subfamily 5, group A, member 1 gene (*NR5A1*; MIM 184757) is located on human chromosome 9q33.3 and encodes for steroidogenic factor 1 (SF1), an intracellular transcription factor that regulates the expression of key genes required for proper sexual development. In human and murine development, NR5A1 is expressed in the developing brain, adrenal gland, and both the XX and XY undifferentiated gonadal somatic cells (Ramayya et al. 1997; Hanley et al. 1999; Lin & Achermann 2008). During sexual differentiation, NR5A1 plays a crucial role in male sex development by governing the regulatory and hormonal networks of male internal and external genital differentiation. In testicular Sertoli cells, *NR5A1* is necessary for the expression of male sexual differentiation genes, such as *SRY* and *SOX9*, and cooperates with the Wilms' tumor gene (*WT1*) to regulate the expression of Anti-Müllerian hormone (AMH) (Nachtigal et al. 1998; Sekido & Lovell-Badge 2008). In testicular Leydig cells, *NR5A1* stimulates the expression of the luteinizing hormone receptor (LHR), insulin-like polypeptide 3 (INSL3), the AMH receptor (AMHR2), and enzymes required for testosterone biosynthesis, thus mediating male testicular descent and external genital virilization (Zimmermann et al. 1998; Fynn-Thompson et al. 2003; Schimmer & White 2010).

In females, NR5A1 expression is persistent from early ovarian development though sex differentiation phases, dictating normal ovarian morphogenesis (Hanley et al. 1999). However, female internal genital duct and external genital development are not dependent upon NR5A1. After puberty, ovarian somatic cell NR5A1 expression becomes important, governing proper ovarian steroidogenesis and follicular cycling (Lourenco et al. 2009).

Targeted deletion of *Nr5a1* in mice results in early postnatal death from failed adrenal development. In xy *Nr5a1*-null mice, complete testicular dysgenesis and male-to-female sex reversal is present with female external genitalia and persistence of Müllerian structures (Luo et al. 1994). Conditional *Nr5a1* inactivation within ovarian granulosa cells results in sterile XX mice with hypoplastic ovaries lacking corpora lutea and containing hemorrhagic cysts (Jeyasuria et al. 2004).

Disorders of sex development (DSD) are human congenital conditions in which development of the chromosomal, gonadal, or anatomic sex is atypical (Hughes et al. 2006). In cases with 46,XY karyotype, the DSD state can be due to either a disorder of androgen synthesis or action or a disorder of gonadal (testicular) development (46,XY DSD due to gonadal dysgenesis [hereafter 46,XY GD]). 46,XY GD can be either complete GD (previously called 'sex reversal'), yielding female external genitalia, streak gonads, and Müllerian structures, or partial GD, yielding ambiguous external genitalia, dysgenetic testes, and partial development of Müllerian and Wolffian structures. Due to phenotypic similarity with *Nr5a1*-null male mice, two 46,XY GD patients with primary adrenal failure were screened for mutations in *NR5A1* and both patients were found to carry loss-of-function mutations in this gene (Achermann et al. 1999; Achermann et al. 2002). Although initially associated with adrenal failure, subsequent studies of *NR5A1* mutations have discovered that loss-of-function mutations in *NR5A1* are more frequent in 46,XY DSD sex reversal patients without adrenal failure than in 46,XY DSD sex reversal patients with adrenal failure (Tajima et al. 2009).

The reported frequency of *NR5A1* loss-of-function mutations is approximately 20% in 46,XY GD patients with impaired androgenization but normal adrenal function (Lin et

al. 2007; Kohler et al. 2008; Philibert et al. 2010) and 15% in patients with severe penoscrotal hypospadias and cryptorchidism (Kohler et al. 2009). The disease-causing variants reported in *NR5A1* range from missense, nonsense, and splicing mutations to small deletions and insertions. In contrast to mutations detectable by sequencing, copy-number variations (CNVs) are deletions or duplications of part of a genomic fragment that change the effective number of DNA copies of a gene. Three *NR5A1* CNVs, one partial deletion and two entire gene deletions, have previously been reported in sporadic patients with 46,XY DSD (Schlaubitz et al. 2007; van Silfhout et al. 2009; Barbaro et al. 2011). However, *NR5A1* CNVs have not been comprehensively searched for in a cohort of 46,XY DSD cases.

Variations in *NR5A1* extend beyond 46,XY DSD and hypospadias phenotypes, to anorchia, male infertility, and premature ovarian failure. Premature ovarian failure (POF; OMIM 612964) is a condition characterized by amenorrhea for at least 4 months before the age of 40 years. In sporadic cases of POF, the mutation frequency of *NR5A1* is approximately 3-8% (Lourenco et al. 2009; Janse et al. 2012). Four families with histories of both 46,XY DSD and 46,XX POF have been identified in which the affected individuals carry *NR5A1* loss-of-function mutations (Lourenco et al. 2009). However, patients with these phenotypes have not been screened for *NR5A1* CNVs.

In this study, we report a pedigree detailing a mother and son with POF and 46,XY GD, respectively, both carrying the same 9q33.3 deletion encompassing *NR5A1*. This case is the first report of a familial *NR5A1* CNV transmitting in a pedigree, causing both the male and female phenotypes associated with *NR5A1* mutations, and the first report of a *NR5A1* CNV associated with POF. Based on the findings of *NR5A1* CNV, we investigated

sporadic cases of unexplained 46,XY DSD, proximal hypospadias, and POF for possible *NR5A1* CNV.

Materials and Methods

Study population

All human subjects were recruited for genetic testing and informed consent obtained per protocol approved by the Institutional Review Board at the University of Texas Southwestern Medical Center. Patients with known chromosomal abnormalities or genetic cause for their disease were excluded from the study. Patients underwent karyotyping and complete phenotyping at the University of Texas Southwestern Medical Center affiliated hospitals and medical records were reviewed. Of the 70 human study subjects, individuals were of varied ethnicity (16 Caucasians, 12 Hispanics, 6 African Americans and 36 Asians) and had either 46,XY DSD (n=12; Table 3.2), 46,XY proximal hypospadias (n=21), 46,XX POF (n=36) or was normal (n=1; subject I-2). All were unrelated except the three subjects comprising the pedigree (Figure 3.1: subjects I-2, II-2, III-1). Genomic DNA was extracted from subjects' peripheral blood lymphocytes (Puregene, Gentra Systems, Minneapolis, MN) per manufacturer's protocols.

Clinical array comparative genomic hybridization

Array CGH was performed using a custom, whole genome 180,000 oligonucleotide array, "V8.1 OLIGO", designed by the Medical Genetics Laboratories at BCM and manufactured by Agilent Technologies (Santa Clara, CA). Digestion, labeling, and hybridization were completed per protocols. BCM web-based software was used for

genomic copy number analysis. The computational methods have been described previously (Schlaubitz et al. 2007). Findings were confirmed via FISH probe RP11-164H5 per standard protocol.

Custom array comparative genomic hybridization

A custom, high-resolution 9q33-q34 array was designed using a 60,000 oligonucleotide array format (Agilent Technologies, Inc., Santa Clara, CA, USA). Average probe spacing was ~1,250 bp per probe. Chromosomal sex-matched DNA samples were used as hybridization reference normal controls. After sample processing and hybridization, data were analyzed using Agilent Genomic Workbench Software (Agilent Technologies, Inc, CA, USA) and plotted using the R Statistical Computing Package (R Core Development Team).

Deletion breakpoint determination

Long range PCR was employed to amplify the deletion-specific junction fragment utilizing the manufacturer's protocol (Takara Bio Inc, Otsu, Japan). PCR primers were designed to flank the familial deletion breakpoints based on array CGH data. PCR products were Sanger sequenced (Lone Star, Houston, TX) and compared to the reference human genome sequence using the UCSC Genome Browser (version hg19).

Inheritance determination

PCR primers were designed to flank HapMap SNPs contained within the deleted region and to produce amplicons containing the SNPs of the mother (II-1) and

grandmother (I-2). Products were Sanger sequenced (Lone Star, Houston, TX) to determine the genotype at each locus.

Multiplex ligation-dependent probe amplification analysis

DNA was screened for *NR5A1* copy-number variations using the SALSA P185-B2 Intersex MLPA kit (MRC-Holland, Amsterdam, The Netherlands), per manufacturer's protocol. This assay includes probes for 5 of the 6 coding exons of *NR5A1*, in addition to probes for other causal DSD genes. Amplified products were separated by size on an ABI3100 genetic analyzer (Applied Biosystems, Foster City, California, USA) and the data were analyzed using GeneMarker V2.2.0 (SoftGenetics, State College, Pennsylvania, USA).

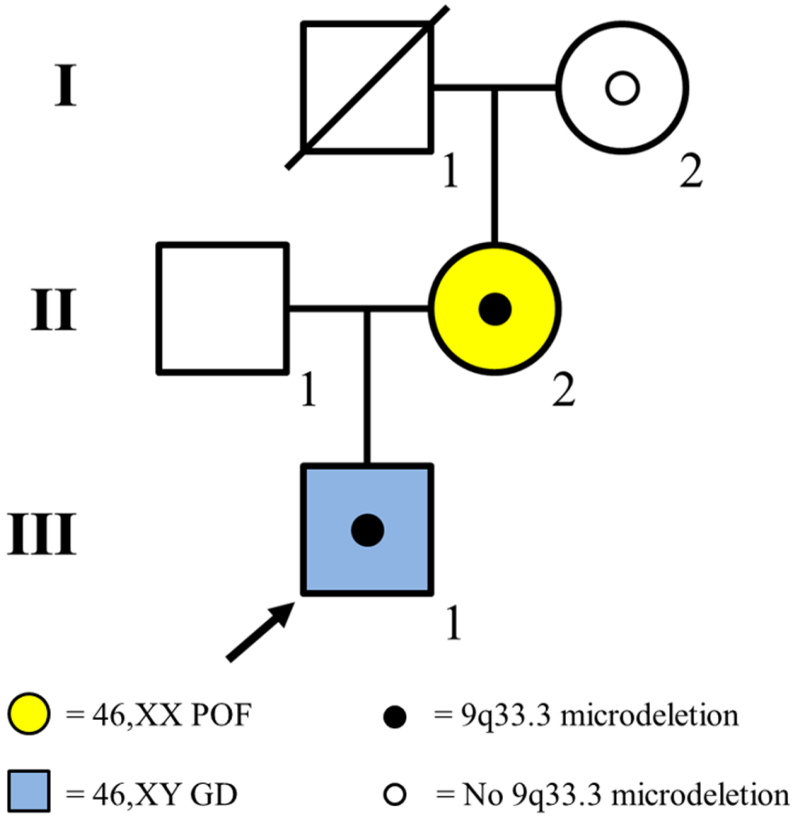

Figure 3.1. GD and POF pedigree with a familial 9q33.3 deletion
In the pedigree, squares represent male family members and circles represent female family members. Blue shaded squares represent 46,XY patient affected with gonadal dysgenesis (GD). Yellow shaded circles represent 46,XX patient affected with POF. A solid circle within an individual indicates that family member was found to harbor a 9q33.3 microdeletion including *NR5A1*. An empty circle within an individual indicates that family member does not carry the 9q33.3 microdeletion. Individuals without an interior circle were not tested for deletion. The index patient is indicated with an arrow.

Results

I. Clinical presentation of child with 46,XY GD and mother with 46,XX POF

A 15 day old full term "female" Caucasian infant (Figure 3.1: subject III-1) was evaluated emergently for fever and found to have ambiguous genitalia, with clitoromegaly, a urogenital sinus, and bilateral labioscrotal masses. Testing identified a urinary tract infection, 46,XY karyotype with neonatal female testosterone levels (testosterone <3 ng/dl), normal adrenal steroidogenic function, no internal Müllerian structures and bilateral labioscrotal testes. At 6 months age, bilateral testicular biopsies demonstrated closely packed seminiferous tubules mostly containing germ cells. Some of the germ cells were bi- or tri-nucleated and located more centrally within the tubules. Neither Leydig cells nor Müllerian structures were observed, consistent with partial gonadal dysgenesis (46,XY GD). The family elected to reassign the child as a male and after testosterone supplementation to stimulate phallic growth, bilateral orchidopexy and proximal hypospadias repair were performed at 6 months of age. At age 11, he has normal intelligence, asthma, attention-deficit-hyperactivity disorder and bipolar disorder. He was retreated with testosterone therapy for lack of spontaneous male puberty and small phallic size.

The proband's mother (Figure 3.1: subject II-2) had menarche at age 12 years and irregular menses prior to her first conception**.** At age 19, she conceived and delivered subject III-1. Following the birth, she had menses every 3 months over the next 3-4 years and thereafter became less frequent. She developed secondary amenorrhea at age 28 unresponsive to multiple hormonal therapies. She had normal genitalia, vagina, cervix and uterus with post-menopausal hormonal values. Computed tomography revealed normal

adrenal glands, moderate hepatomegaly and diverticulosis of the sigmoid colon. Her comorbidities included bipolar disorder, dyslexia, obesity, obstructive sleep apnea, gastroesophageal reflux disease, hiatal hernia, sigmoid diverticulosis and type II diabetes. Her past surgical history included appendectomy, cholecystectomy and knee repair. Family history is negative for disorders of sex development or premature ovarian failure and subject II-2's mother (Figure 3.1; subject I-2) did not have POF. Family history is positive for colon cancer and coronary artery disease in paternal grandparents and a strong bilineal family history of bipolar disorder.

II. Microdeletion of NR5A1 in child with 46,XY GD and mother with 46,XX POF

Clinical chromosomal microarray analysis of the 46,XY GD proband (subject III-1) revealed a 0.232 Mb microdeletion of chromosome band 9q33.3, involving *NR5A1* and four additional RefSeq genes. No disease-associated *NR5A1* mutations were found in the other allele by sequencing the coding region (exons 2-7) in the proband. FISH testing revealed that the deletion present in the 46,XY GD proband (subject III-1) was also harbored by his mother (subject II-2) but was absent from the maternal grandmother (subject I-2).

To determine the extent of the familial 9q33.3 deletion, we performed custom, high-resolution 9q33-q34 array CGH followed by long range PCR and Sanger sequencing (Figure 3.2). Breakpoint analysis revealed the deletion of chr9:127,251,113-127,487,356 (GRChr37/hg19), impacting five RefSeq genes: *NR5A1* (exons 1-6), *NR6A1* (exons 3-10), *MIR181A2HG* (whole gene), *MIR181A2* (whole gene), and *MIR181B2* (whole gene).

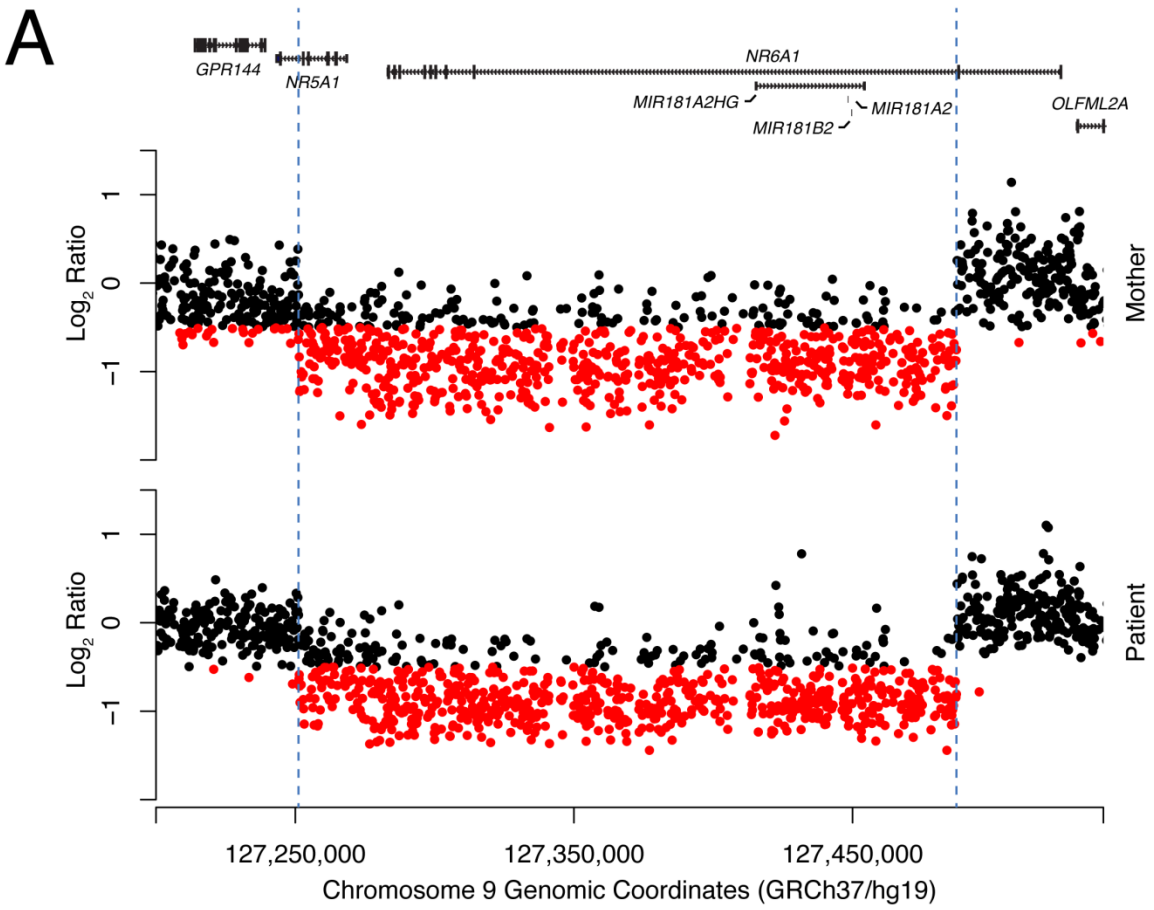

Figure 3.2. Genomic extent of the familial 9q33.3 deletion.
A) Custom-designed high-resolution aCGH analysis of the 9q33.3 region. Array CGH probes with log2 subject:control ratios less than -0.5 are colored red for ease of visualization. The locations of the RefSeq genes in the region are indicated along the top of the graph as black rectangles. B) Breakpoint sequence of the patient from this study. The reference sequence of the proximal intact segment of the chromosome harboring the deletion allele is shown in red while the distal intact segment is shown in blue. The patient's sequence is shown in between. A single thymidine base of microhomology is shown in green. All coordinates and reference sequences are provided in the GRChr37/hg19 2009 assembly

To confirm that the *NR5A1* deletion was not inherited from the deceased maternal grandfather (subject I-1) we performed genotyping of HapMap (hapmap.org) SNPs contained within the deleted region to assure that the *NR5A1* CNV did not segregate with this phenotypically normal individual who was unavailable for testing. Sanger sequencing of one of the SNPs, rs10986358, revealed a genotype in the mother (subject II-2) that was incompatible with the genotype of the grandmother (subject I-2) (Figure 3.3). Since the mother has only one allele at the rs10986358 locus (on the intact chromosome) and it is incompatible with the grandmother's genotype, the intact chromosome is most likely inherited from the grandfather. Thus, the chromosome harboring the deletion in the mother is most likely inherited from the grandmother. A *de novo* point mutation between generations resulting in an rs10986358 T allele on a chromosome inherited from the grandmother cannot be excluded. However, given low locus-specific mutation rates and the fact that the haplotype of the mother's intact chromosome is the most common among chromosomes of individuals with Northern and Western European ancestry (91/234 HapMap Phase III CEU phased chromosomes, data not shown), the probability of a mutation explaining the data is extremely low.

To test for the possibility of low-level mosaicism in the grandmother, we also subjected DNA isolated from her peripheral blood leukocytes to PCR testing. There was no evidence of the deletion in the grandmother. Since the deletion is most likely located on the chromosome nine inherited from the grandmother and we were unable to detect evidence of the deletion in her peripheral blood genomic DNA, we concluded that the deletion arose *de novo* in generation II.

III. Screening of NR5A1 CNVs in patients with 46,XY DSD, 46,XY proximal hypospadias, and 46,XX POF

To assess the frequency of *NR5A1* CNVs in DSD states, we screened 11 patients with 46,XY DSD phenotypes (described in Table 3.2), 21 patients with proximal hypospadias (with or without cryptorchidism), and 35 patients with POF for *NR5A1* CNV via *NR5A1* MLPA. The MLPA assay did not identify any additional *NR5A1* CNVs in the DSD, proximal hypospadias, or POF patient groups but did confirm the familial *NR5A1* microdeletion (exons 1-6) in subjects II-2 and III-1. The MLPA kit did not include a probe for the unaffected *NR5A1* exon 7.

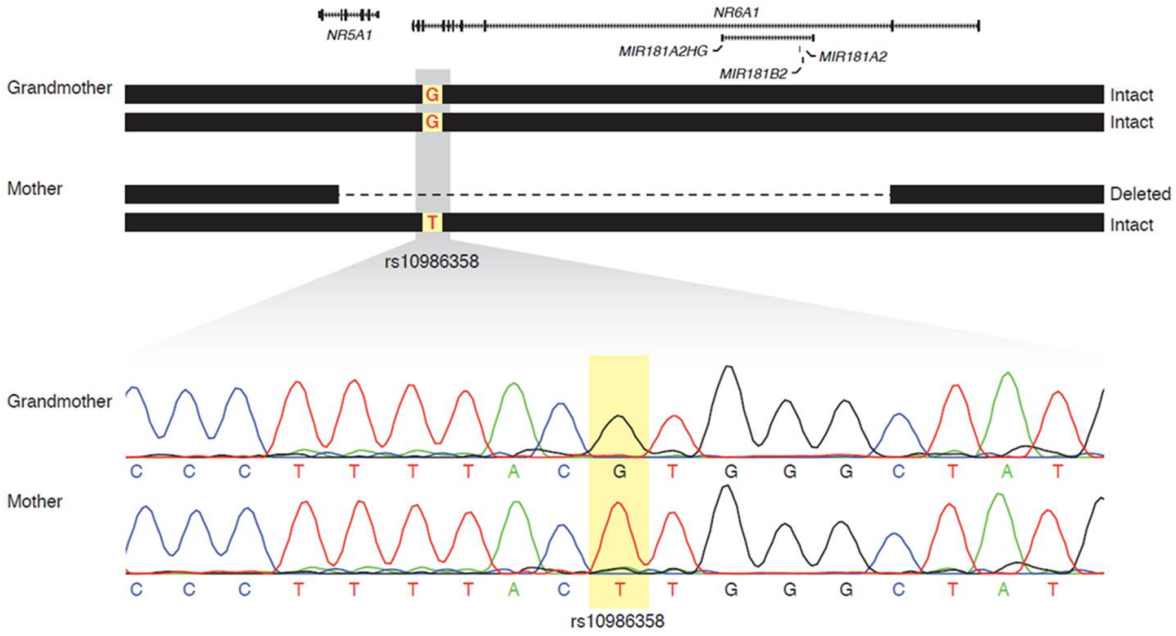

Figure 3.3. Determination of parent of origin of the chromosome harboring the *NR5A1* deletion.

Genotyping of SNPs from the HapMap project reveals that the mother's intact chromosome is inherited from her father because the genotype of rs10986358 is incompatible with her mother's genotype. Top, schematic representation of the genotypes of the mother and grandmother. The mother is hemizygous for the minor allele (T), while the grandmother is homozygous for the reference allele (G). Thus, the mother's intact chromosome is most likely inherited from the grandfather. Therefore, the chromosome harboring the deletion is most likely inherited from the grandmother. Bottom, Sanger sequencing traces of the rs10986358 locus in both individuals. Twelve other HapMap SNPs were also genotyped but were uninformative. No sample was available from the grandfather

Case; Sex	External Genital Phenotype	Müllerian Structures	Wollfian Structures	Testes Position /History	aCGH Results	Normal Genetic Testing
1/F	Clitoromegaly, short UGS	Hemiuterus; vaginal duplication	No vas bilaterally	IA/ Normal	Normal	*SRY NR5A1 WT1 DHH*
2/F	Normal clitoris, short UGS	None	None	IA/ Dysgenetic	Normal	*SRY AR WT1 SRD5A2*
3/F	Clitoromegaly, short UGS	None	Normal	IG/ Atrophy	Normal	N.D.
4/F	Clitoromegaly, UGS	Uterus, vagina	Normal	IA/ Atrophy	N.D.	N.D.
5/F	Clitoromegaly, short UGS	No uterus; vagina present	Normal	IG/ Fibrotic	Normal	*AR*
6/M	Hypospadias, microphallus, penoscrotal transposition	Hemiuterus; large vagina	Mixed	Left: IG/ Dysgenetic; Right: absent	N.D.	N.D.
7/F	Clitoromegaly	No uterus; short vagina	Normal	IG/ Normal	Normal	N.D.
8/F	Clitoromegaly, UGS	No uterus; short vagina	Unknown	Unknown	N.D.	N.D.
9/F	Clitoromegaly, UGS	No uterus; short vagina	Normal	IA/ Dysgenetic	N.D.	*AR*
10/M	Microphallus	No uterus; no vagina	Normal	IG/ Microtestes	N.D.	N.D.
11/F	Clitoromegaly, UGS	Hemiuterus; vagina	Normal	IA/ Dysgenetic	N.D.	*SRY NR5A1 WT1 DHH*
Index Case (III-1) /M	Clitoromegaly, UGS	None	Normal	Labioscrotal / Dysgenetic	Microdel (9q33.3)	*NR5A1*

Table 3.2. Clinical and genetic characteristics of 12 patients with 46,XY DSD
Sex, sex of rearing; aCGH, array comparative genomic hybridization; UGS, urogenital sinus; IA, intraabdominal; IG, inguinal; N.D., not done; *SRY*, sex-determining region Y; *NR5A1*, nuclear receptor subfamily 5 group A member 1; *AR*, androgen receptor; *WT1*, Wilms tumor 1; *DHH*, desert hedgehog; *SRD5A2*, 5α-reductase type 2 gene

Discussion

We identified a novel 0.232 Mb microdeletion on 9q33.3 in a 46,XY GD patient with partial gonadal dysgenesis. Breakpoint mapping revealed that the deletion involves chr9:127,251,113-127,487,356 (GRChr37/hg19), impacting five RefSeq genes (*NR5A1*, *NR6A1*, *MIR181A2HG*, *MIR181A2*, and *MIR181B2*). The patient's mother, diagnosed with POF, was found to carry the same 9q33.3 microdeletion. Subsequent studies utilizing SNP genotyping and PCR analysis determined that the deletion arose *de novo* between generations I and II (Figure 3.1). A single thymidine base pair of microhomology was detected at the breakpoint (Figure 3.2.B). Microhomology is the hallmark of replicative mechanisms of CNV formation such as microhomology mediated break-induced replication or fork stalling and template switching; however non-homologous end joining cannot be excluded (Liu et al. 2012).

One of the genes implicated in the familial 9q33.3 microdeletion is *NR5A1*, also known as steroidogenic factor 1 (SF1), a transcription factor that regulates the expression of key genes required for proper sexual development, such as *SRY*, *SOX9*, and *AMH*. *NR5A1* is a confirmed causal gene for DSD as *NR5A1* sequence mutations account for approximately 20% of 46,XY GD cases (Lin et al. 2007; Kohler et al. 2008; Philibert et al. 2010). Additionally, three *NR5A1* CNV have previously been reported in cases of 46,XY DSD (Schlaubitz et al. 2007; van Silfhout et al. 2009; Barbaro et al. 2011). *NR5A1* sequence mutations were previously identified in affected members from four families with histories of both 46,XY DSD and 46,XX POF *(Lourenco et al. 2009)*. We report the first pedigree with both 46,XY DSD and 46,XX POF due to *NR5A1* CNV.

Aside from *NR5A1*, four other genes are located in the 9q33.3 deletion reported in this pedigree. Of these four genes, only *NR6A1* is expressed in tissues related to sexual development. However, *NR6A1* has not been associated with sex reversal in humans and is not deleted in a 46,XY GD patient reported by Barbaro *et al* with only partial *NR5A1* deletion, suggesting that *NR5A1* haploinsufficiency alone is sufficient to cause the patient's abnormal sexual development (Barbaro et al. 2011).

Mutations in known sex-determination genes, such as *SRY*, *SOX9*, *WNT4*, *DAX1*, and *NR5A1* account for almost 50% of 46,XY GD, suggesting the genetic basis for the remaining 50% of patients is unknown (White et al. 2011). However, screening for mutations in the known sex-determining genes typically only identifies point mutations, while genomic rearrangements, such as CNV, are often missed by sequencing and are too small to be detected by karyotyping. Two recent publications have identified causal CNV in 13-30% patients with unexplained, syndromic or non-syndromic 46,XY GD (Ledig et al. 2010; White et al. 2011), rates in range with our observed 17% in a similar patient cohort (Harrison et al., In review). Additionally, 22% of DSD patients with phenotypes including ambiguous genitalia, hypospadias, and cryptorchidism, had a clinically relevant CNV, 74% of which were undetectable by karyotype (Tannour-Louet et al. 2010).

Making the correct molecular diagnosis can have significant implications for gender assignment and thus the likely response to hormone treatment as well as genetic counseling for the family. As only 15-20% of 46,XY DSD and proximal hypospadias cases and 3% of POF cases have *NR5A1* sequence mutations, copy-number variations in *NR5A1*, such as the deletion reported in this pedigree, are another genomic cause to consider. These data suggest that *NR5A1* CNVs are an infrequent cause of these disorders;

however, copy number tests, such as array CGH and MLPA, are useful genomic screening tools to uncover the genetic basis of such unexplained 46,XY DSD cases.

CHAPTER 3 PART C:

DNA COPY-NUMBER VARIATIONS IN 46,XY DISORDERS OF SEX DEVELOPMENT

Steven M. Harrison[1]; Candace F. Granberg MD[2]; Carlos Villanueva MD[3]; Melise Keays MD[1], Gwen M. Grimsby MD[1], and Linda A. Baker MD[1,4]

[1]Department of Urology, University of Texas Southwestern Medical Center, Dallas, TX

[2]Department of Urology, Mayo Clinic, Rochester, MN

[3]Children's Specialty Physicians, Omaha, NE

[4]McDermott Center for Human Growth and Development, University of Texas Southwestern Medical Center, Dallas, TX

Submitted to Genetics in Medicine

February 20, 2014

Abstract

Purpose: Less than 50% of 46,XY disorders of sex development (DSD) cases are genetically defined after karyotyping and/or sequencing of known DSD causal genes. As copy-number variations (CNVs) are often missed by karyotyping and sequencing, the goal of this study was to assess cases of unexplained 46,XY DSD by array-comparative genomic hybridization (aCGH) for possible disease-causing genomic variants.

Methods: DNA from 46,XY DSD cases were tested by whole genome aCGH. In cases wherein novel CNVs were detected, parental testing was performed to identify whether CNV was *de novo* or inherited.

Results: Of the 12 cases who underwent aCGH testing, two had possible DSD-causing CNV, both maternally-inherited microdeletions. The first case, with a maternal history of premature ovarian failure, had a co-segregating microdeletion on 9q33.3 involving *NR5A1*. The second case, with a maternal family history of congenital heart disease, was found to have a co-segregating microdeletion on 8p23.1 upstream of *GATA4*.

Conclusion: In this cohort, CNVs involving or adjacent to known 46,XY DSD-causing genes lead to 46,XY DSD in 2 of 12 (17%) previously unexplained cases. CNV testing is clinically indicated for unexplained 46,XY DSD cases to aid in genetic counseling for family planning.

Introduction

The determination of a sexual phenotype in humans depends on the presence and activity of regulatory networks that stimulate the bipotential gonad to develop into either a testis or ovary. In males, sex-determining region Y (*SRY*) initiates male sex determination by stimulating the differentiation of Sertoli cells through a genetically-controlled network. Deregulation of this network can result in partial or complete failure of testis determination. After sex determination, male sex differentiation involves Müllerian duct regression, Wolffian duct development and virilization of the external genitalia which rely on Sertoli-cell derived anti-Müllerian hormone (*AMH*) and Leydig-cell derived testosterone, respectively. Disruption of the sex-determination or sex-differentiation networks causes disorders of sex development (DSD), defined as congenital conditions in which development of chromosomal, gonadal, or anatomical sex is atypical (Hughes et al. 2006). The DSD phenotype can range from external and internal genital abnormalities to complete sex reversal.

DSD cases with a 46,XY karyotype are clinically and genetically heterogeneous but can be classified as 1) gonadal (testicular) dysgenesis, 2) decreased fetal androgen biosynthesis, 3) decreased fetal AMH production/action, or 4) defects in androgen action. While the genetic basis of the last three categories is better understood, the 46,XY DSD/gonadal dysgenesis (46,XY DSD/GD) group is incompletely characterized. Phenotypically speaking, 46,XY DSD/GD can be either complete GD (previously called 'sex reversal'), yielding female external genitalia, streak gonads, and Müllerian structures, or partial GD, yielding ambiguous external genitalia, dysgenetic testes, and partial development of Müllerian and Wolffian structures.

Gene	Chr	Gene OMIM	CNV associated with 46,XY DSD/GD
DMRT1	9p24.3	602424	Deletion
GATA4	8p23.1	600576	Deletion (Case #2; current study)
NR0B1 (DAX1)	Xp21.2	300473	Deletion
NR5A1 (SF1)	9q33.3	184757	Deletion (Case #1; current study)
SOX9	17q24.3	608160	Deletion/ Duplication
SRY	Yp11.3	480000	Deletion
WNT4	1p36.12	603490	Duplication
WT1	11p13	607102	Deletion
WWOX	16q23.1	605131	Deletion

Table 3.3. Dosage sensitive genes associated with 46,XY disorders of sex development due to gonadal dysgenesis (DSD/GD)
Data collected from: Disteche et al. (1986); Muroya et al. (2000); Le Caignec et al. (2007); Schlaubitz et al. (2007); Smyk et al. (2007); White et al. (2011); White et al. (2012)

As seen in Table 3.3, many genes have been identified that are crucial for proper testis determination and thus mediate testicular dysgenesis when genetically disrupted. As expected, mutations in these genes in 46,XY individuals can cause gain or loss of function. These genomic variations can be detected by gene sequencing. In addition, larger genomic rearrangements of 46,XY DSD/GD causal genes can cause a copy-number variation (CNV) yielding deletions (del) or duplications (dup) of the genes or their regulatory regions in 46,XY DSD/GD patients. Unfortunately, these genomic variations can be missed on karyotyping. For example, CNVs of *SRY* (del), *SOX9* (del) and *DAX1* (dup) are known to cause 46,XY DSD/GD. Array- comparative genomic hybridization (aCGH), also known as chromosome microarray analysis or cytogenomic microarray analysis, is a convenient microarray-based genomic copy-number analysis test capable of testing for CNVs throughout the genome.

Mutations in known sex-determination genes (Table 3.3) account for almost 50% of 46,XY DSD cases, meaning the genetic basis for the remaining 50% of patients is unknown (White et al. 2011). This data is suspect however, since screening for mutations in the known sex-determining genes typically only identifies point mutations, while genomic rearrangements, such as CNVs, are often missed by sequencing and are too small to be detected by karyotyping. Alternatively, the genetic basis for the remaining 50% could be due to mutations in yet-to-be-identified 46,XY DSD genes.

To determine whether CNVs can account for previously unexplained cases of 46,XY DSD, the goal of this study was to screen patients with 46,XY DSD by aCGH to access for variations in novel gonadal genes, variations in the regulatory elements of

known gonadal genes, or variations in known gonadal genes that were not detected by karyotyping or candidate gene sequencing.

Materials and Methods

Study population

All human subjects were recruited for genetic testing and informed consent obtained according to a protocol approved by the Institutional Review Board at the University of Texas Southwestern Medical Center. Patients with known chromosomal abnormalities or genetic cause for their disease were excluded from the study. Patients underwent karyotyping and complete phenotyping at the University of Texas Southwestern Medical Center affiliated hospitals and medical records were reviewed. Genomic DNA was extracted from subjects' peripheral blood lymphocytes via the Puregene DNA isolation kit (Gentra Systems, Minneapolis, MN) according to the manufacturer's protocols.

Array-comparative genomic hybridization

Custom-designed exon-targeted aCGH was performed using versions V8.1 or V8.3 (180,000 or 400,000 oligonucleotides, respectively) both designed by the Medical Genetics Laboratories at Baylor College of Medicine and manufactured by Agilent Technologies (Santa Clara, CA). Digestion, labeling, and hybridization were completed following the manufacturers' protocols. BCM web-based software was used for genomic copy-number analysis. The computational methods have been described previously (Schlaubitz et al.

2007). Confirmatory and parental FISH analyses were performed using standard procedures by Medical Genetics Laboratories at Baylor College of Medicine.

Multiplex ligation-dependent probe amplification analysis

DNA was screened for copy-number variations using the SALSA P234-A1 GATA4 MLPA kit (MRC-Holland, Amsterdam, The Netherlands), as instructed by the manufacturer. Amplified products were separated by size on an ABI3100 genetic analyzer (Applied Biosystems, Foster City, California, USA) and the data were analyzed using GeneMarker V2.2.0 (SoftGenetics, State College, Pennsylvania, USA).

Results

Of the 12 46,XY DSD human study subjects, individuals were of varied ethnicity (8 Caucasians, 3 Hispanics, 1 African-American). The urogenital phenotype as well as genetic testing results can be seen in Table 3.4. Of the 12 patients screened for genomic rearrangements via aCGH, four had previously unreported genomic rearrangements. Two of these patients were shown to have 0.076-0.263Mb microduplications of Xp21.1 and 15q12q13.1, both of which are remote from any genes associated with sexual development and thus are of unclear clinical significance. More importantly, two patients had maternally-inherited microdeletions affecting genes known to have a role in gonadal development.

Table 3.4. Clinical characteristics and aCGH results of 12 patients with 46,XY DSD

Case; Sex	External Genital Phenotype	Müllerian Structures	Wolffian Structures	Testes Position /History	aCGH Results	Normal Genetic Testing
1/M	Clitoromegaly, UGS	None	Normal	Labioscrotal /Dysgenetic	Loss 9q33.3 (Maternal)	*NR5A1*
2/M	Perineal hypospadias	None	Normal	Scrotal/ Hypoplasia	Loss 8p23.1 (Maternal)	N.D.
3/M	Small phallus, hypospadias	None	Normal	IG/ Normal	Gain 15q13.1 (Maternal)	N.D.
4/M	Small phallus, perineal hypospadias	None	Normal	IG/ Normal	Gain Xp21.1	*AR* *SRD5A2*
5/F	Clitoromegaly, short UGS	No uterus; vagina present	Normal	IG/ Fibrotic	Normal	*AR*
6/F	Clitoromegaly, short UGS	Hemiuterus; vaginal duplication	No vas bilaterally	IA/ Normal	Normal	*SRY* *NR5A1* *WT1* *DHH*
7/F	Normal clitoris, short UGS	None	None	IA/ Dysgenetic	Normal	*SRY* *AR* *WT1* *SRD5A2*
8/M	Small phallus, perineal hypospadias	None	Normal	IG/ Unknown	Normal	*AR* *SRD5A2*
9/F	Clitoromegaly, short UGS	Hemiuterus; vaginal duplication	No vas bilaterally	IA/ Atrophic	Normal	*SRY* *NR5A1* *WT1* *DHH*
10/F	Small phallus, UGS	Atretic vagina	None	IG/ Normal	Normal	*AR* *SRD5A2*
11/M	Small phallus, perineal hypospadias	None	Normal	IG/ Unknown	Normal	*AR*
12/F	Normal clitoris	Small vagina; no uterus	Unknown	Labial/ Unknown	Normal	*AR*

Sex, sex of rearing; aCGH, array comparative genomic hybridization; UGS, urogenital sinus; IA, intraabdominal; IG, inguinal; N.D., not done; *SRY*, sex-determining region Y; *NR5A1*, nuclear receptor subfamily 5 group A member 1; *AR*, androgen receptor; *WT1*, Wilms tumor 1; *DHH*, desert hedgehog; *SRD5A2*, 5α-reductase type 2 gene

The first patient (Figure 3.4) was assigned female sex at birth and presented at day of life 15 with a febrile urinary tract infection. Physical exam revealed ambiguous genitalia with a small phallus, perineal hypospadias, and bilateral gonads palpable in the labioscrotal folds. Karyotype was 46,XY and after appropriate testing and counseling, the family elected to raise the child as male. He subsequently underwent testosterone stimulation, bilateral orchidopexy, and proximal hypospadias repair.

At age 14 years, aCGH testing of this patient revealed a copy-number loss of chromosome band 9q33.3 of approximately 0.24 Mb, implicating a known DSD/GD causal gene *NR5A1* (exons 1-6), and four additional RefSeq genes: *NR6A1* (partial gene deletion), *MIR181A2HG* (whole gene deletion), *MIR181A2* (whole gene deletion), and *MIR181B2* (whole gene deletion). No disease-associated mutations were identified in the coding region (exons 2-7) of the intact *NR5A1* allele in the patient. The patient's mother had developed secondary amenorrhea at age 19 years, consistent with premature ovarian failure (POF). FISH analysis of the mother showed the same 9q33.3 microdeletion as observed in her child. FISH analysis of the maternal grandmother showed no evidence of the 9q33.3 microdeletion observed in her child or grandchild. Subsequent studies utilizing SNP genotyping and FISH analysis determined that the deletion arose *de novo* between generations I and II (Figure 3.4). This familial case of *NR5A1* deletion has been previously reported in greater detail (Harrison et al. 2013).

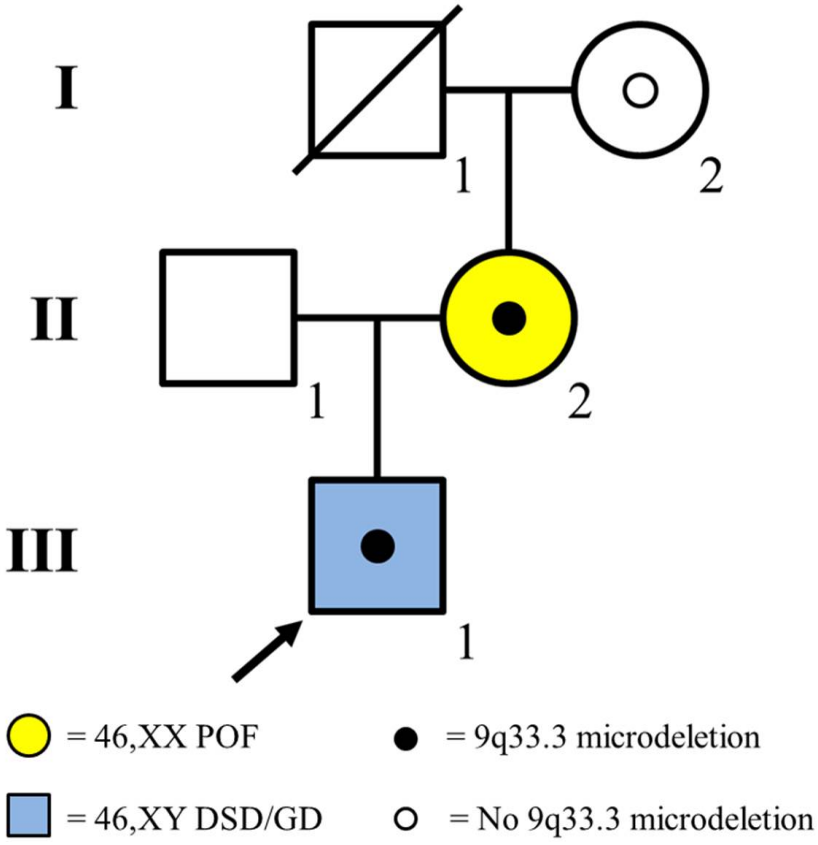

Figure 3.4. A 46,XY GD and 46,XX POF pedigree with a familial 9q33.3 deletion
A 46,XY disorder of sex development due to gonadal dysgenesis (DSD/GD) and premature ovarian failure (POF) pedigree with a familial 9q33.3 deletion. In the pedigree, squares represent XY male family members and circles represent XX female family members. The blue-shaded square represents a XY patient affected with DSD/GD. The yellow-shaded circle represents a XX patient affected with POF. A solid small dot within an individual indicates that family member was found to harbor a 9q33.3 microdeletion including NR5A1. An empty small dot within an individual indicates that family member does not carry the 9q33.3 microdeletion. Individuals without an interior small dot were not tested for deletion. The index patient is indicated with an arrow.

The second patient (Figure 3.5) was also initially assigned female sex, but was subsequently found to have ambiguous genitalia with perineal hypospadias, bifid scrotum with penoscrotal transposition, no Müllerian structures, and bilateral descended testes. After hormonal testing and karyotype detected 46,XY, the family reassigned the patient as male. The infant underwent surgical repair of his hypospadias and genital anomalies after testosterone stimulation. At age 4 years, aCGH testing revealed a copy-number loss of chromosome band 8p23.1 of approximately 0.22 Mb, immediately upstream of *GATA4* and implicating 4 RefSeq genes: *C8orf12* (partial gene deletion), *FAM167A* (partial gene deletion), *BLK* (whole gene deletion), and *LINC00208* (whole gene deletion). FISH analysis of the mother showed the same 8p23.1 microdeletion as observed in her child. Pedigree analysis indicates a family history of congenital heart disease (CHD) in the maternal grandmother (Figure 3.5). Screening for copy-number deletion upstream of GATA4 in this pedigree using the MLPA P234-A1 GATA4 kit confirmed the presence of the 8p23.1 microdeletion in the index case and his mother (III:1 and II:3, respectively) and confirmed the maternal grandmother with CHD (I:2) carries this same microdeletion.

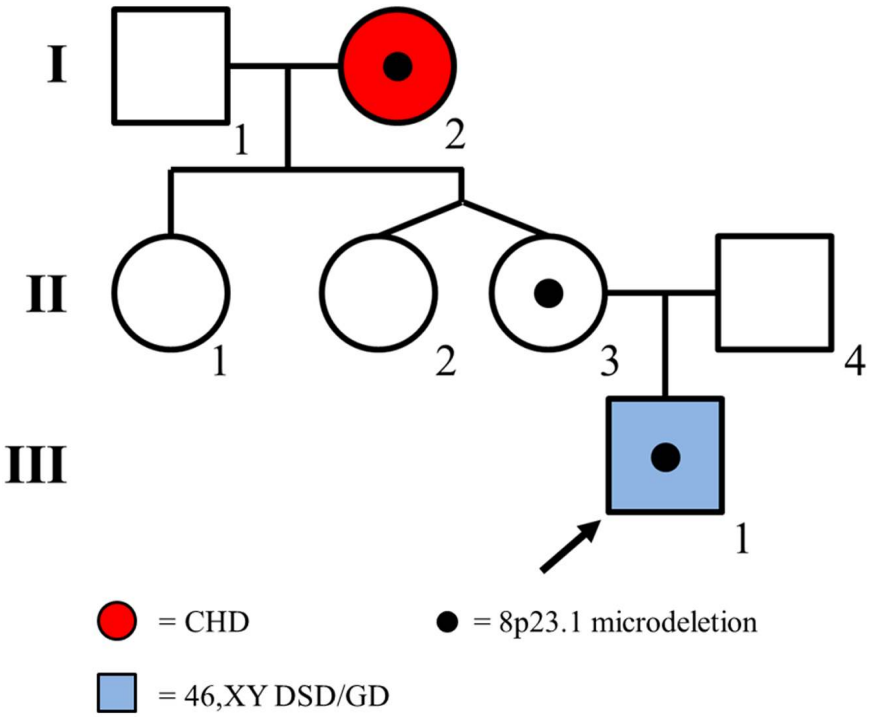

Figure 3.5 - A 46, XY DSD/GD and CHD pedigree with a familial 8p23.1 deletion
A 46,XY DSD/GD and congenital heart disease (CHD) pedigree with a familial 8p23.1 deletion. In the pedigree, squares represent XY male family members and circles represent XX female family members. The grey-shaded square represents a XY patient affected with DSD/GD. The vertical-striped circle represents a XX patient affected with CHD. A solid dot within an individual indicates that family member was found to harbor a 8p23.1 microdeletion. The index patient is indicated with an arrow.

Discussion

Maternally-inherited CNVs involving or adjacent to known 46,XY DSD-causing genes were identified in 2 of 12 (17%) previously unexplained DSD patients. The first patient, with a maternal history of POF, was found to have a co-segregating 0.24Mb microdeletion on 9q33.3 implicating nuclear receptor subfamily 5, group A, member 1 (*NR5A1*; MIM 184757). The *NR5A1* gene encodes for steroidogenic factor 1 (SF1), an intracellular protein transcription factor that regulates the expression of key genes required for testicular determination and proper sexual development, such as *SRY*, *SOX9*, and *AMH*. Consequently, targeted deletion of *Nr5a1* in XY mice results in failed adrenal development, complete testicular dysgenesis, and XY sex reversal with female external genitalia and persistence of Müllerian structures(Luo et al. 1994). Due to studies with knockout mice and the discovery of *NR5A1* mutations in patients with 46,XY sex reversal, *NR5A1* became a candidate gene for DSD. Variations in *NR5A1* extend beyond 46,XY DSD phenotypes, to anorchia, male infertility, and POF in 46,XX cases. The reported frequency of *NR5A1* mutations in 46, XY DSD/GD patients is approximately 20% and in POF patients approximately 3% (Lin et al. 2007; Kohler et al. 2008; Lourenco et al. 2009; Philibert et al. 2010; Janse et al. 2012). Three *NR5A1* copy-number variations, two whole gene deletions and one partial gene deletion, have previously been reported in 46,XY DSD patients (Schlaubitz et al. 2007; van Silfhout et al. 2009; Barbaro et al. 2011). Affected members of four families with histories of both 46, XY DSD and 46,XX POF were found to carry sequence mutations in *NR5A1* (Lourenco et al. 2009). However, this pedigree seen in Figure 3.4 represents the first family with both 46,XY DSD and 46,XX POF caused by a *NR5A1* CNV.

The second patient, with a maternal family history of CHD, was found to have a maternally inherited 0.22Mb microdeletion on 8p23.1 immediately upstream of GATA–binding protein 4 (*GATA4*; MIM 600576). The maternal grandmother with CHD was also found to have the same 8p23.1 microdeletion. In humans and mice, *GATA4* is strongly expressed in the somatic cell population of the developing gonad before and during the time of sex determination (Viger et al. 1998). Mice lacking *Gata4* die *in utero* due to abnormalities in ventral morphogenesis and heart tube formation (Kuo et al. 1997; Molkentin et al. 1997). In humans, mutations in *GATA4* have been well associated with CHD, including septal defects (Garg et al. 2003). Additionally, microdeletions of 8p encompassing GATA4 have previously been identified in 46,XY patients with genitourinary anomalies (Devriendt et al. 1999). Recently however, a familial case of 46, XY DSD and CHD was reported in which affected individuals were found to carry a heterozygous mutation in *GATA4* with incomplete penetrance demonstrating the role of this gene in testis determination (Lourenco et al. 2011). Interestingly, phenotypic variation and incomplete penetrance with regards to *GATA4* variations are also observed in mice heterozygous for a *Gata4* deletion (Jay et al. 2007).

Mutations in known sex-determination genes, such as *SRY*, *SOX9*, *WNT4*, and *DAX1*, account for almost 50% of 46, XY DSD, meaning the genetic basis for the remaining 50% is unknown (White et al. 2011). Screening for mutations in the known sex-determining genes typically only identifies point mutations, while genomic rearrangements, such as CNVs, are often missed by sequencing and are too small to be detected by karyotyping. Others have performed studies to assess the possibility of causal CNVs via microarray-based tests in patients with unexplained, non-syndromic 46,XY

DSD/GD, revealing that approximately 18% of these patients carried CNVs that are likely the cause of DSD/GD(Ledig et al. 2010; White et al. 2011). More broadly, 22% of all types of DSD patients, with phenotypes ranging from isolated hypospadias and isolated cryptorchidism to genital ambiguity and sex reversal, were found to carry clinically relevant CNVs as detected by aCGH (Tannour-Louet et al. 2010). Of these identified clinically-relevant CNVs, 74% were undetectable by karyotype (Tannour-Louet et al. 2010).

The International Standard Cytogenomic Array (ISCA) Consortium recommends aCGH as first-tier genetic testing, in place of karyotyping, for patients with unexplained congenital anomalies (Miller et al. 2010). The ISCA Consortium found that aCGH offers a much higher diagnostic yield (15%-20%) for genetic testing of individuals with congenital anomalies and/or development delay compared to karyotyping diagnostic yield (3%) due to the inability of karyotypes to detect microdeletions and microduplications (<3 Mb) (Miller et al. 2010).

CNV screening, via array-based testing, identified the first reported deletion CNV of WWOX in a 46,XY DSD patient (White et al. 2012). Two different Wwox knockout mice have shown gonadal abnormalities, suggesting WWOK as a causal gene in 46,XY DSD pathogenesis and thus should be screened in additional cases of unexplained DSD. This approach of using CNV testing to identify candidate genes or loci in diseases has previously been utilized to study the genetic causes of idiopathic infertility due to spermatogenic impairment (Tuttelmann et al. 2011; Krausz et al. 2012) and Mayer-Rokitansky-Kuster-Hauser syndrome (Ledig et al. 2011).

Despite the high incidence of sequence mutations associated with DSD, copy-number variations, such as the microdeletions reported in these patients, are another cause of DSD. Thus, in the assessment, treatment, and diagnosis of 46, XY DSD, copy-number analysis by CGH testing should be performed. Making the correct diagnosis can have implications for gender assignment, response to hormone treatment, gonadal malignant potential as well as genetic counseling for the family's future reproductive risk of recurrence.

CHAPTER 3: CONCLUSIONS

Familial cases of congenital anomalies are frequently used to identify candidate genes or genomic loci by comparing genetic variations between affected and healthy family members. In the absence of familial history, sporadic cases can be utilized to identify candidate genes or causal mutations by genome-wide studies, such as aCGH. In studying genital anomalies, familial recurrence is not necessary to hypothesize a genetic cause as causal variants may be inherited from an unaffected parent given the sex-limiting phenotype of persistent cloaca and sex-influenced phenotypes of DSD.

Testing persistent cloaca females via aCGH identified two novel CNVs: a paternally-inherited duplication on 16p13.2 and a *de novo* deletion on 1q32.1q32.3. Both CNV standout as a paternally-inherited duplication supports a sex-limited phenotype of persistent cloaca and *de novo* deletions are a likely pathogenic category of CNVs. Thus, both CNVs provide candidate loci for a severe disorder of unknown genetic cause.

Patients with DSD were also selected for aCGH genotyping, identifing maternally-inherited likely-causal CNVs in two patients with no family history of DSD. A lack of familial history may suggest that an inherited DSD is benign; however subsequent phenotyping of both families identified family members with additional anomalies associated with the gene of interest. In one family, a microdeletion of *NR5A1* was identified in both a DSD patient and his mother with POF. In the second family, a microdeletion of the regulatory region of *GATA4* was identified in both a DSD patient and his maternal grandmother with CHD. Both *NR5A1* and *GATA4* are known to cause DSD in 46,XY individuals and POF or CHD in 46,XX individuals, respectively (Devriendt et al. 1999; Garg et al. 2003; Lourenco et al. 2009).

Given these findings with cloaca and DSD, discounting CNVs inherited from unaffected parents may be erroneous as the phenotypic effects of a CNV can vary by sex. Additionally, excluding CNVs present in DGV as causal may also be erroneous as DGV does not routinely record sex or all phenotypic anomalies of each case. As the phenotypic spectrum associated with CNVs can vary by sex or age, as seen in this study, excluding these CNVs may incorrectly categorize a pathogenic CNV as benign.

Implementation of aCGH has identified novel genes and variants for anomalies of the genital system, including severe oligozoospermia, CHARGE syndrome, and Mayer-Rokitansky-Kuster-Hauser syndrome (Ledig et al. 2010; Ledig et al. 2011; Tuttelmann et al. 2011). Continued use of aCGH on patients with genital anomalies can uncover addition causal variants and candidate genes and potentially help clinicians make well-informed decisions regarding the management of these patients. For instance, in the case of suspected cloaca during pregnancy, a prenatal genetic diagnosis might in the future be correlated with severity of cloaca and impact prenatal care and outcomes. In patients with DSD, identification of a molecular cause can help in diagnosis and give strong indications or predictors regarding gender assignment, response to hormone treatment, and gonadal malignant potential.

CHAPTER 4: CONCLUSIONS AND FUTURE DIRECTIONS

I. Prune belly syndrome

Sequencing the exomes of PBS-affected brothers identified a hypothesized-causal variant in FLNA. This finding is significant as PBS has long been hypothesized to be an X-linked disorder; however, a PBS candidate gene on chrX had not previously been proposed. Confirmation of this FLNA variant in an unrelated, possibly-mosaic PBS patient will also be significant as this finding would be the first report of a PBS variant in unrelated patients. Additionally, analysis of the candidate genes identified by sequencing the exomes of unrelated PBS patients proposes a common mechanistic or pathway model for PBS pathogenesis.

To identify the genetic basis of PBS, multiple steps are needed to validate the proposed candidate genes from WES and develop a genotype-phenotype correlation. Comparing the exomes of the 19 sporadic PBS patients did not identify a single gene affected in all patients. In fact, the gene with the highest overlap in this patient cohort (*IGFN1*) is implicated in only six patients. Given the hypothesized genetic heterogeneity of PBS, screening the remaining 65 sporadic PBS for rare variants in the proposed candidate genes is recommended, starting with the strongest candidate genes, including *IGFN1*, *ITGB2*, *RYR2*, and *ITPR2*.

Continued use of WES on this patient population is also recommended, but with specific selection criteria of samples. Given the relatively low overlap of candidate genes in the sequenced exomes, selection of sporadic patients with similar non-PBS phenotypes for WES is recommended. While the cardinal PBS features are present in all patients in this study, associated skeletal, facial, neurological, and cardiopulmonary abnormalities

vary. By selecting patients with the most similar phenotypes (across all organs), genetic heterogeneity may be minimized, ideally resulting in enrichment of candidate genes. Continued use of WES in sporadic cases without this selection may exclude a potentially-causal PBS gene due to low occurrence within a subset of PBS samples.

Screening proposed candidate genes in a larger cohort of sporadic PBS patients and continued use of WES in phenotypically-matched PBS patients may result in a genotype-phenotype correlation within this patient population. This correlation may result in prioritization of candidate genes to be screened on a case-by-case basis depending on the phenotypic spectrum of the patient as well as permit the creation of phenotype sub-classes within the PBS spectrum. PBS sub-classification may aid clinical care of these complex patients by identifying patients at greatest risk for life-threatening disorders, such as excess surgical bleeding from platelet dysfunction or aortic aneurysm dissection, for example.

II. Genital anomalies

This dissertation research details the use of aCGH to identify the genetic basis of genital anomalies as the genetic cause of persistent cloaca is unknown and causative mutations in known genes account for only 20-50% of 46,XY DSD. Two persistent cloaca patients were found to have possibly pathogenic CNVs due to concordance of CNV inheritance with the sex-limited phenotype of cloacal anomalies. Further studies of the genes affected by these structural variations, with regards to gene function, expression, and known disorders associated with the gene, are recommended as this knowledge can potentially narrow down these regions to a few candidate cloaca-causing genes. Additionally, to better understand these structural variations and their potential impact on

cloacal pathogenesis, continued screening of persistent cloaca patients by aCGH, followed by parental testing if abnormal, is highly recommended. Given the rarity of this phenotype, identification of recurrent or overlapping CNVs in multiple patients would identify the strongest candidate regions for containing cloacal-causing genes.

Patients presenting with DSD are routinely screened for causative variations by karyotyping or sequencing known sex-determining genes. However, this study of 46,XY DSD patients identified causative CNVs that are missed by these traditional genetic tests. Sanger sequencing candidate DSD genes only detects variants in the protein-coding sequences; however, variants in the regulatory elements of many DSD genes, including the microdeletion upstream of *GATA4* from this study, are also associated with DSD pathogenesis. Sanger sequencing is inefficient at detecting whole gene deletions or duplications, thus CNVs encompassing the coding region of a DSD gene, including the microdeletion of *NR5A1* in this study, are also missed by Sanger sequencing. Additionally, as karyotyping can only detect large structure variations (>3 Mb), 74% of clinically relevant CNV identified in 46,XY DSD patients, including the two reported in this study, go undetected (Tannour-Louet et al. 2010).

This research indicates that CNVs are a significant and common cause of DSD. Thus, in the assessment, treatment, and diagnosis of 46, XY DSD, copy-number analysis by CGH testing is recommended as the correct molecular diagnosis can significantly impact gender assignment and predicted response to hormone treatment.

III. Disease gene identification

Of the estimated 5000 rare monogenic diseases, the underlying causative genes are only known for half (Gilissen et al. 2012). Many common disorders hypothesized to be caused by complex multifactorial inheritance, such as autism and intellectually disability, are now thought to represent heterogeneous collections of rare monogenic disorders (McClellan & King 2010; Vissers et al. 2010). Reclassification of these disorders will facilitate disease gene identification by insuring variant data from aCGH and WES is compared across phenotypically-matched individuals, potentially limiting the impact of genetic heterogeneity within a patient cohort.

Identification of disease-causing genes by aCGH or WES is the first step in understanding the physiological roles of the identified protein and elucidating a causative pathway. An understanding of physiological pathways implicated then serves as a starting point for developing therapeutic interventions. Thus, continued use of genome-wide tests, including WES and aCGH, in patients with rare congenital disorders will continue to be a powerful tool in not only molecular studies of disease pathogenesis but also clinical care. Many genitourinary malformations are extremely rare, highly morbid and rarely familial. There is much to gain in identifying the genetic basis of these disorders, including improved prenatal testing, *in utero* counseling and management, improved family counseling for carriers and for future pregnancy risk, and development of novel therapies to prevent the malformation or improve the lives of affected individuals.

BIBLIOGRAPHY

A P. & MA L. (2006) Cloaca. In: *Operative Pediatric Surgery* (eds. by L S & AG C), pp. 503-20. CRC Press, Boca Raton.

Abecasis G.R., Altshuler D., Auton A., Brooks L.D., Durbin R.M., Gibbs R.A., Hurles M.E. & McVean G.A. (2010) A map of human genome variation from population-scale sequencing. *Nature* **467**, 1061-73.

Achermann J.C., Ito M., Hindmarsh P.C. & Jameson J.L. (1999) A mutation in the gene encoding steroidogenic factor-1 causes XY sex reversal and adrenal failure in humans. *Nat Genet* **22**, 125-6.

Achermann J.C., Ozisik G., Ito M., Orun U.A., Harmanci K., Gurakan B. & Jameson J.L. (2002) Gonadal determination and adrenal development are regulated by the orphan nuclear receptor steroidogenic factor-1, in a dose-dependent manner. *J Clin Endocrinol Metab* **87**, 1829-33.

Adams M., Simms R.J., Abdelhamed Z., Dawe H.R., Szymanska K., Logan C.V., Wheway G., Pitt E., Gull K., Knowles M.A., Blair E., Cross S.H., Sayer J.A. & Johnson C.A. (2012) A meckelin-filamin A interaction mediates ciliogenesis. *Hum Mol Genet* **21**, 1272-86.

Adeyokunnu AA & Familusi JB (1982) Prune belly syndrome in two siblings and a first cousin: possible genetic implications. *Am J Dis Child* **136**, 23-5.

Afifi AK, Rebeiz J, Mire J, Andonian J & der K.V. (1972) The mycopathology of the prune belly syndrome. *J Neurol Sci* **15**, 153-65.

Aggarwal V., Krishnamurthy S., Seth A., Bingham C., Ellard S., Mukherjee S.B. & Aneja S. (2010) The renal cysts and diabetes (RCAD) syndrome in a child with deletion of the hepatocyte nuclear factor-1beta gene. *Indian J Pediatr* **77**, 1429-31.

Allen R.C., Zoghbi H.Y., Moseley A.B., Rosenblatt H.M. & Belmont J.W. (1992) Methylation of HpaII and HhaI sites near the polymorphic CAG repeat in the human androgen-receptor gene correlates with X chromosome inactivation. *Am J Hum Genet* **51**, 1229-39.

Amos-Landgraf J.M., Cottle A., Plenge R.M., Friez M., Schwartz C.E., Longshore J. & Willard H.F. (2006) X chromosome-inactivation patterns of 1,005 phenotypically unaffected females. *Am J Hum Genet* **79**, 493-9.

Arner A., Malmqvist U. & Uvelius B. (1990) Metabolism and force in hypertrophic smooth muscle from rat urinary bladder. *Am J Physiol* **258**, C923-32.

Balaji K.C., Patil A., Townes P.L., Primack W., Skare J. & Hopkins T. (2000) Concordant prune belly syndrome in monozygotic twins. *Urology* **55**, 949.

Baldwin E.L., Lee J.Y., Blake D.M., Bunke B.P., Alexander C.R., Kogan A.L., Ledbetter D.H. & Martin C.L. (2008) Enhanced detection of clinically relevant genomic imbalances using a targeted plus whole genome oligonucleotide microarray. *Genet Med* **10**, 415-29.

Barbacci E., Reber M., Ott M.O., Breillat C., Huetz F. & Cereghini S. (1999) Variant hepatocyte nuclear factor 1 is required for visceral endoderm specification. *Development* **126**, 4795-805.

Barbaro M., Cools M., Looijenga L.H., Drop S.L. & Wedell A. (2011) Partial deletion of the NR5A1 (SF1) gene detected by synthetic probe MLPA in a patient with XY gonadal disorder of sex development. *Sex Dev* **5**, 181-7.

Beatham J., Romero R., Townsend S.K., Hacker T., van der Ven P.F. & Blanco G. (2004) Filamin C interacts with the muscular dystrophy KY protein and is abnormally distributed in mouse KY deficient muscle fibres. *Hum Mol Genet* **13**, 2863-74.

Becknell B., Pais P., Onimoe G., Rangarajan H., Schwaderer A.L., McHugh K., Ranalli M.A. & Hains D.S. (2011) Hepatoblastoma and prune belly syndrome: a potential association. *Pediatr Nephrol* **26**, 1269-73.

Berry F.B., O'Neill M.A., Coca-Prados M. & Walter M.A. (2005) FOXC1 transcriptional regulatory activity is impaired by PBX1 in a filamin A-mediated manner. *Mol Cell Biol* **25**, 1415-24.

Bingham C, Ellard S, van't Hoff WG, Simmonds HA, Marinaki AM, Badman MK, Winocour PH, Stride A, Lockwood CR, Nicholls AJ, Owen KR, Spyer G, Pearson ER & Hattersley AT (2003) Atypical familial juvenile hyperuricemic nephropathy associated with a hepatocyte nuclear factor-1β gene mutation. *Kidney Int* **63**, 1645-51.

Bingham C & Hattersley AT (2004) Renal cysts and diabetes syndrome resulting from mutations in hepatocyte nuclear factor-1beta. *Nephrol Dial Transplant* **19**, 2703-8.

Bogart M.M., Arnold H.E. & Greer K.E. (2006) Prune-belly syndrome in two children and review of the literature. *Pediatr Dermatol* **23**, 342-5.

Boycott K.M., Vanstone M.R., Bulman D.E. & MacKenzie A.E. (2013) Rare-disease genetics in the era of next-generation sequencing: discovery to translation. *Nat Rev Genet* **14**, 681-91.

Buglino J.A. & Resh M.D. (2008) Hhat is a palmitoylacyltransferase with specificity for N-palmitoylation of Sonic Hedgehog. *J Biol Chem* **283**, 22076-88.

Calderwood D.A., Huttenlocher A., Kiosses W.B., Rose D.M., Woodside D.G., Schwartz M.A. & Ginsberg M.H. (2001) Increased filamin binding to beta-integrin cytoplasmic domains inhibits cell migration. *Nat Cell Biol* **3**, 1060-8.

Chan Y & Bird LM (2004) Vertically transmitted hypoplasia of the abdominal wall musculature. *Clin Dysmorphol* **13**, 7-10.

Chen H.S., Kolahi K.S. & Mofrad M.R. (2009) Phosphorylation facilitates the integrin binding of filamin under force. *Biophys J* **97**, 3095-104.

Chen M.H., Li Y.J., Kawakami T., Xu S.M. & Chuang P.T. (2004) Palmitoylation is required for the production of a soluble multimeric Hedgehog protein complex and long-range signaling in vertebrates. *Genes Dev* **18**, 641-59.

Chen Y.Z., Gao Q., Zhao X.Z., Bennett C.L., Xiong X.S., Mei C.L., Shi Y.Q. & Chen X.M. (2010) Systematic review of TCF2 anomalies in renal cysts and diabetes syndrome/maturity onset diabetes of the young type 5. *Chin Med J (Engl)* **123**, 3326-33.

Cheng W., Li B., Kajstura J., Li P., Wolin M.S., Sonnenblick E.H., Hintze T.H., Olivetti G. & Anversa P. (1995) Stretch-induced programmed myocyte cell death. *J Clin Invest* **96**, 2247-59.

Christianson A., Howson C. & Modell B. (2006) March of Dimes global report on birth defects, 2006.

Clayton-Smith J., Walters S., Hobson E., Burkitt-Wright E., Smith R., Toutain A., Amiel J., Lyonnet S., Mansour S., Fitzpatrick D., Ciccone R., Ricca I., Zuffardi O. & Donnai D. (2009) Xq28 duplication presenting with intestinal and bladder dysfunction and a distinctive facial appearance. *Eur J Hum Genet* **17**, 434-43.

Clements K.M., Bee Z.C., Crossingham G.V., Adams M.A. & Sharif M. (2001) How severe must repetitive loading be to kill chondrocytes in articular cartilage? *Osteoarthritis Cartilage* **9**, 499-507.

Coffinier C., Barra J., Babinet C. & Yaniv M. (1999) Expression of the vHNF1/HNF1beta homeoprotein gene during mouse organogenesis. *Mech Dev* **89**, 211-3.

Cook E.H., Jr. & Scherer S.W. (2008) Copy-number variations associated with neuropsychiatric conditions. *Nature* **455**, 919-23.

Cooper G.M., Stone E.A., Asimenos G., Green E.D., Batzoglou S. & Sidow A. (2005) Distribution and intensity of constraint in mammalian genomic sequence. *Genome Res* **15**, 901-13.

Cunningham C.C., Gorlin J.B., Kwiatkowski D.J., Hartwig J.H., Janmey P.A., Byers H.R. & Stossel T.P. (1992) Actin-binding protein requirement for cortical stability and efficient locomotion. *Science* **255**, 325-7.

D'Addario M., Arora P.D., Ellen R.P. & McCulloch C.A. (2002) Interaction of p38 and Sp1 in a mechanical force-induced, beta 1 integrin-mediated transcriptional circuit that regulates the actin-binding protein filamin-A. *J Biol Chem* **277**, 47541-50.

Desai V., Donsante A., Swoboda K.J., Martensen M., Thompson J. & Kaler S.G. (2011) Favorably skewed X-inactivation accounts for neurological sparing in female carriers of Menkes disease. *Clin Genet* **79**, 176-82.

Devriendt K., Matthijs G., Van Dael R., Gewillig M., Eyskens B., Hjalgrim H., Dolmer B., McGaughran J., Brondum-Nielsen K., Marynen P., Fryns J.P. & Vermeesch J.R. (1999) Delineation of the critical deletion region for congenital heart defects, on chromosome 8p23.1. *Am J Hum Genet* **64**, 1119-26.

Disteche C.M., Casanova M., Saal H., Friedman C., Sybert V., Graham J., Thuline H., Page D.C. & Fellous M. (1986) Small deletions of the short arm of the Y chromosome in 46,XY females. *Proc Natl Acad Sci U S A* **83**, 7841-4.

Donnenfeld A.E., Conard K.A., Roberts N.S., Borns P.F. & Zackai E.H. (1987) Melnick-Needles syndrome in males: a lethal multiple congenital anomalies syndrome. *Am J Med Genet* **27**, 159-73.

Dravis C., Yokoyama N., Chumley M.J., Cowan C.A., Silvany R.E., Shay J., Baker L.A. & Henkemeyer M. (2004) Bidirectional signaling mediated by ephrin-B2 and EphB2 controls urorectal development. *Dev Biol* **271**, 272-90.

Druschel C.M. (1995) A descriptive study of prune belly in New York State, 1983 to 1989. *Arch Pediatr Adolesc Med* **149**, 70-6.

Edghill EL, Bingham C, Ellard S & Hattersley AT (2006) Mutations in hepatocyte nuclear factor-1B and their related phenotypes. *J Med Genet* **43**, 84-90.

Edghill E.L., Oram R.A., Owens M., Stals K.L., Harries L.W., Hattersley A.T., Ellard S. & Bingham C. (2008) Hepatocyte nuclear factor-1beta gene deletions--a common cause of renal disease. *Nephrol Dial Transplant* **23**, 627-35.

Edghill E.L., Stals K., Oram R.A., Shepherd M.H., Hattersley A.T. & Ellard S. (2013) HNF1B deletions in patients with young-onset diabetes but no known renal disease. *Diabet Med* **30**, 114-7.

Ekman M., Uvelius B., Albinsson S. & Sward K. (2014) HIF-mediated metabolic switching in bladder outlet obstruction mitigates the relaxing effect of mitochondrial inhibition. *Lab Invest*.

Eksioglu Y.Z., Scheffer I.E., Cardenas P., Knoll J., DiMario F., Ramsby G., Berg M., Kamuro K., Berkovic S.F., Duyk G.M., Parisi J., Huttenlocher P.R. & Walsh C.A. (1996) Periventricular heterotopia: an X-linked dominant epilepsy locus causing aberrant cerebral cortical development. *Neuron* **16**, 77-87.

Engler A.J., Sen S., Sweeney H.L. & Discher D.E. (2006) Matrix elasticity directs stem cell lineage specification. *Cell* **126**, 677-89.

Farrand K., Jovanovic L., Delahunt B., McIver B., Hay I.D., Eberhardt N.L. & Grebe S.K. (2002) Loss of heterozygosity studies revisited: prior quantification of the amplifiable DNA content of archival samples improves efficiency and reliability. *J Mol Diagn* **4**, 150-8.

Feige A F.K., Rempen A, Osterhage HR. (1984) Prenatal diagnosis of prune belly syndrome occurring in siblings in 2 consecutive pregnancies. *Z Geburtshilfe Perinatol* **188**, 239-43.

Feng Y., Chen M.H., Moskowitz I.P., Mendonza A.M., Vidali L., Nakamura F., Kwiatkowski D.J. & Walsh C.A. (2006) Filamin A (FLNA) is required for cell-cell contact in vascular development and cardiac morphogenesis. *Proc Natl Acad Sci U S A* **103**, 19836-41.

Fink J.M., Dobyns W.B., Guerrini R. & Hirsch B.A. (1997) Identification of a duplication of Xq28 associated with bilateral periventricular nodular heterotopia. *Am J Hum Genet* **61**, 379-87.

Folch M., Pigem I. & Konje J.C. (2000) Mullerian agenesis: etiology, diagnosis, and management. *Obstet Gynecol Surv* **55**, 644-9.

Forrester M.B. & Merz R.D. (2004) Impact of excluding cases with known chromosomal abnormalities on the prevalence of structural birth defects, Hawaii, 1986-1999. *Am J Med Genet A* **128A**, 383-8.

Fowler C.J., Griffiths D. & de Groat W.C. (2008) The neural control of micturition. *Nat Rev Neurosci* **9**, 453-66.

Fox J.W., Lamperti E.D., Eksioglu Y.Z., Hong S.E., Feng Y., Graham D.A., Scheffer I.E., Dobyns W.B., Hirsch B.A., Radtke R.A., Berkovic S.F., Huttenlocher P.R. & Walsh C.A. (1998) Mutations in filamin 1 prevent migration of cerebral cortical neurons in human periventricular heterotopia. *Neuron* **21**, 1315-25.

Froyen G., Corbett M., Vandewalle J., Jarvela I., Lawrence O., Meldrum C., Bauters M., Govaerts K., Vandeleur L., Van Esch H., Chelly J., Sanlaville D., van Bokhoven H., Ropers H.H., Laumonnier F., Ranieri E., Schwartz C.E., Abidi F., Tarpey P.S., Futreal P.A., Whibley A., Raymond F.L., Stratton M.R., Fryns J.P., Scott R., Peippo M., Sipponen M., Partington M., Mowat D., Field M., Hackett A., Marynen P., Turner G. & Gecz J. (2008) Submicroscopic duplications of the hydroxysteroid dehydrogenase HSD17B10 and the E3 ubiquitin ligase HUWE1 are associated with mental retardation. *Am J Hum Genet* **82**, 432-43.

Fynn-Thompson E., Cheng H. & Teixeira J. (2003) Inhibition of steroidogenesis in Leydig cells by Mullerian-inhibiting substance. *Mol Cell Endocrinol* **211**, 99-104.

Gaboardi F, Sterpa A, Thiebat E, Cornali R, Manfredi M, Bianchi C, Giacomoni MA & L B. (1982) Prune-belly syndrome: report of three siblings. *Helv Paediatr Acta* **37**, 283-8.

Garg V., Kathiriya I.S., Barnes R., Schluterman M.K., King I.N., Butler C.A., Rothrock C.R., Eapen R.S., Hirayama-Yamada K., Joo K., Matsuoka R., Cohen J.C. & Srivastava D. (2003) GATA4 mutations cause human congenital heart defects and reveal an interaction with TBX5. *Nature* **424**, 443-7.

Gargiulo A., Auricchio R., Barone M.V., Cotugno G., Reardon W., Milla P.J., Ballabio A., Ciccodicola A. & Auricchio A. (2007) Filamin A is mutated in X-linked chronic idiopathic intestinal pseudo-obstruction with central nervous system involvement. *Am J Hum Genet* **80**, 751-8.

Garlinger P & Ott J (1974) Prune belly syndrome: possible genetic implications. *Birth Defects* **10**, 173-80.

Gearhart J.P., Lee B.R., Partin A.W., Epstein J.I. & Gosling J.A. (1995) A quantitative histological evaluation of the dilated ureter of childhood. II: Ectopia, posterior urethral valves and the prune belly syndrome. *J Urol* **153**, 172-6.

Gehler S., Baldassarre M., Lad Y., Leight J.L., Wozniak M.A., Riching K.M., Eliceiri K.W., Weaver V.M., Calderwood D.A. & Keely P.J. (2009) Filamin A-beta1 integrin complex tunes epithelial cell response to matrix tension. *Mol Biol Cell* **20**, 3224-38.

Giannone G. & Sheetz M.P. (2006) Substrate rigidity and force define form through tyrosine phosphatase and kinase pathways. *Trends Cell Biol* **16**, 213-23.

Gilissen C., Hoischen A., Brunner H.G. & Veltman J.A. (2012) Disease gene identification strategies for exome sequencing. *Eur J Hum Genet* **20**, 490-7.

Glogauer M., Arora P., Chou D., Janmey P.A., Downey G.P. & McCulloch C.A. (1998) The role of actin-binding protein 280 in integrin-dependent mechanoprotection. *J Biol Chem* **273**, 1689-98.

Gosling J.A., Kung L.S., Dixon J.S., Horan P., Whitbeck C. & Levin R.M. (2000) Correlation between the structure and function of the rabbit urinary bladder following partial outlet obstruction. *J Urol* **163**, 1349-56.

Granberg C.F., Harrison S.M., Dajusta D., Zhang S., Hajarnis S., Igarashi P. & Baker L.A. (2012) Genetic basis of prune belly syndrome: screening for HNF1beta gene. *J Urol* **187**, 272-8.

Grenet P, Le Calvé G, Badoual J, Gallet JP & JM B. (1972) Congenital aplasia of the abdominal wall: a familial case. *Ann Pediatr* **19**, 523-8.

Guillen D.R., Lowichik A., Schneider N.R., Cohen D.S., Garcia S. & Zinn A.R. (1997) Prune-belly syndrome and other anomalies in a stillborn fetus with a ring X chromosome lacking XIST. *Am J Med Genet* **70**, 32-6.

Gunst S.J. & Zhang W. (2008) Actin cytoskeletal dynamics in smooth muscle: a new paradigm for the regulation of smooth muscle contraction. *Am J Physiol Cell Physiol* **295**, C576-87.

Guo D.C., Pannu H., Tran-Fadulu V., Papke C.L., Yu R.K., Avidan N., Bourgeois S., Estrera A.L., Safi H.J., Sparks E., Amor D., Ades L., McConnell V., Willoughby C.E., Abuelo D., Willing M., Lewis R.A., Kim D.H., Scherer S., Tung P.P., Ahn C., Buja L.M., Raman C.S., Shete S.S. & Milewicz D.M. (2007) Mutations in smooth muscle alpha-actin (ACTA2) lead to thoracic aortic aneurysms and dissections. *Nat Genet* **39**, 1488-93.

Guo D.C., Papke C.L., Tran-Fadulu V., Regalado E.S., Avidan N., Johnson R.J., Kim D.H., Pannu H., Willing M.C., Sparks E., Pyeritz R.E., Singh M.N., Dalman R.L., Grotta J.C., Marian A.J., Boerwinkle E.A., Frazier L.Q., LeMaire S.A., Coselli J.S., Estrera A.L., Safi H.J., Veeraraghavan S., Muzny D.M., Wheeler D.A., Willerson J.T., Yu R.K., Shete S.S., Scherer S.E., Raman C.S., Buja L.M. & Milewicz D.M. (2009) Mutations in smooth muscle alpha-actin (ACTA2) cause coronary artery disease, stroke, and Moyamoya disease, along with thoracic aortic disease. *Am J Hum Genet* **84**, 617-27.

Haeri S., Devers P.L., Kaiser-Rogers K.A., Moylan V.J., Jr., Torchia B.S., Horton A.L., Wolfe H.M. & Aylsworth A.S. (2010) Deletion of hepatocyte nuclear factor-1-beta in an infant with prune belly syndrome. *Am J Perinatol* **27**, 559-63.

Hanley N.A., Ball S.G., Clement-Jones M., Hagan D.M., Strachan T., Lindsay S., Robson S., Ostrer H., Parker K.L. & Wilson D.I. (1999) Expression of steroidogenic factor 1 and Wilms' tumour 1 during early human gonadal development and sex determination. *Mech Dev* **87**, 175-80.

Harley LM, Chen Y & Rattner WH (1972) Prune belly syndrome. *J Urol* **108**, 174-6.

Harrison S.M., Campbell I.M., Keays M., Granberg C.F., Villanueva C., Tannin G., Zinn A.R., Castrillon D.H., Shaw C.A., Stankiewicz P. & Baker L.A. (2013) Screening and familial characterization of copy-number variations in NR5A1 in 46,XY disorders of sex development and premature ovarian failure. *Am J Med Genet A* **161**, 2487-94.

Hart A.W., Morgan J.E., Schneider J., West K., McKie L., Bhattacharya S., Jackson I.J. & Cross S.H. (2006) Cardiac malformations and midline skeletal defects in mice lacking filamin A. *Hum Mol Genet* **15**, 2457-67.

Hendren W.H. (1992) Cloacal malformations: experience with 105 cases. *J Pediatr Surg* **27**, 890-901.

Henrichsen C.N., Chaignat E. & Reymond A. (2009) Copy number variants, diseases and gene expression. *Hum Mol Genet* **18**, R1-8.

Hiesberger T, Bai Y, Shao X, McNally BT, Sinclair AM, Tian X, Somlo S & P I. (2004) Mutations of hepatocyte nuclear factor-1B inhibits Pkhd1 gene expression and produces renal cysts in mice. *J Clin Invest* **113**, 814-25.

Holder J.P. (1989) Pathophysiologic and anesthetic correlations of the prune-belly syndrome. *AANA J* **57**, 137-41.

Hood R.L., Lines M.A., Nikkel S.M., Schwartzentruber J., Beaulieu C., Nowaczyk M.J., Allanson J., Kim C.A., Wieczorek D., Moilanen J.S., Lacombe D., Gillessen-Kaesbach G., Whiteford M.L., Quaio C.R., Gomy I., Bertola D.R., Albrecht B., Platzer K., McGillivray G., Zou R., McLeod D.R., Chudley A.E., Chodirker B.N., Marcadier J., Majewski J., Bulman D.E., White S.M. & Boycott K.M. (2012) Mutations in SRCAP, encoding SNF2-related CREBBP activator protein, cause Floating-Harbor syndrome. *Am J Hum Genet* **90**, 308-13.

Hoskins BE, Cramer CH, Tasic V, Kehinde EO, Ashraf S, Bogdanovic R, Hoefele J, Pohl M & F H. (2008) Missense mutations in EYA1 and TCF2 are a rare cause of urinary tract malformations. *Nephrol Dial Transplant* **23**, 777-9.

Hughes I.A., Houk C., Ahmed S.F. & Lee P.A. (2006) Consensus statement on management of intersex disorders. *J Pediatr Urol* **2**, 148-62.

Iafrate A.J., Feuk L., Rivera M.N., Listewnik M.L., Donahoe P.K., Qi Y., Scherer S.W. & Lee C. (2004) Detection of large-scale variation in the human genome. *Nat Genet* **36**, 949-51.

Ibadin M.O., Ademola A.A. & Ofovwe G.E. (2012) Familial prune belly syndrome in a Nigerian family. *Saudi J Kidney Dis Transpl* **23**, 338-42.

Ithychanda S.S., Das M., Ma Y.Q., Ding K., Wang X., Gupta S., Wu C., Plow E.F. & Qin J. (2009a) Migfilin, a molecular switch in regulation of integrin activation. *J Biol Chem* **284**, 4713-22.

Ithychanda S.S., Hsu D., Li H., Yan L., Liu D.D., Das M., Plow E.F. & Qin J. (2009b) Identification and characterization of multiple similar ligand-binding repeats in filamin: implication on filamin-mediated receptor clustering and cross-talk. *J Biol Chem* **284**, 35113-21.

Itsara A., Cooper G.M., Baker C., Girirajan S., Li J., Absher D., Krauss R.M., Myers R.M., Ridker P.M., Chasman D.I., Mefford H., Ying P., Nickerson D.A. & Eichler E.E. (2009) Population analysis of large copy number variants and hotspots of human genetic disease. *Am J Hum Genet* **84**, 148-61.

Ives E.J. (1974) The abdominal muscle deficiency triad syndrome--experience with ten cases. *Birth Defects Orig Artic Ser* **10**, 127-35.

Janse F., de With L.M., Duran K.J., Kloosterman W.P., Goverde A.J., Lambalk C.B., Laven J.S., Fauser B.C. & Giltay J.C. (2012) Limited contribution of NR5A1 (SF-1) mutations in women with primary ovarian insufficiency (POI). *Fertil Steril* **97**, 141-6 e2.

Janson L.W., Kolega J. & Taylor D.L. (1991) Modulation of contraction by gelation/solation in a reconstituted motile model. *J Cell Biol* **114**, 1005-15.

Jay P.Y., Bielinska M., Erlich J.M., Mannisto S., Pu W.T., Heikinheimo M. & Wilson D.B. (2007) Impaired mesenchymal cell function in Gata4 mutant mice leads to diaphragmatic hernias and primary lung defects. *Dev Biol* **301**, 602-14.

Jenkins D., Bitner-Glindzicz M., Malcolm S., Hu C.C., Allison J., Winyard P.J., Gullett A.M., Thomas D.F., Belk R.A., Feather S.A., Sun T.T. & Woolf A.S. (2005) De novo Uroplakin IIIa heterozygous mutations cause human renal adysplasia leading to severe kidney failure. *J Am Soc Nephrol* **16**, 2141-9.

Jenkins D., Bitner-Glindzicz M., Thomasson L., Malcolm S., Warne S.A., Feather S.A., Flanagan S.E., Ellard S., Bingham C., Santos L., Henkemeyer M., Zinn A., Baker L.A., Wilcox D.T. & Woolf A.S. (2007) Mutational analyses of UPIIIA, SHH, EFNB2 and HNF1beta in persistent cloaca and associated kidney malformations. *J Pediatr Urol* **3**, 2-9.

Jeyasuria P., Ikeda Y., Jamin S.P., Zhao L., De Rooij D.G., Themmen A.P., Behringer R.R. & Parker K.L. (2004) Cell-specific knockout of steroidogenic factor 1 reveals its essential roles in gonadal function. *Mol Endocrinol* **18**, 1610-9.

Johnson C.P., Tang H.Y., Carag C., Speicher D.W. & Discher D.E. (2007) Forced unfolding of proteins within cells. *Science* **317**, 663-6.

Jordan B.K., Mohammed M., Ching S.T., Delot E., Chen X.N., Dewing P., Swain A., Rao P.N., Elejalde B.R. & Vilain E. (2001) Up-regulation of WNT-4 signaling and dosage-sensitive sex reversal in humans. *Am J Hum Genet* **68**, 1102-9.

Kainulainen T., Pender A., D'Addario M., Feng Y., Lekic P. & McCulloch C.A. (2002) Cell death and mechanoprotection by filamin a in connective tissues after challenge by applied tensile forces. *J Biol Chem* **277**, 21998-2009.

Kamm R.D. & Kaazempur-Mofrad M.R. (2004) On the molecular basis for mechanotransduction. *Mech Chem Biosyst* **1**, 201-9.

Kapur R.P., Robertson S.P., Hannibal M.C., Finn L.S., Morgan T., van Kogelenberg M. & Loren D.J. (2010) Diffuse abnormal layering of small intestinal smooth muscle is present in patients with FLNA mutations and x-linked intestinal pseudo-obstruction. *Am J Surg Pathol* **34**, 1528-43.

Kasza K.E., Nakamura F., Hu S., Kollmannsberger P., Bonakdar N., Fabry B., Stossel T.P., Wang N. & Weitz D.A. (2009) Filamin A is essential for active cell stiffening but not passive stiffening under external force. *Biophys J* **96**, 4326-35.

Kelley R.I. & Hennekam R.C. (2000) The Smith-Lemli-Opitz syndrome. *J Med Genet* **37**, 321-35.

Kiema T., Lad Y., Jiang P., Oxley C.L., Baldassarre M., Wegener K.L., Campbell I.D., Ylanne J. & Calderwood D.A. (2006) The molecular basis of filamin binding to integrins and competition with talin. *Mol Cell* **21**, 337-47.

Kim E.J., Park J.S. & Um S.J. (2007) Filamin A negatively regulates the transcriptional activity of p73alpha in the cytoplasm. *Biochem Biophys Res Commun* **362**, 1101-6.

Kim H., Sengupta A., Glogauer M. & McCulloch C.A. (2008) Filamin A regulates cell spreading and survival via beta1 integrins. *Exp Cell Res* **314**, 834-46.

Kinahan T.J., Churchill B.M., McLorie G.A., Gilmour R.F. & Khoury A.E. (1992) The efficiency of bladder emptying in the prune belly syndrome. *J Urol* **148**, 600-3.

Kohler B., Lin L., Ferraz-de-Souza B., Wieacker P., Heidemann P., Schroder V., Biebermann H., Schnabel D., Gruters A. & Achermann J.C. (2008) Five novel mutations in steroidogenic factor 1 (SF1, NR5A1) in 46,XY patients with severe underandrogenization but without adrenal insufficiency. *Hum Mutat* **29**, 59-64.

Kohler B., Lin L., Mazen I., Cetindag C., Biebermann H., Akkurt I., Rossi R., Hiort O., Gruters A. & Achermann J.C. (2009) The spectrum of phenotypes associated with mutations in steroidogenic factor 1 (SF-1, NR5A1, Ad4BP) includes severe penoscrotal hypospadias in 46,XY males without adrenal insufficiency. *Eur J Endocrinol* **161**, 237-42.

Kolatsi-Joannou M., Bingham C., Ellard S., Bulman M.P., Allen L.I., Hattersley A.T. & Woolf A.S. (2001) Hepatocyte nuclear factor-1beta: a new kindred with renal cysts and diabetes and gene expression in normal human development. *J Am Soc Nephrol* **12**, 2175-80.

Krausz C., Giachini C., Lo Giacco D., Daguin F., Chianese C., Ars E., Ruiz-Castane E., Forti G. & Rossi E. (2012) High resolution X chromosome-specific array-CGH detects new CNVs in infertile males. *PLoS One* **7**, e44887.

Kuo C.T., Morrisey E.E., Anandappa R., Sigrist K., Lu M.M., Parmacek M.S., Soudais C. & Leiden J.M. (1997) GATA4 transcription factor is required for ventral morphogenesis and heart tube formation. *Genes Dev* **11**, 1048-60.

Kyndt F., Gueffet J.P., Probst V., Jaafar P., Legendre A., Le Bouffant F., Toquet C., Roy E., McGregor L., Lynch S.A., Newbury-Ecob R., Tran V., Young I., Trochu J.N., Le Marec H. & Schott J.J. (2007) Mutations in the gene encoding filamin A as a cause for familial cardiac valvular dystrophy. *Circulation* **115**, 40-9.

Lad Y., Harburger D.S. & Calderwood D.A. (2007a) Integrin cytoskeletal interactions. *Methods Enzymol* **426**, 69-84.

Lad Y., Kiema T., Jiang P., Pentikainen O.T., Coles C.H., Campbell I.D., Calderwood D.A. & Ylanne J. (2007b) Structure of three tandem filamin domains reveals auto-inhibition of ligand binding. *EMBO J* **26**, 3993-4004.

Le Caignec C., Delnatte C., Vermeesch J.R., Boceno M., Joubert M., Lavenant F., David A. & Rival J.M. (2007) Complete sex reversal in a WAGR syndrome patient. *Am J Med Genet A* **143A**, 2692-5.

Ledig S., Hiort O., Scherer G., Hoffmann M., Wolff G., Morlot S., Kuechler A. & Wieacker P. (2010) Array-CGH analysis in patients with syndromic and non-syndromic XY gonadal dysgenesis: evaluation of array CGH as diagnostic tool and search for new candidate loci. *Hum Reprod* **25**, 2637-46.

Ledig S., Schippert C., Strick R., Beckmann M.W., Oppelt P.G. & Wieacker P. (2011) Recurrent aberrations identified by array-CGH in patients with Mayer-Rokitansky-Kuster-Hauser syndrome. *Fertil Steril* **95**, 1589-94.

Lee C., Iafrate A.J. & Brothman A.R. (2007) Copy number variations and clinical cytogenetic diagnosis of constitutional disorders. *Nat Genet* **39**, S48-54.

Li H. & Durbin R. (2009) Fast and accurate short read alignment with Burrows-Wheeler transform. *Bioinformatics* **25**, 1754-60.

Li H., Handsaker B., Wysoker A., Fennell T., Ruan J., Homer N., Marth G., Abecasis G. & Durbin R. (2009) The Sequence Alignment/Map format and SAMtools. *Bioinformatics* **25**, 2078-9.

Lilleoja R., Sarapik A., Reimann E., Reemann P., Jaakma U., Vasar E. & Koks S. (2012) Sequencing and annotated analysis of an Estonian human genome. *Gene* **493**, 69-76.

Lin L. & Achermann J.C. (2008) Steroidogenic factor-1 (SF-1, Ad4BP, NR5A1) and disorders of testis development. *Sex Dev* **2**, 200-9.

Lin L., Philibert P., Ferraz-de-Souza B., Kelberman D., Homfray T., Albanese A., Molini V., Sebire N.J., Einaudi S., Conway G.S., Hughes I.A., Jameson J.L., Sultan C., Dattani M.T. & Achermann J.C. (2007) Heterozygous missense mutations in steroidogenic factor 1 (SF1/Ad4BP, NR5A1) are associated with 46,XY disorders of sex development with normal adrenal function. *J Clin Endocrinol Metab* **92**, 991-9.

Liu P., Carvalho C.M., Hastings P.J. & Lupski J.R. (2012) Mechanisms for recurrent and complex human genomic rearrangements. *Curr Opin Genet Dev* **22**, 211-20.

Livak K.J. & Schmittgen T.D. (2001) Analysis of relative gene expression data using real-time quantitative PCR and the 2(-Delta Delta C(T)) Method. *Methods* **25**, 402-8.

Loane M., Dolk H., Kelly A., Teljeur C., Greenlees R. & Densem J. (2011) Paper 4: EUROCAT statistical monitoring: identification and investigation of ten year trends of congenital anomalies in Europe. *Birth Defects Res A Clin Mol Teratol* **91 Suppl 1**, S31-43.

Lockhart JL, Reeve HR, Bredael JJ & Krueger RP (1979) Siblings with prune belly syndrome and associated pulmonic stensosis, mental retardation, and deafness. *Urology* **14**, 140-2.

Lourenco D., Brauner R., Lin L., De Perdigo A., Weryha G., Muresan M., Boudjenah R., Guerra-Junior G., Maciel-Guerra A.T., Achermann J.C., McElreavey K. & Bashamboo A. (2009) Mutations in NR5A1 associated with ovarian insufficiency. *N Engl J Med* **360**, 1200-10.

Lourenco D., Brauner R., Rybczynska M., Nihoul-Fekete C., McElreavey K. & Bashamboo A. (2011) Loss-of-function mutation in GATA4 causes anomalies of human testicular development. *Proc Natl Acad Sci U S A* **108**, 1597-602.

Loy C.J., Sim K.S. & Yong E.L. (2003) Filamin-A fragment localizes to the nucleus to regulate androgen receptor and coactivator functions. *Proc Natl Acad Sci U S A* **100**, 4562-7.

Luo X., Ikeda Y. & Parker K.L. (1994) A cell-specific nuclear receptor is essential for adrenal and gonadal development and sexual differentiation. *Cell* **77**, 481-90.

Malin G., Tonks A.M., Morris R.K., Gardosi J. & Kilby M.D. (2012) Congenital lower urinary tract obstruction: a population-based epidemiological study. *BJOG* **119**, 1455-64.

Matsui M., Motomura D., Karasawa H., Fujikawa T., Jiang J., Komiya Y., Takahashi S. & Taketo M.M. (2000) Multiple functional defects in peripheral autonomic organs in mice lacking muscarinic acetylcholine receptor gene for the M3 subtype. *Proc Natl Acad Sci U S A* **97**, 9579-84.

McClellan J. & King M.C. (2010) Genetic heterogeneity in human disease. *Cell* **141**, 210-7.

McKenna A., Hanna M., Banks E., Sivachenko A., Cibulskis K., Kernytsky A., Garimella K., Altshuler D., Gabriel S., Daly M. & DePristo M.A. (2010) The Genome Analysis Toolkit: a MapReduce framework for analyzing next-generation DNA sequencing data. *Genome Res* **20**, 1297-303.

Mefford HC, Clauin S, Sharp AJ, Moller RS, Ullmann R, Kapur R, Pinkel D, Cooper GM, Ventura M, Ropers HH, Tommerup N, Eichler EE & C B.-C. (2007) Recurrent

reciprocal genomic rearrangements of 17q12 are associated with renal disease, diabetes, and epilepsy. *Am J Hum Genet* **81**, 1057-69.

Mefford H.C., Clauin S., Sharp A.J., Moller R.S., Ullmann R., Kapur R., Pinkel D., Cooper G.M., Ventura M., Ropers H.H., Tommerup N., Eichler E.E. & Bellanne-Chantelot C. (2007) Recurrent reciprocal genomic rearrangements of 17q12 are associated with renal disease, diabetes, and epilepsy. *Am J Hum Genet* **81**, 1057-69.

Melnick J.C. & Needles C.F. (1966) An undiagnosed bone dysplasia. A 2 family study of 4 generations and 3 generations. *Am J Roentgenol Radium Ther Nucl Med* **97**, 39-48.

Menon R., Deng M., Boehm D., Braun M., Fend F., Biskup S. & Perner S. (2012) Exome Enrichment and SOLiD Sequencing of Formalin Fixed Paraffin Embedded (FFPE) Prostate Cancer Tissue. *Int J Mol Sci* **13**, 8933-42.

Milewicz D.M., Ostergaard J.R., Ala-Kokko L.M., Khan N., Grange D.K., Mendoza-Londono R., Bradley T.J., Olney A.H., Ades L., Maher J.F., Guo D., Buja L.M., Kim D., Hyland J.C. & Regalado E.S. (2010) De novo ACTA2 mutation causes a novel syndrome of multisystemic smooth muscle dysfunction. *Am J Med Genet A* **152A**, 2437-43.

Miller D.T., Adam M.P., Aradhya S., Biesecker L.G., Brothman A.R., Carter N.P., Church D.M., Crolla J.A., Eichler E.E., Epstein C.J., Faucett W.A., Feuk L., Friedman J.M., Hamosh A., Jackson L., Kaminsky E.B., Kok K., Krantz I.D., Kuhn R.M., Lee C., Ostell J.M., Rosenberg C., Scherer S.W., Spinner N.B., Stavropoulos D.J., Tepperberg J.H., Thorland E.C., Vermeesch J.R., Waggoner D.J., Watson M.S., Martin C.L. & Ledbetter D.H. (2010) Consensus statement: chromosomal microarray is a first-tier clinical diagnostic test for individuals with developmental disabilities or congenital anomalies. *Am J Hum Genet* **86**, 749-64.

Miller M., Kaufman G., Reed G., Bilenker R. & Schinzel A. (1979) Familial, balanced insertional translocation of chromosome 7 leading to offspring with deletion and duplication of the inserted segment, 7p15 leads to 7p21. *Am J Med Genet* **4**, 323-32.

Mininberg D.T., Montoya F., Okada K., Galioto F. & Presutti R. (1973) Subcellular muscle studies in the prune belly syndrome. *J Urol* **109**, 524-6.

Mo R., Kim J.H., Zhang J., Chiang C., Hui C.C. & Kim P.C. (2001) Anorectal malformations caused by defects in sonic hedgehog signaling. *Am J Pathol* **159**, 765-74.

Moerman P., Fryns J.P., Goddeeris P. & Lauweryns J.M. (1984) Pathogenesis of the prune-belly syndrome: a functional urethral obstruction caused by prostatic hypoplasia. *Pediatrics* **73**, 470-5.

Molkentin J.D., Lin Q., Duncan S.A. & Olson E.N. (1997) Requirement of the transcription factor GATA4 for heart tube formation and ventral morphogenesis. *Genes Dev* **11**, 1061-72.

Montoli A, Colussi G, Massa O, Caccia R, Rizzoni G, Civati G & Barbetti F (2002) Renal cysts and diabetes syndrome linked to mutations of the hepatocyte nuclear factor-1β gene: description of a new family with associated liver involvement. *Am J Kidney Dis* **40**, 397-402.

Moro F., Carrozzo R., Veggiotti P., Tortorella G., Toniolo D., Volzone A. & Guerrini R. (2002) Familial periventricular heterotopia: missense and distal truncating mutations of the FLN1 gene. *Neurology* **58**, 916-21.

Muroya K., Okuyama T., Goishi K., Ogiso Y., Fukuda S., Kameyama J., Sato H., Suzuki Y., Terasaki H., Gomyo H., Wakui K., Fukushima Y. & Ogata T. (2000) Sex-determining gene(s) on distal 9p: clinical and molecular studies in six cases. *J Clin Endocrinol Metab* **85**, 3094-100.

Murray P.J., Thomas K., Mulgrew C.J., Ellard S., Edghill E.L. & Bingham C. (2008) Whole gene deletion of the hepatocyte nuclear factor-1beta gene in a patient with the prune-belly syndrome. *Nephrol Dial Transplant* **23**, 2412-5.

Nachtigal M.W., Hirokawa Y., Enyeart-VanHouten D.L., Flanagan J.N., Hammer G.D. & Ingraham H.A. (1998) Wilms' tumor 1 and Dax-1 modulate the orphan nuclear receptor SF-1 in sex-specific gene expression. *Cell* **93**, 445-54.

Nagano T., Morikubo S. & Sato M. (2004) Filamin A and FILIP (Filamin A-Interacting Protein) regulate cell polarity and motility in neocortical subventricular and intermediate zones during radial migration. *J Neurosci* **24**, 9648-57.

Nakamura F., Osborn T.M., Hartemink C.A., Hartwig J.H. & Stossel T.P. (2007) Structural basis of filamin A functions. *J Cell Biol* **179**, 1011-25.

Ng S.B., Bigham A.W., Buckingham K.J., Hannibal M.C., McMillin M.J., Gildersleeve H.I., Beck A.E., Tabor H.K., Cooper G.M., Mefford H.C., Lee C., Turner E.H., Smith J.D., Rieder M.J., Yoshiura K., Matsumoto N., Ohta T., Niikawa N., Nickerson D.A., Bamshad M.J. & Shendure J. (2010a) Exome sequencing identifies MLL2 mutations as a cause of Kabuki syndrome. *Nat Genet* **42**, 790-3.

Ng S.B., Buckingham K.J., Lee C., Bigham A.W., Tabor H.K., Dent K.M., Huff C.D., Shannon P.T., Jabs E.W., Nickerson D.A., Shendure J. & Bamshad M.J. (2010b) Exome sequencing identifies the cause of a mendelian disorder. *Nat Genet* **42**, 30-5.

Ng S.B., Turner E.H., Robertson P.D., Flygare S.D., Bigham A.W., Lee C., Shaffer T., Wong M., Bhattacharjee A., Eichler E.E., Bamshad M., Nickerson D.A. & Shendure J. (2009) Targeted capture and massively parallel sequencing of 12 human exomes. *Nature* **461**, 272-6.

Okello J.B., Zurek J., Devault A.M., Kuch M., Okwi A.L., Sewankambo N.K., Bimenya G.S., Poinar D. & Poinar H.N. (2010) Comparison of methods in the recovery of nucleic acids from archival formalin-fixed paraffin-embedded autopsy tissues. *Anal Biochem* **400**, 110-7.

Olbrich H., Schmidts M., Werner C., Onoufriadis A., Loges N.T., Raidt J., Banki N.F., Shoemark A., Burgoyne T., Al Turki S., Hurles M.E., Kohler G., Schroeder J., Nurnberg G., Nurnberg P., Chung E.M., Reinhardt R., Marthin J.K., Nielsen K.G., Mitchison H.M. & Omran H. (2012) Recessive HYDIN mutations cause primary ciliary dyskinesia without randomization of left-right body asymmetry. *Am J Hum Genet* **91**, 672-84.

Ono M. & Harley V.R. (2013) Disorders of sex development: new genes, new concepts. *Nat Rev Endocrinol* **9**, 79-91.

Oram RA, Edghill EL, Blackman J, Taylor MJO, Kay T, Flanagan SE, Ismail-Pratt I, Creighton SM, Ellard S, Hattersley AT & C B. (2010) Mutations in the hepatocyte nuclear factor-1B (HNF1B) gene are common with combined uterine and renal malformations but are not found with isolated uterine malformations. *Am J Obstet Gynecol* **203**, 364.

Ozanne D.M., Brady M.E., Cook S., Gaughan L., Neal D.E. & Robson C.N. (2000) Androgen receptor nuclear translocation is facilitated by the f-actin cross-linking protein filamin. *Mol Endocrinol* **14**, 1618-26.

Paria N., Copley L.A., Herring J.A., Kim H.K., Richards B.S., Sucato D.J., Wise C.A. & Rios J.J. (2013) Whole-exome sequencing: discovering genetic causes of orthopaedic disorders. *J Bone Joint Surg Am* **95**, e1851-8.

Pentikainen U. & Ylanne J. (2009) The regulation mechanism for the auto-inhibition of binding of human filamin A to integrin. *J Mol Biol* **393**, 644-57.

Pfaff M., Liu S., Erle D.J. & Ginsberg M.H. (1998) Integrin beta cytoplasmic domains differentially bind to cytoskeletal proteins. *J Biol Chem* **273**, 6104-9.

Philibert P., Leprieur E., Zenaty D., Thibaud E., Polak M., Frances A.M., Lespinasse J., Raingeard I., Servant N., Audran F., Paris F. & Sultan C. (2010) Steroidogenic factor-1 (SF-1) gene mutation as a frequent cause of primary amenorrhea in 46,XY female adolescents with low testosterone concentration. *Reprod Biol Endocrinol* **8**, 28.

Pinto V.I., Senini V.W., Wang Y., Kazembe M.P. & McCulloch C.A. (2014) Filamin A protects cells against force-induced apoptosis by stabilizing talin- and vinculin-containing cell adhesions. *FASEB J* **28**, 453-63.

Pohl H.G., Joyce G.F., Wise M. & Cilento B.G., Jr. (2007) Cryptorchidism and hypospadias. *J Urol* **177**, 1646-51.

Qi B.Q., Williams A., Beasley S. & Frizelle F. (2000) Clarification of the process of separation of the cloaca into rectum and urogenital sinus in the rat embryo. *J Pediatr Surg* **35**, 1810-6.

Rabbani B., Tekin M. & Mahdieh N. (2014) The promise of whole-exome sequencing in medical genetics. *J Hum Genet* **59**, 5-15.

Ramalho-Santos M., Melton D.A. & McMahon A.P. (2000) Hedgehog signals regulate multiple aspects of gastrointestinal development. *Development* **127**, 2763-72.

Ramasamy R., Haviland M., Woodard J.R. & Barone J.G. (2005) Patterns of inheritance in familial prune belly syndrome. *Urology* **65**, 1227.

Ramayya M.S., Zhou J., Kino T., Segars J.H., Bondy C.A. & Chrousos G.P. (1997) Steroidogenic factor 1 messenger ribonucleic acid expression in steroidogenic and nonsteroidogenic human tissues: Northern blot and in situ hybridization studies. *J Clin Endocrinol Metab* **82**, 1799-806.

Ramos F.J., McDonald-McGinn D.M., Emanuel B.S. & Zackai E.H. (1992) Tricho-rhino-phalangeal syndrome type II (Langer-Giedion) with persistent cloaca and prune belly sequence in a girl with 8q interstitial deletion. *Am J Med Genet* **44**, 790-4.

Rasouly H.M. & Lu W. (2013) Lower urinary tract development and disease. *Wiley Interdiscip Rev Syst Biol Med* **5**, 307-42.

Reinberg Y., Manivel J.C., Pettinato G. & Gonzalez R. (1991) Development of renal failure in children with the prune belly syndrome. *J Urol* **145**, 1017-9.

Riccardi VM & Grum CM (1977) The prune belly anomaly: heterogeneity and superficial X-linkage mimicry. *J Med Genet* **14**, 266-70.

Richer J., Milewicz D.M., Gow R., de Nanassy J., Maharajh G., Miller E., Oppenheimer L., Weiler G. & O'Connor M. (2012) R179H mutation in ACTA2 expanding the phenotype to include prune-belly sequence and skin manifestations. *Am J Med Genet A* **158A**, 664-8.

Rink R.C., Herndon C.D., Cain M.P., Kaefer M., Dussinger A.M., King S.J. & Casale A.J. (2005) Upper and lower urinary tract outcome after surgical repair of cloacal malformations: a three-decade experience. *BJU Int* **96**, 131-4.

Robertson S.P. (2005) Filamin A: phenotypic diversity. *Curr Opin Genet Dev* **15**, 301-7.

Robertson S.P., Twigg S.R., Sutherland-Smith A.J., Biancalana V., Gorlin R.J., Horn D., Kenwrick S.J., Kim C.A., Morava E., Newbury-Ecob R., Orstavik K.H., Quarrell O.W., Schwartz C.E., Shears D.J., Suri M., Kendrick-Jones J. & Wilkie A.O. (2003) Localized mutations in the gene encoding the cytoskeletal protein filamin A cause diverse malformations in humans. *Nat Genet* **33**, 487-91.

Rognoni L., Stigler J., Pelz B., Ylanne J. & Rief M. (2012) Dynamic force sensing of filamin revealed in single-molecule experiments. *Proc Natl Acad Sci U S A* **109**, 19679-84.

Routh J.C., Huang L., Retik A.B. & Nelson C.P. (2010) Contemporary epidemiology and characterization of newborn males with prune belly syndrome. *Urology* **76**, 44-8.

Sanna-Cherchi S., Ravani P., Corbani V., Parodi S., Haupt R., Piaggio G., Innocenti M.L., Somenzi D., Trivelli A., Caridi G., Izzi C., Scolari F., Mattioli G., Allegri L. & Ghiggeri G.M. (2009) Renal outcome in patients with congenital anomalies of the kidney and urinary tract. *Kidney Int* **76**, 528-33.

Sanna-Cherchi S., Sampogna R.V., Papeta N., Burgess K.E., Nees S.N., Perry B.J., Choi M., Bodria M., Liu Y., Weng P.L., Lozanovski V.J., Verbitsky M., Lugani F., Sterken R., Paragas N., Caridi G., Carrea A., Dagnino M., Materna-Kiryluk A., Santamaria G., Murtas C., Ristoska-Bojkovska N., Izzi C., Kacak N., Bianco B., Giberti S., Gigante M., Piaggio G., Gesualdo L., Kosuljandic Vukic D., Vukojevic K., Saraga-Babic M., Saraga M., Gucev Z., Allegri L., Latos-Bielenska A., Casu D., State M., Scolari F., Ravazzolo R., Kiryluk K., Al-Awqati Q., D'Agati V.D., Drummond I.A., Tasic V., Lifton R.P., Ghiggeri G.M. & Gharavi A.G. (2013) Mutations in DSTYK and dominant urinary tract malformations. *N Engl J Med* **369**, 621-9.

Sasaki A., Masuda Y., Ohta Y., Ikeda K. & Watanabe K. (2001) Filamin associates with Smads and regulates transforming growth factor-beta signaling. *J Biol Chem* **276**, 17871-7.

Schimmer B.P. & White P.C. (2010) Minireview: steroidogenic factor 1: its roles in differentiation, development, and disease. *Mol Endocrinol* **24**, 1322-37.

Schlaubitz S., Yatsenko S.A., Smith L.D., Keller K.L., Vissers L.E., Scott D.A., Cai W.W., Reardon W., Abdul-Rahman O.A., Lammer E.J., Lifchez C.A., Magenis E., Veltman J.A., Stankiewicz P., Zabel B.U. & Lee B. (2007) Ovotestes and XY sex reversal in a female with an interstitial 9q33.3-q34.1 deletion encompassing NR5A1 and LMX1B causing features of Genitopatellar syndrome. *Am J Med Genet A* **143A**, 1071-81.

Sebat J., Lakshmi B., Malhotra D., Troge J., Lese-Martin C., Walsh T., Yamrom B., Yoon S., Krasnitz A., Kendall J., Leotta A., Pai D., Zhang R., Lee Y.H., Hicks J., Spence S.J., Lee A.T., Puura K., Lehtimaki T., Ledbetter D., Gregersen P.K., Bregman J., Sutcliffe J.S., Jobanputra V., Chung W., Warburton D., King M.C., Skuse D., Geschwind D.H., Gilliam T.C., Ye K. & Wigler M. (2007) Strong association of de novo copy number mutations with autism. *Science* **316**, 445-9.

Sebat J., Lakshmi B., Troge J., Alexander J., Young J., Lundin P., Maner S., Massa H., Walker M., Chi M., Navin N., Lucito R., Healy J., Hicks J., Ye K., Reiner A., Gilliam T.C., Trask B., Patterson N., Zetterberg A. & Wigler M. (2004) Large-scale copy number polymorphism in the human genome. *Science* **305**, 525-8.

Sekido R. & Lovell-Badge R. (2008) Sex determination involves synergistic action of SRY and SF1 on a specific Sox9 enhancer. *Nature* **453**, 930-4.

Sheen V.L., Dixon P.H., Fox J.W., Hong S.E., Kinton L., Sisodiya S.M., Duncan J.S., Dubeau F., Scheffer I.E., Schachter S.C., Wilner A., Henchy R., Crino P., Kamuro K., DiMario F., Berg M., Kuzniecky R., Cole A.J., Bromfield E., Biber M., Schomer D., Wheless J., Silver K., Mochida G.H., Berkovic S.F., Andermann F., Andermann E., Dobyns W.B., Wood N.W. & Walsh C.A. (2001) Mutations in the X-linked filamin 1 gene cause periventricular nodular heterotopia in males as well as in females. *Hum Mol Genet* **10**, 1775-83.

Shimizu T., Ihara Y., Yomura W., Ando N. & Nishimura R. (1992) Antenatal diagnosis of prune belly syndrome. *Arch Gynecol Obstet* **251**, 211-4.

Shoukier M., Klein N., Auber B., Wickert J., Schroder J., Zoll B., Burfeind P., Bartels I., Alsat E.A., Lingen M., Grzmil P., Schulze S., Keyser J., Weise D., Borchers M., Hobbiebrunken E., Robl M., Gartner J., Brockmann K. & Zirn B. (2013) Array CGH in patients with developmental delay or intellectual disability: are there phenotypic clues to pathogenic copy number variants? *Clin Genet* **83**, 53-65.

Smyk M., Berg J.S., Pursley A., Curtis F.K., Fernandez B.A., Bien-Willner G.A., Lupski J.R., Cheung S.W. & Stankiewicz P. (2007) Male-to-female sex reversal associated with an approximately 250 kb deletion upstream of NR0B1 (DAX1). *Hum Genet* **122**, 63-70.

Stephens F.D. & Gupta D. (1994) Pathogenesis of the prune belly syndrome. *J Urol* **152**, 2328-31.

Stitziel N.O., Kiezun A. & Sunyaev S. (2011) Computational and statistical approaches to analyzing variants identified by exome sequencing. *Genome Biol* **12**, 227.

Sutherland R.S., Mevorach R.A. & Kogan B.A. (1995) The prune-belly syndrome: current insights. *Pediatr Nephrol* **9**, 770-8.

Sutton E., Hughes J., White S., Sekido R., Tan J., Arboleda V., Rogers N., Knower K., Rowley L., Eyre H., Rizzoti K., McAninch D., Goncalves J., Slee J., Turbitt E., Bruno D., Bengtsson H., Harley V., Vilain E., Sinclair A., Lovell-Badge R. & Thomas P. (2011) Identification of SOX3 as an XX male sex reversal gene in mice and humans. *J Clin Invest* **121**, 328-41.

Tadokoro S., Shattil S.J., Eto K., Tai V., Liddington R.C., de Pereda J.M., Ginsberg M.H. & Calderwood D.A. (2003) Talin binding to integrin beta tails: a final common step in integrin activation. *Science* **302**, 103-6.

Tajima T., Fujiwara F. & Fujieda K. (2009) A novel heterozygous mutation of steroidogenic factor-1 (SF-1/Ad4BP) gene (NR5A1) in a 46, XY disorders of sex development (DSD) patient without adrenal failure. *Endocr J* **56**, 619-24.

Tannour-Louet M., Han S., Corbett S.T., Louet J.F., Yatsenko S., Meyers L., Shaw C.A., Kang S.H., Cheung S.W. & Lamb D.J. (2010) Identification of de novo copy number variants associated with human disorders of sexual development. *PLoS One* **5**, e15392.

Thomas R., Sanna-Cherchi S., Warady B.A., Furth S.L., Kaskel F.J. & Gharavi A.G. (2011) HNF1B and PAX2 mutations are a common cause of renal hypodysplasia in the CKiD cohort. *Pediatr Nephrol* **26**, 897-903.

Toro C., Olive M., Dalakas M.C., Sivakumar K., Bilbao J.M., Tyndel F., Vidal N., Farrero E., Sambuughin N. & Goldfarb L.G. (2013) Exome sequencing identifies titin mutations causing hereditary myopathy with early respiratory failure (HMERF) in families of diverse ethnic origins. *BMC Neurol* **13**, 29.

Tsai M.H., Kamm K.E. & Stull J.T. (2012) Signalling to contractile proteins by muscarinic and purinergic pathways in neurally stimulated bladder smooth muscle. *J Physiol* **590**, 5107-21.

Tu Y., Wu S., Shi X., Chen K. & Wu C. (2003) Migfilin and Mig-2 link focal adhesions to filamin and the actin cytoskeleton and function in cell shape modulation. *Cell* **113**, 37-47.

Tuttelmann F., Simoni M., Kliesch S., Ledig S., Dworniczak B., Wieacker P. & Ropke A. (2011) Copy number variants in patients with severe oligozoospermia and Sertoli-cell-only syndrome. *PLoS One* **6**, e19426.

Van den Veyver I.B. (2001) Skewed X inactivation in X-linked disorders. *Semin Reprod Med* **19**, 183-91.

van der Flier A., Kuikman I., Kramer D., Geerts D., Kreft M., Takafuta T., Shapiro S.S. & Sonnenberg A. (2002) Different splice variants of filamin-B affect myogenesis, subcellular distribution, and determine binding to integrin [beta] subunits. *J Cell Biol* **156**, 361-76.

van der Werf C.S., Sribudiani Y., Verheij J.B., Carroll M., O'Loughlin E., Chen C.H., Brooks A.S., Liszewski M.K., Atkinson J.P. & Hofstra R.M. (2013) Congenital short bowel syndrome as the presenting symptom in male patients with FLNA mutations. *Genet Med* **15**, 310-3.

van Silfhout A., Boot A.M., Dijkhuizen T., Hoek A., Nijman R., Sikkema-Raddatz B. & van Ravenswaaij-Arts C.M. (2009) A unique 970kb microdeletion in 9q33.3, including the NR5A1 gene in a 46,XY female. *Eur J Med Genet* **52**, 157-60.

Viger R.S., Mertineit C., Trasler J.M. & Nemer M. (1998) Transcription factor GATA-4 is expressed in a sexually dimorphic pattern during mouse gonadal development and is a potent activator of the Mullerian inhibiting substance promoter. *Development* **125**, 2665-75.

Virtanen H.E., Bjerknes R., Cortes D., Jorgensen N., Rajpert-De Meyts E., Thorsson A.V., Thorup J. & Main K.M. (2007) Cryptorchidism: classification, prevalence and long-term consequences. *Acta Paediatr* **96**, 611-6.

Vissers L.E., de Ligt J., Gilissen C., Janssen I., Steehouwer M., de Vries P., van Lier B., Arts P., Wieskamp N., del Rosario M., van Bon B.W., Hoischen A., de Vries B.B., Brunner H.G. & Veltman J.A. (2010) A de novo paradigm for mental retardation. *Nat Genet* **42**, 1109-12.

Vissers L.E., van Ravenswaaij C.M., Admiraal R., Hurst J.A., de Vries B.B., Janssen I.M., van der Vliet W.A., Huys E.H., de Jong P.J., Hamel B.C., Schoenmakers E.F., Brunner H.G., Veltman J.A. & van Kessel A.G. (2004) Mutations in a new member of the chromodomain gene family cause CHARGE syndrome. *Nat Genet* **36**, 955-7.

Vulto-van Silfhout A.T., Hehir-Kwa J.Y., van Bon B.W., Schuurs-Hoeijmakers J.H., Meader S., Hellebrekers C.J., Thoonen I.J., de Brouwer A.P., Brunner H.G., Webber C., Pfundt R., de Leeuw N. & de Vries B.B. (2013) Clinical significance of de novo and inherited copy-number variation. *Hum Mutat* **34**, 1679-87.

Warne S.A., Hiorns M.P., Curry J. & Mushtaq I. (2011) Understanding cloacal anomalies. *Arch Dis Child* **96**, 1072-6.

Warne S.A., Wilcox D.T., Ledermann S.E. & Ransley P.G. (2002) Renal outcome in patients with cloaca. *J Urol* **167**, 2548-51; discussion 51.

Weber S. (2012) Novel genetic aspects of congenital anomalies of kidney and urinary tract. *Curr Opin Pediatr* **24**, 212-8.

Weber S., Moriniere V., Knuppel T., Charbit M., Dusek J., Ghiggeri G.M., Jankauskiene A., Mir S., Montini G., Peco-Antic A., Wuhl E., Zurowska A.M., Mehls O., Antignac C., Schaefer F. & Salomon R. (2006) Prevalence of mutations in renal developmental genes in children with renal hypodysplasia: results of the ESCAPE study. *J Am Soc Nephrol* **17**, 2864-70.

Weber S., Thiele H., Mir S., Toliat M.R., Sozeri B., Reutter H., Draaken M., Ludwig M., Altmuller J., Frommolt P., Stuart H.M., Ranjzad P., Hanley N.A., Jennings R., Newman W.G., Wilcox D.T., Thiel U., Schlingmann K.P., Beetz R., Hoyer P.F., Konrad M., Schaefer F., Nurnberg P. & Woolf A.S. (2011) Muscarinic Acetylcholine Receptor M3 Mutation Causes Urinary Bladder Disease and a Prune-Belly-like Syndrome. *Am J Hum Genet* **89**, 668-74.

Wheatley J.M., Stephens F.D. & Hutson J.M. (1996) Prune-belly syndrome: ongoing controversies regarding pathogenesis and management. *Semin Pediatr Surg* **5**, 95-106.

White S., Hewitt J., Turbitt E., van der Zwan Y., Hersmus R., Drop S., Koopman P., Harley V., Cools M., Looijenga L. & Sinclair A. (2012) A multi-exon deletion

within WWOX is associated with a 46,XY disorder of sex development. *Eur J Hum Genet* **20**, 348-51.

White S., Ohnesorg T., Notini A., Roeszler K., Hewitt J., Daggag H., Smith C., Turbitt E., Gustin S., van den Bergen J., Miles D., Western P., Arboleda V., Schumacher V., Gordon L., Bell K., Bengtsson H., Speed T., Hutson J., Warne G., Harley V., Koopman P., Vilain E. & Sinclair A. (2011) Copy number variation in patients with disorders of sex development due to 46,XY gonadal dysgenesis. *PLoS One* **6**, e17793.

Wu X., Ferrara C., Shapiro E. & Grishina I. (2009) Bmp7 expression and null phenotype in the urogenital system suggest a role in re-organization of the urethral epithelium. *Gene Expr Patterns* **9**, 224-30.

Yoshida N., Ogata T., Tanabe K., Li S., Nakazato M., Kohu K., Takafuta T., Shapiro S., Ohta Y., Satake M. & Watanabe T. (2005) Filamin A-bound PEBP2beta/CBFbeta is retained in the cytoplasm and prevented from functioning as a partner of the Runx1 transcription factor. *Mol Cell Biol* **25**, 1003-12.

Yu S., Bittel D.C., Kibiryeva N., Zwick D.L. & Cooley L.D. (2009) Validation of the Agilent 244K oligonucleotide array-based comparative genomic hybridization platform for clinical cytogenetic diagnosis. *Am J Clin Pathol* **132**, 349-60.

Zentner G.E., Layman W.S., Martin D.M. & Scacheri P.C. (2010) Molecular and phenotypic aspects of CHD7 mutation in CHARGE syndrome. *Am J Med Genet A* **152A**, 674-86.

Zhang F., Gu W., Hurles M.E. & Lupski J.R. (2009) Copy number variation in human health, disease, and evolution. *Annu Rev Genomics Hum Genet* **10**, 451-81.

Zheng X., Zhou A.X., Rouhi P., Uramoto H., Boren J., Cao Y., Pereira T., Akyurek L.M. & Poellinger L. (2014) Hypoxia-induced and calpain-dependent cleavage of filamin A regulates the hypoxic response. *Proc Natl Acad Sci U S A* **111**, 2560-5.

Zhou A.X., Hartwig J.H. & Akyurek L.M. (2010) Filamins in cell signaling, transcription and organ development. *Trends Cell Biol* **20**, 113-23.

Zhou X., Boren J. & Akyurek L.M. (2007) Filamins in cardiovascular development. *Trends Cardiovasc Med* **17**, 222-9.

Zimmerman R.A., Tomasek J.J., McRae J., Haaksma C.J., Schwartz R.J., Lin H.K., Cowan R.L., Jones A.N. & Kropp B.P. (2004) Decreased expression of smooth muscle alpha-actin results in decreased contractile function of the mouse bladder. *J Urol* **172**, 1667-72.

Zimmermann S., Schwarzler A., Buth S., Engel W. & Adham I.M. (1998) Transcription of the Leydig insulin-like gene is mediated by steroidogenic factor-1. *Mol Endocrinol* **12**, 706-13.

Zitzmann M., Depenbusch M., Gromoll J. & Nieschlag E. (2004) X-chromosome inactivation patterns and androgen receptor functionality influence phenotype and social characteristics as well as pharmacogenetics of testosterone therapy in Klinefelter patients. *J Clin Endocrinol Metab* **89**, 6208-17.